Chapter 6

FUTURE DIRECTIONS

This chapter contains a few contributions related to future possibilities for the extraction of the CKM elements and of the CP violating phases. They include general strategies for the determination of the CKM matrix elements, radiative rare B decays, weak phase determination from hadronic B decays and rare $\mathrm{K} \to \pi\nu\bar{\nu}$ decays. Since these topics have not been the subject of a dedicated working group at this meeting of the Workshop, we present them in the form of collected papers under individual authorship.

1. General strategies for the CKM matrix

A.J. Buras, F. Parodi and A. Stocchi

During the last two decades several strategies have been proposed that should allow one to determine the CKM matrix and the related unitarity triangle (UT). We have already discussed a number of processes that can be used for the determination of the CKM parameters in Chapters 2–4. Additional processes and the related strategies will be discussed in this part. They are also reviewed in [1–5]. In this first opening section we want to address the determination of the CKM matrix and of the UT in general terms leaving the discussion of specific strategies to the following sections.

To be specific let us first choose as the independent parameters

$$|V_{us}|, \qquad |V_{cb}|, \qquad \bar{\varrho}, \qquad \bar{\eta}\,. \tag{1}$$

The best place to determine $|V_{us}|$ and $|V_{cb}|$, as discussed already in detail in Chapters 2 and 3, are the semi-leptonic K and B decays, respectively. The question that we want address here is the determination of the remaining two parameters $(\bar{\varrho}, \bar{\eta})$.

There are many ways to determine $(\bar{\varrho}, \bar{\eta})$. As the length of one side of the rescaled unitarity triangle is fixed to unity, we have to our disposal two sides, R_b and R_t and three angles, α, β and γ. These five quantities can be measured by means of rare K and B decays and in particular by studying CP-violating observables. While until recently only a handful of strategies could be realized, the present decade should allow several independent determinations of $(\bar{\varrho}, \bar{\eta})$ that will test the KM picture of CP violation and possibly indicate the physics beyond the Standard Model (SM).

The determination of $(\bar{\varrho}, \bar{\eta})$ in a given strategy is subject to experimental and theoretical errors and it is important to identify those strategies that are experimentally feasible and in which hadronic uncertainties are as much as possible under control. Such strategies are reviewed in [1–5] and in the following sections below.

Here we want to address a different question. The determination of $(\bar{\varrho}, \bar{\eta})$ requires at least two independent measurements. In most cases these are the measurements of two sides of the UT, of one side

and one angle or the measurements of two angles. Sometimes $\bar{\eta}$ can be directly measured and combining it with the knowledge of one angle or one side of the UT, $\bar{\varrho}$ can be found. Analogous comments apply to measurements in which $\bar{\varrho}$ is directly measured. Finally in more complicated strategies one measures various linear combinations of angles, sides or $\bar{\varrho}$ and $\bar{\eta}$.

Restricting first our attention to measurements in which sides and angles of the UT can be measured independently of each other, we end up with ten different pairs of measurements that allow the determination of $(\bar{\varrho}, \bar{\eta})$. The question then arises which of the pairs in question is most efficient in the determination of the UT? That is, given the same relative errors on R_b, R_t, α, β and γ, we want to find which of the pairs gives the most accurate determination of $(\bar{\varrho}, \bar{\eta})$.

The answer to this question depends necessarily on the values of R_b, R_t, α, β and γ but as we will see below just the requirement of the consistency of R_b with the measured value of $|V_{ub}/V_{cb}|$ implies a hierarchy within the ten strategies mentioned above.

During the 1970's and 1980's α_{QED}, the Fermi constant G_F and the sine of the Weinberg angle ($\sin\theta_W$) measured in the ν-N scattering were the fundamental parameters in terms of which the electroweak tests of the SM were performed. After the Z^0 boson was discovered and its mass precisely measured at LEP-I, $\sin\theta_W$ has been replaced by M_Z and the fundamental set used in the electroweak precision studies in the 1990's has been (α_{QED}, G_F, M_Z). It is to be expected that when M_W will be measured precisely this set will be changed to (α_{QED}, M_W, M_Z) or (G_F, M_W, M_Z).

We anticipate that an analogous development will happen in this decade in connection with the CKM matrix. While the set (1) has clearly many virtues and has been used extensively in the literature, one should emphasize that presently no direct independent measurements of $\bar{\eta}$ and $\bar{\varrho}$ are available. $|\bar{\eta}|$ can be measured cleanly in the decay $\mathrm{K}_L \to \pi^0\nu\bar{\nu}$. On the other hand to our knowledge there does not exist any strategy for a clean independent measurement of $\bar{\varrho}$.

Taking into account the experimental feasibility of various measurements and their theoretical cleanness, the most obvious candidate for the fundamental set in the quark flavour physics for the coming years appears to be [6]

$$|V_{us}|, \qquad |V_{cb}|, \qquad R_t, \qquad \beta \tag{2}$$

with the last two variables describing the V_{td} coupling that can be measured by means of the $\mathrm{B}^0 - \bar{B}^0$ mixing ratio $\Delta M_d/\Delta M_s$ and the CP-asymmetry $a_{\psi \mathrm{K}_S}$, respectively. In this context, we investigate [6], in analogy to the $(\bar{\varrho}, \bar{\eta})$ plane and the planes $(\sin 2\beta, \sin 2\alpha)$ [7] and $(\gamma, \sin 2\beta)$ [8] considered in the past, the (R_t, β) plane for the exhibition of various constraints on the CKM matrix. We also provide the parametrization of the CKM matrix given directly in terms of the variables (2).

While the set (2) appears to be the best choice for the coming years, our analysis shows that in the long run other choices could turn out to be preferable. In this context it should be emphasized that several of the results and formulae presented here are not entirely new and have been already discussed by us and other authors in the past. In particular in [9] it has been pointed out that only a moderately precise measurement of $\sin 2\alpha$ can be as useful for the UT as a precise measurement of the angle β. This has been recently reemphasized in [10–12], see contribution in this Chapter, Sec. 3.3.. Similarly the measurement of the pair (α, β) has been found to be a very efficient tool for the determination of the UT [13,14] and the construction of the full CKM matrix from the angles of various unitarity triangles has been presented in [15]. Next, the importance of the pair $(R_t, \sin 2\beta)$ has been emphasized recently in a number of papers [16–20]. Many useful relations relevant for the unitarity triangle can also be found in [21,22]. Finally, in a recent paper [6] we have presented a systematic classification of the strategies in question and their comparison. In fact the results of this paper constitute the main part of this section.

1.1. Basic formulae

Let us begin our presentation by listing the formulae for $\bar{\varrho}$ and $\bar{\eta}$ in the strategies in question that are labeled by the two measured quantities as discussed above.

$\boldsymbol{R_t}$ and $\boldsymbol{\beta}$

$$\bar{\varrho} = 1 - R_t \cos\beta, \qquad \bar{\eta} = R_t \sin\beta \; . \tag{3}$$

$\boldsymbol{R_b}$ and $\boldsymbol{\gamma}$

$$\bar{\varrho} = R_b \cos\gamma, \qquad \bar{\eta} = R_b \sin\gamma \; . \tag{4}$$

$\boldsymbol{R_b}$ and $\boldsymbol{R_t}$

$$\bar{\varrho} = \frac{1}{2}(1 + R_b^2 - R_t^2), \qquad \bar{\eta} = \sqrt{R_b^2 - \bar{\varrho}^2} \tag{5}$$

where $\bar{\eta} > 0$ has been assumed.

$\boldsymbol{R_t}$ and $\boldsymbol{\gamma}$

This strategy uses (4) with

$$R_b = \cos\gamma \pm \sqrt{R_t^2 - \sin^2\gamma} \; . \tag{6}$$

The two possibilities can be distinguished by the measured value of R_b.

$\boldsymbol{R_b}$ and $\boldsymbol{\beta}$

This strategy uses (3) and

$$R_t = \cos\beta \pm \sqrt{R_b^2 - \sin^2\beta} \; . \tag{7}$$

The two possibilities can be distinguished by the measured value of R_t.

$\boldsymbol{R_t}$ and $\boldsymbol{\alpha}$

$$\bar{\varrho} = 1 - R_t^2 \sin^2\alpha + R_t \cos\alpha \sqrt{1 - R_t^2 \sin^2\alpha}, \tag{8}$$

$$\bar{\eta} = R_t \sin\alpha \left[R_t \cos\alpha + \sqrt{1 - R_t^2 \sin^2\alpha} \right] \tag{9}$$

where $\cos\gamma > 0$ has been assumed. For $\cos\gamma < 0$ the signs in front of the square roots should be reversed.

$\boldsymbol{R_b}$ and $\boldsymbol{\alpha}$

$$\bar{\varrho} = R_b^2 \sin^2\alpha - R_b \cos\alpha \sqrt{1 - R_b^2 \sin^2\alpha}, \tag{10}$$

$$\bar{\eta} = R_b \sin\alpha \left[R_b \cos\alpha + \sqrt{1 - R_b^2 \sin^2\alpha} \right] \tag{11}$$

where $\cos\beta > 0$ has been assumed.

$\boldsymbol{\beta}$ and $\boldsymbol{\gamma}$

$$R_t = \frac{\sin\gamma}{\sin(\beta+\gamma)}, \qquad R_b = \frac{\sin\beta}{\sin(\beta+\gamma)} \tag{12}$$

and (5).

$\boldsymbol{\alpha}$ and $\boldsymbol{\gamma}$

$$R_t = \frac{\sin\gamma}{\sin\alpha}, \qquad R_b = \frac{\sin(\alpha+\gamma)}{\sin\alpha} \tag{13}$$

and (5).

$\boldsymbol{\alpha}$ and $\boldsymbol{\beta}$

$$R_t = \frac{\sin(\alpha+\beta)}{\sin\alpha}, \qquad R_b = \frac{\sin\beta}{\sin\alpha} \tag{14}$$

and (5).

Finally we give the formulae for the strategies in which $\bar{\eta}$ is directly measured and the strategy allows to determine $\bar{\varrho}$.

$\bar{\boldsymbol{\eta}}$ and $\boldsymbol{R_t}$ or $\boldsymbol{R_b}$

$$\bar{\varrho} = 1 - \sqrt{R_t^2 - \bar{\eta}^2}, \qquad \bar{\varrho} = \pm\sqrt{R_b^2 - \bar{\eta}^2}\,, \tag{15}$$

where in the first case we have excluded the + solution in view of $R_b \leq 0.5$ as extracted from the experimental data on $|V_{ub}|$.

$\bar{\boldsymbol{\eta}}$ and $\boldsymbol{\beta}$ or $\boldsymbol{\gamma}$

$$\bar{\varrho} = 1 - \frac{\bar{\eta}}{\tan\beta}, \qquad \bar{\varrho} = \frac{\bar{\eta}}{\tan\gamma}\,. \tag{16}$$

1.2. CKM matrix and the fundamental variables

It is useful for phenomenological purposes to express the CKM matrix directly in terms of the parameters selected in a given strategy. This can be easily done by inserting the formulae for $\bar{\varrho}$ and $\bar{\eta}$ presented here into the known expressions for the CKM elements in terms of these variables [23,13] as given in Chapter 1.

Here we give explicit result only for the set (2). In order to simplify the notation we use λ instead of $|V_{us}|$ as $V_{us} = \lambda + \mathcal{O}(\lambda^7)$. We find

$$V_{ud} = 1 - \frac{1}{2}\lambda^2 - \frac{1}{8}\lambda^4 + \mathcal{O}(\lambda^6), \qquad V_{ub} = \frac{\lambda}{1-\lambda^2/2}|V_{cb}|\left[1 - R_t e^{i\beta}\right], \tag{17}$$

$$V_{cd} = -\lambda + \frac{1}{2}\lambda|V_{cb}|^2 - \lambda|V_{cb}|^2\left[1 - R_t e^{-i\beta}\right] + \mathcal{O}(\lambda^7), \tag{18}$$

$$V_{cs} = 1 - \frac{1}{2}\lambda^2 - \frac{1}{8}\lambda^4 - \frac{1}{2}|V_{cb}|^2 + \mathcal{O}(\lambda^6), \tag{19}$$

$$V_{tb} = 1 - \frac{1}{2}|V_{cb}|^2 + \mathcal{O}(\lambda^6), \qquad V_{td} = \lambda|V_{cb}|R_t e^{-i\beta} + \mathcal{O}(\lambda^7), \tag{20}$$

$$V_{ts} = -|V_{cb}| + \frac{1}{2}\lambda^2|V_{cb}| - \lambda^2|V_{cb}|\left[1 - R_t e^{-i\beta}\right] + \mathcal{O}(\lambda^6)\,. \tag{21}$$

1.3. Hierarchies of the various strategies

The numerical analysis of various strategies listed above was performed using the Bayesian approach as described in the previous Chapter. The main results of this analysis are depicted in Figs. 6.1, 6.2, 6.3 and 6.4. In Figs. 6.1 and 6.2 we plot the correlation between the precisions on the variables relevant for a given strategy required to reach the assumed precision on $\bar{\eta}$ and $\bar{\varrho}$, respectively. For this exercise we have used, for $\bar{\eta}$ and $\bar{\rho}$, the central values obtained in the previous Chapter. Obviously strategies described by curves in Figs. 6.1 and 6.2 that lie far from the origin are more effective in the determination of the unitarity triangle than those corresponding to curves placed close to the origin.

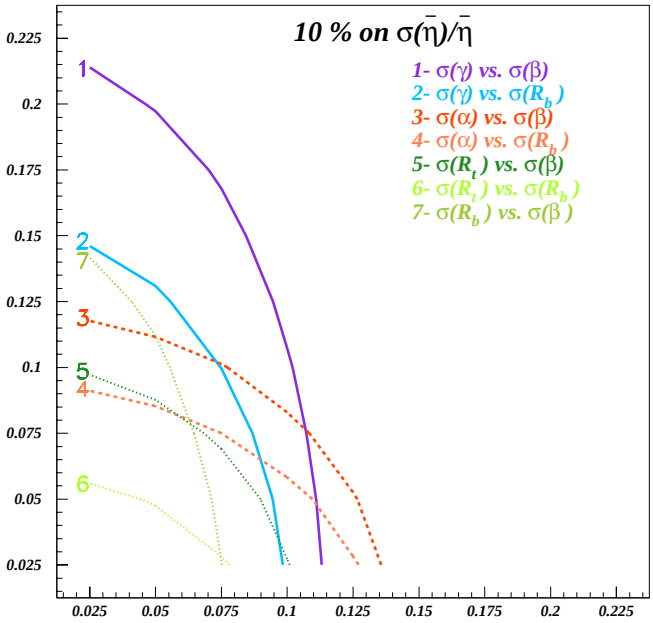

Fig. 6.1: *The plot shows the curves of the 10% relative precision on $\bar{\eta}$ as a function of the precision on the variables of the given strategy.*

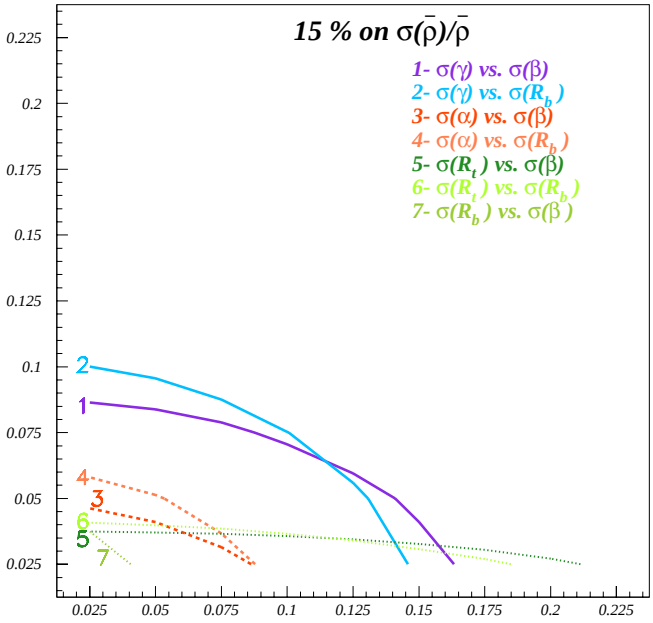

Fig. 6.2: *The plot shows the curves of the 15% relative precision on $\bar{\varrho}$ as a function of the precision on the variables of the given strategy.*

Figures 6.1 and 6.2 reveal certain hierarchies within the strategies in question. In order to find these hierarchies and to eliminate the weakest ones not shown in these figures we divided first the five variables under consideration into two groups:

$$(R_t, \alpha, \gamma), \qquad (R_b, \beta)\ . \tag{22}$$

It turned out then that the four strategies (R_t, α), (R_t, γ), (α, γ) and (R_b, β) which involve pairs of variables belonging to the same group are not particularly useful in the determination of $(\bar{\varrho}, \bar{\eta})$. In the case of (R_b, β) this is related to the existence of two possible solutions as stated above. If one of these solutions can easily be excluded on the basis of R_t, then the effectiveness of this strategy can be increased. We have therefore included this strategy in our numerical analysis. The strategy (R_t, γ) turns out to be less useful in this respect. Similarly the strategy (γ, α) is not particularly useful due to strong correlation between the variables in question as discussed previously by many authors in the literature.

The remaining six strategies that involve pairs of variables belonging to different groups in (22) are all interesting. While some strategies are better suited for the determination of $\bar{\eta}$ and the other for $\bar{\varrho}$, as clearly seen in Figs. 6.1 and 6.2, on the whole a clear ranking of strategies seems to emerge from our analysis.

If we assume the same relative error on α, β, γ, R_b and R_t we find the following hierarchy:

$$1)\ (\gamma, \beta), \quad (\gamma, R_b) \qquad 2)\ (\alpha, \beta), \quad (\alpha, R_b) \qquad 3)\ (R_t, \beta), \quad (R_t, R_b), \quad (R_b, \beta). \tag{23}$$

We observe that in particular the strategies involving R_b and γ are very high on this ranking list. This is related to the fact that $R_b < 0.5 < R_t$ and consequently the action in the $(\bar{\varrho}, \bar{\eta})$ plane takes place closer to the origin of this plane than to the corner of the UT involving the angle β. Consequently the accuracy on R_b and γ does not have to be as high as for R_t and β in order to obtain the same accuracy for $(\bar{\varrho}, \bar{\eta})$. This is clearly seen in Figs. 6.1 and 6.2.

This analysis shows how important is the determination of R_b and γ in addition to β that is already well known. On the other hand the strategy involving R_t and β will be most probably the cleanest one before the LHC experiments unless the error on angle γ from B factories and Tevatron can be significantly decreased below 10% and the accuracy on R_b considerably improved. The explicit strategies for the determination of γ are discussed in the following sections.

The strategies involving α are in our second best class. However, it has to be noticed that in order to get $10\%(15\%)$ relative precision on $\bar{\eta}(\bar{\rho})$ it is necessary (see Figs. 6.1 and 6.2) to determine α with better than 10% relative precision. If $\sin 2\alpha$ could be directly measured this could be soon achieved due to the high sensitivity of $\sin 2\alpha$ to α for α in the ball park of 90° as obtained from the standard analysis of the unitarity triangle. However, from the present perspective this appears to be very difficult in view of the penguin pollution that could be substantial as indicated by the most recent data from Belle [24]. On the other hand, as the BaBar data [25] do not indicate this pollution, the situation is unclear at present. These issues are discussed in detail in the following sections.

We have also performed a numerical analysis for the strategies in which $|\bar{\eta}|$ can be directly measured. The relevant formulae are given in (15) and (16). It turns out that the strategy $(\gamma, \bar{\eta})$ can be put in the first best class in (23) together with the strategies (γ, β) and (γ, R_b).

In Fig. 6.3 we show the resulting regions in the $(\bar{\varrho}, \bar{\eta})$ plane obtained from leading strategies assuming that each variable is measured with 10% accuracy. This figure is complementary to Figs. 6.1 and 6.2 and demonstrates clearly the ranking given in (23).

While at present the set (2) appears to be the leading candidate for the fundamental parameter set in the quark flavour physics for the coming years, it is not clear which set will be most convenient in the

second half of this decade when the B-factories and Tevatron will improve considerably their measurements and LHC will start its operation. Therefore it is of interest to investigate how the measurements of three variables out of $\alpha,\ \beta,\ \gamma\ , R_b$ and R_t will determine the allowed values for the remaining two variables. We illustrate this in Fig. 6.4 assuming a relative error of 10% for the constraints used in each plot. While this figure is self explanatory a striking feature consistent with the hierarchical structure in (23) can be observed. While the measurements of (α, R_t, R_b) and (α, β, R_t) as seen in the first two plots do not appreciably constrain the parameters of the two leading strategies (β, γ) and (R_b, γ), respectively, the opposite is true in the last two plots. There the measurements of (R_b, γ, α) and (β, γ, α) give strong constraints in the (β, R_t) and (R_b, R_t) plane, respectively. The last two plots illustrate also clearly that measuring only α and γ does not provide a strong constraint on the unitarity triangle.

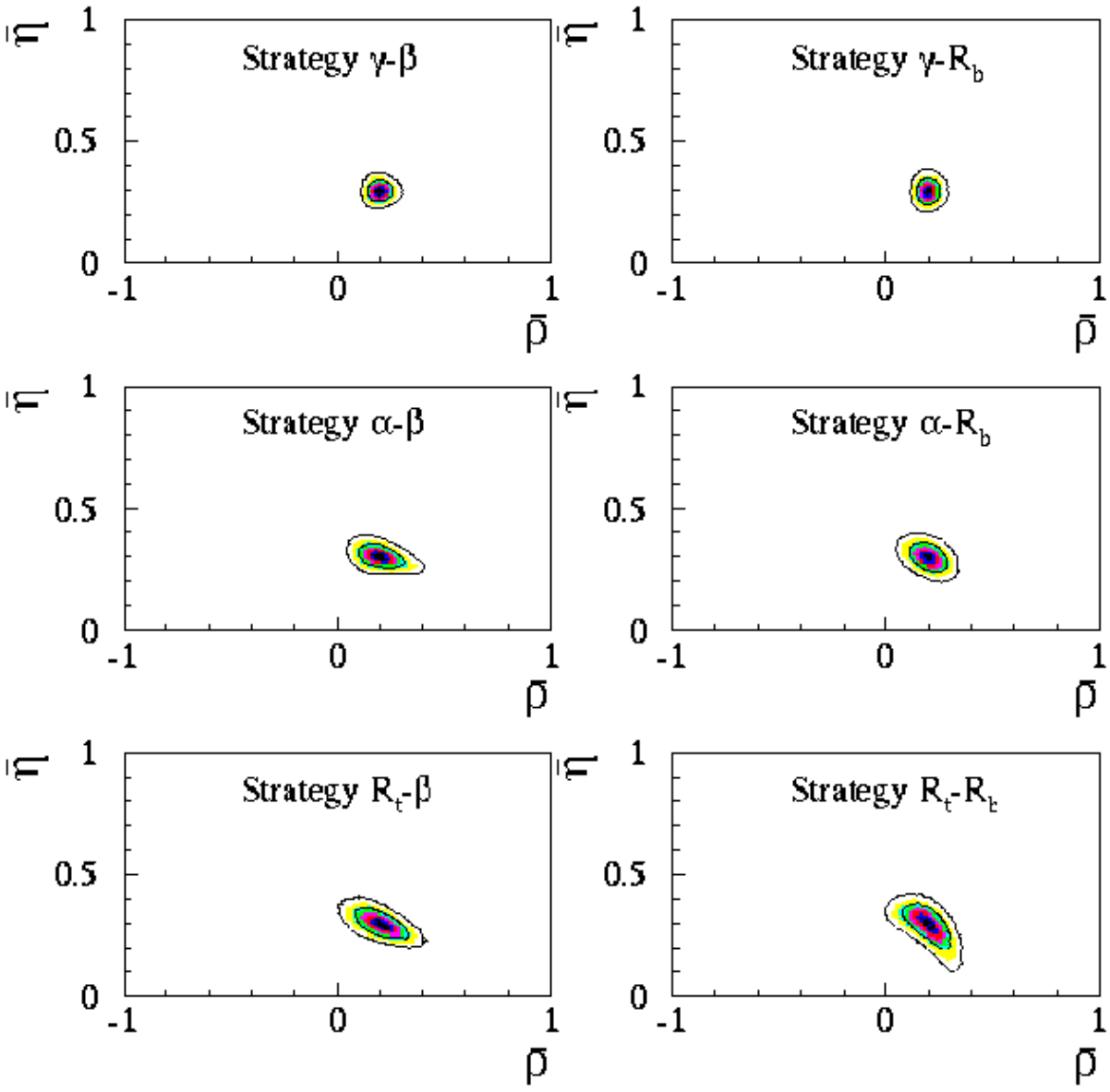

Fig. 6.3: *The plots show the allowed regions (68% and 95%) in the $(\bar{\varrho}, \bar{\eta})$ plane obtained from the leading strategies assuming that each variable is measured with* 10% *accuracy.*

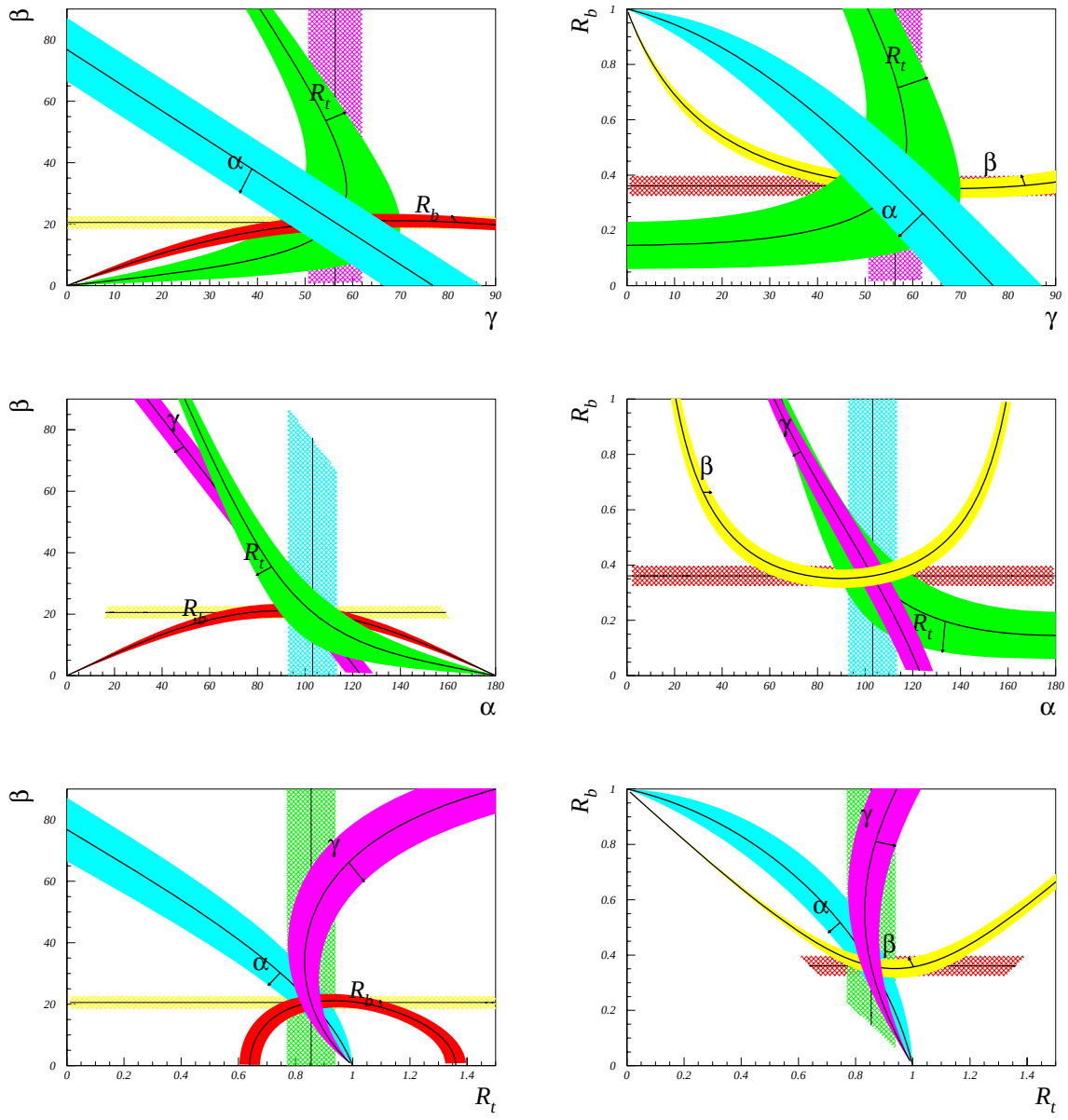

Fig. 6.4: *The plots show the different constraints (assuming a relative error of 10%) in the different planes corresponding to the leading stategies of equation 23. The small arrow indicates the range corresponding to an increase of 10% of the corresponding quantity.*

1.4. Results for the presently available strategies

At present the concrete results can be obtained only for the strategies (R_t, β), (R_b, R_t) and (R_b, β) as no direct measurements of γ and α are available.

The results for $\bar{\rho}$ and $\bar{\eta}$ for the three strategies in question are presented in Table 6.1 and in Figs. 6.5, 6.6 and 6.7. To obtain these results we have used the direct measurement of sin 2β [26], R_t as extracted from ΔM_d and $\Delta M_d/\Delta M_s$ by means of the formulae in [5,27] and R_b as extracted from $|V_{ub}|$.

Strategy	$\bar{\rho}$	$\bar{\eta}$
(R_t, β)	$0.157\ ^{+0.056}_{-0.054}$	$0.367\ ^{+0.036}_{-0.034}$
	[0.047-0.276]	[0.298-0.439]
(R_t, R_b)	$0.161^{+0.055}_{-0.057}$	$0.361\ ^{+0.041}_{-0.045}$
	[0.043-0.288]	[0.250-0.438]
(R_b, β)	$0.137\ ^{+0.135}_{-0.135}$	$0.373\ ^{+0.049}_{-0.063}$
	[-0.095-0.357]	[0.259-0.456]

Table 6.1: *Results for $\bar{\rho}$ and $\bar{\eta}$ for the three indicated strategies using the present knowledge summarized in Table 5.1 in Chapter 5. For the strategy (R_t, β), the solution compatible with the region selected by the R_b constraint has been considered. In squared brackets the 95% probability regions are also given.*

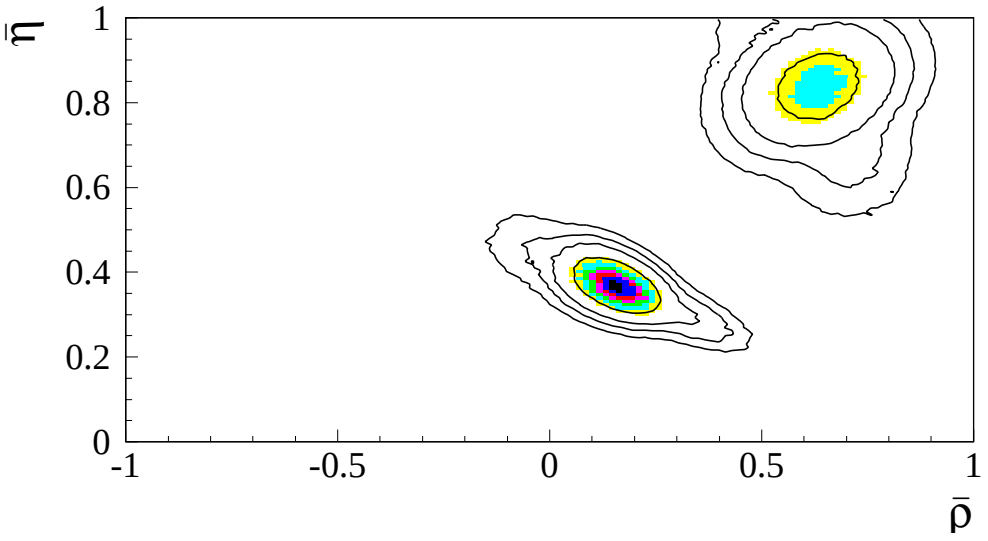

Fig. 6.5: *The plot shows the presently allowed regions (68%,95%,99% and 99.9%) in the $(\bar{\rho}, \bar{\eta})$ plane using the (R_t, β) strategy: the direct measurement of sin 2β and R_t from ΔM_d and $\Delta M_d/\Delta M_s$.*

The experimental and theoretical inputs are summarized in Chapter 4 It should be emphasized that these three presently available strategies are the weakest among the leading strategies listed in (23). Among them (R_t, β) and (R_t, R_b) appear to be superior to (R_b, β) at present. We expect that once ΔM_s has been measured and the error on $\sin 2\beta$ reduced, the strategy (R_t, β) will be leading among these three. Therefore in Fig. 6.8 we show how the presently available constraints look like in the (R_t, β) plane.

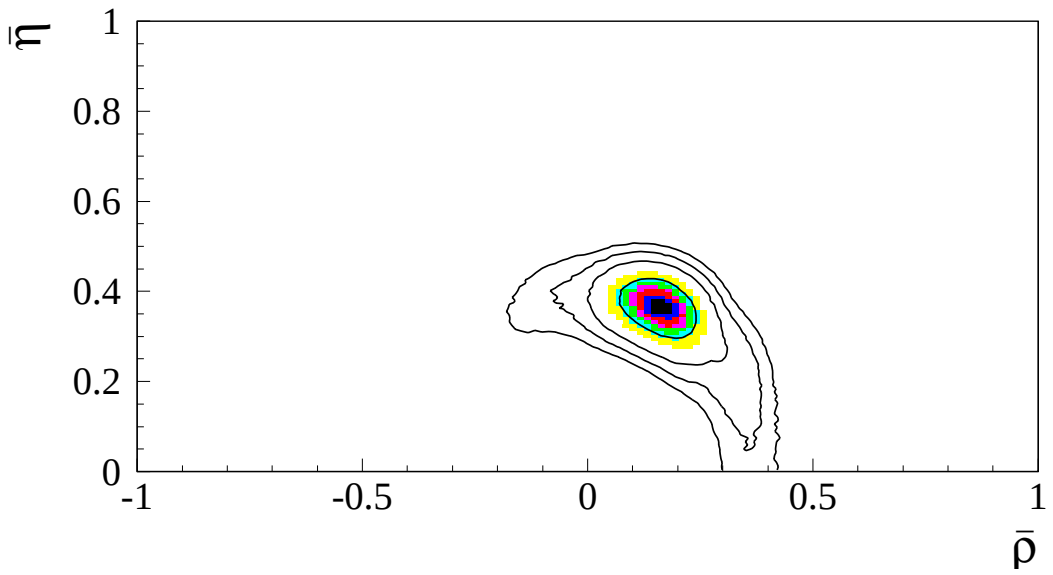

Fig. 6.6: *The plot shows the allowed regions (68%,95%,99% and 99.9%) in the $(\bar{\rho}, \bar{\eta})$ plane using the (R_t, R_b) strategy: R_t from ΔM_d and $\Delta M_d/\Delta M_s$ and R_b from $|V_{ub}|$.*

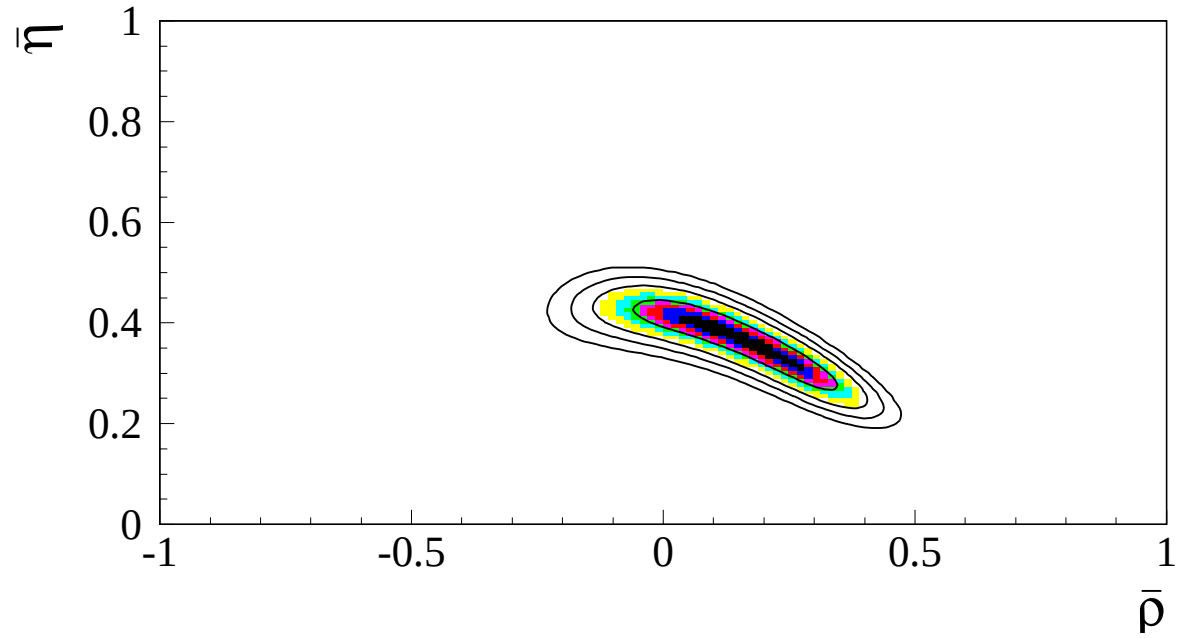

Fig. 6.7: *The plot shows the allowed regions (68%,95%,99% and 99.9%) in the $(\bar{\rho}, \bar{\eta})$ plane using the (R_b, β) strategy: direct measurement of sin 2β and R_b from $|V_{ub}/V_{cb}|$.*

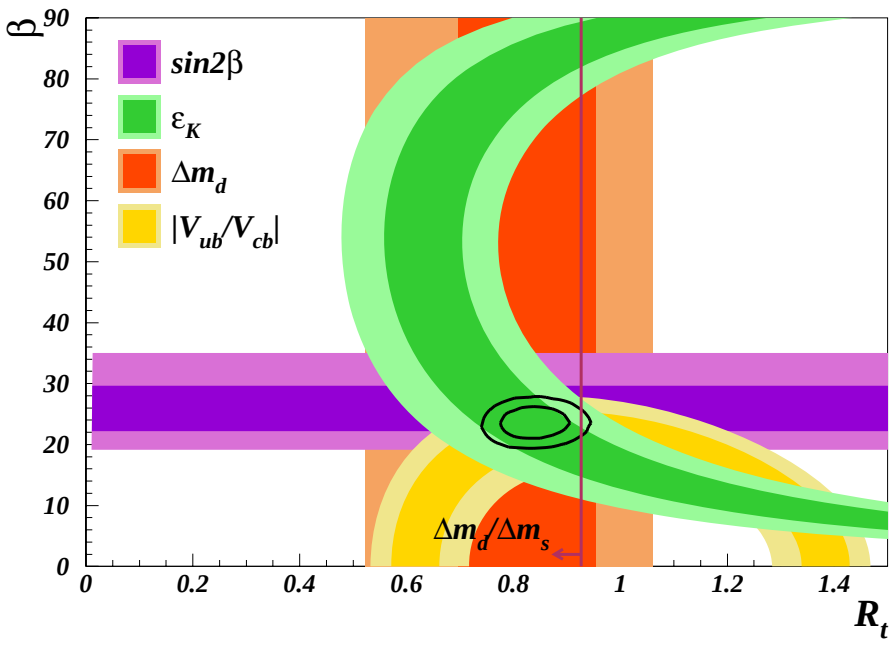

Fig. 6.8: *The plot shows the allowed regions (68% and 95%) in the (R_t, β) plane. Different constraints are also shown.*

1.5. Summary

We have presented a numerical analysis of the unitarity triangle from a different point of view, that emphasizes the role of different strategies in the precise determination of the unitarity triangle parameters. While we have found that the pairs (γ, β), (γ, R_b) and $(\gamma, \bar{\eta})$ are most efficient in determining $(\bar{\varrho}, \bar{\eta})$, we expect that the pair (R_t, β) will play the leading role in the UT fits in the coming years, in particular, when ΔM_s will be measured and the theoretical error on ξ decreased. For this reason we have proposed to plot available constraints on the CKM matrix in the (R_t, β) plane.

It will be interesting to compare in the future the allowed ranges for $(\bar{\varrho}, \bar{\eta})$ resulting from different strategies in order to see whether they are compatible with each other. Any discrepancies will signal the physics beyond the SM. We expect that the strategies involving γ will play a very important role in this comparison.

For the fundamental set of parameters in the quark flavour physics given in (2) we find within the SM

$$|V_{us}| = 0.2240 \pm 0.0036,\ |V_{cb}| = (41.3 \pm 0.7)10^{-3},\ R_t = 0.91 \pm 0.05,\ \beta = (22.4 \pm 1.4)^\circ,$$

where the errors represent one standard deviations and the result for β corresponds to $\sin 2\beta = 0.705 \pm 0.035$.

A complete analysis of the usefulness of a given strategy should also include the discussion of its experimental feasibility and theoretical cleanness. Extensive studies of these two issues can be found in [1–5] and in these proceedings. Again among various strategies, the (R_t, β) strategy is exceptional as the theoretical uncertainties in the determination of these two variables are small and the corresponding experiments are presently feasible. In the long run, when γ will be cleanly measured in $\mathrm{B}_l \to \mathrm{D}\pi$ and $\mathrm{B}_s \to \mathrm{D}_s\mathrm{K}$ decays and constrained through other decays as reviewed in the following sections, we expect that the strategy (γ, β) will take over the leading role. Eventually the independent direct determinations of the five variables in question will be crucial for the tests of the SM and its extensions.

2. Radiative rare B decays

A. Ali and M. Misiak

The transitions $b \to s(d)\gamma$ and $b \to s(d)\ell^+\ell^-$ receive sizable contributions from loops involving the top quark (Fig. 6.9). Their dependence on V_{ts} and V_{td} may be used to test unitarity of the CKM matrix and to overconstrain the Wolfenstein parameters $\bar\rho$ and $\bar\eta$. The considered transitions manifest themselves in exclusive $\overline{\rm B}$-meson decays like $\overline{\rm B} \to {\rm K}^\star\gamma$, $\overline{\rm B} \to {\rm K}^*\ell^+\ell^-$, $\overline{\rm B} \to \rho\gamma$ and $\overline{\rm B} \to \rho\ell^+\ell^-$. The corresponding inclusive decays $\overline{\rm B} \to X_{s(d)}\gamma$ and $\overline{\rm B} \to X_{s(d)}\ell^+\ell^-$ are experimentally more challenging, but the theoretical predictions are significantly more accurate, thanks to the use of OPE and HQET. The exclusive processes remain interesting due to possible new physics effects in observables other than just the total branching ratios (photon polarization, isospin- and CP-asymmetries), as well as due to information they provide on non-perturbative form-factors. This information is particularly required in analyzing exclusive modes generated by the $b \to d\gamma$ transition, in which case there is little hope for an inclusive measurement.

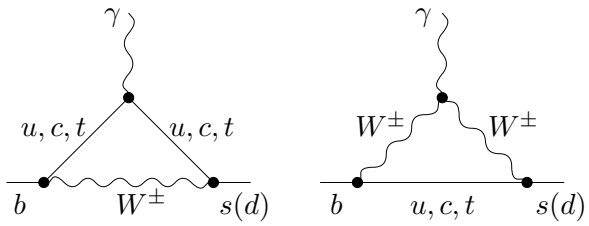

Fig. 6.9: *Leading-order Feynman diagrams for $b \to s(d)\gamma$ in the SM.*

In this section we discuss briefly the generic features of the CKM phenomenology in the considered rare B-decays. The transitions $b \to s\gamma$ and $b \to s\ell^+\ell^-$ involve the CKM matrix elements from the second and third column of this matrix, with the unitarity constraint taking the form $\sum_{u,c,t}\lambda_i = 0$, with $\lambda_i = V_{ib}V_{is}^*$. This equation yields a unitarity triangle which is highly squashed, as one of the sides of this triangle $\lambda_u = V_{ub}V_{us}^* \simeq A\lambda^4(\bar\rho - i\bar\eta)$ is doubly Cabibbo suppressed, compared to the other two sides $\lambda_c \simeq -\lambda_t = A\lambda^2 + ...$ Hence, the transitions $b \to s\gamma$ and $b \to s\ell^+\ell^-$ are not expected to yield useful information on the parameters $\bar\rho$ and $\bar\eta$, which define the apex of the unitarity triangle of current interest (see Chapt. 1). The test of unitarity for the $b \to s$ transitions in rare B-decays lies in checking the relation $\lambda_t \simeq -\lambda_c$, which holds up to corrections of order λ^2.

The impact of the decays $b \to d\gamma$ and $b \to d\ell^+\ell^-$ on the CKM phenomenology is, however, quite different. These transitions involve the CKM matrix elements in the first and third column, with the unitarity constraints taking the form $\sum_{u,c,t}\xi_i = 0$, with $\xi_i = V_{ib}V_{id}^*$. Now, all three matrix elements are of order λ^3, with $\xi_u \simeq A\lambda^3(\bar\rho - i\bar\eta)$, $\xi_c \simeq -A\lambda^3$, and $\xi_t \simeq A\lambda^3(1 - \bar\rho - i\bar\eta)$. This equation leads to the same unitarity triangle as studied through the constraints V_{ub}/V_{cb}, ΔM_{B_d} (or $\Delta M_{B_d}/\Delta M_{B_s}$). Hence, the transitions $b \to d\gamma$ and $b \to d\ell^+\ell^-$ lead to complementary constraints on the CKM parameters $\bar\rho$ and $\bar\eta$, as illustrated in the following. Thus, the role of rare B-decays is that they provide complementary constraints on the CKM matrix elements, hence test the CKM unitarity, but they also constrain extensions of the Standard Model, and by that token can act as harbinger of new physics.

A theoretical framework for analyzing the $b \to s\gamma$ transition is set by the effective interaction Hamiltonian

$$\mathcal{H}_{\rm eff} = -\frac{4G_F}{\sqrt{2}}V_{ts}^*V_{tb}\sum_{i=1}^{8}C_i(\mu)Q_i. \qquad (24)$$

The generic structure of the operators Q_i is as follows:

$$Q_i = \begin{cases} (\bar{s}\Gamma_i c)(\bar{c}\Gamma'_{\underline{i}} b), & i = 1, 2, \\ (\bar{s}\Gamma_i b)\sum_q (\bar{q}\Gamma'_{\underline{i}} q), & i = 3, 4, 5, 6, \qquad (q = u, d, s, c, b) \\ \frac{e m_b}{16\pi^2}\bar{s}_L \sigma^{\mu\nu} b_R F_{\mu\nu}, & i = 7, \\ \frac{g_s m_b}{16\pi^2}\bar{s}_L \sigma^{\mu\nu} T^a b_R G^a_{\mu\nu}, & i = 8. \end{cases} \tag{25}$$

Here, Γ_i and Γ'_i denote various combinations of the colour and Dirac matrices. Everything that is not important for $b \to s\gamma$ at the leading order in $\alpha_{\rm em}$, m_b/m_W, m_s/m_b and V_{ub}/V_{cb} has been neglected in Eq. (24).

Perturbative calculations (see Ref. [28] and refs. therein) are used to find the Wilson coefficients in the $\overline{\rm MS}$ scheme, at the renormalization scale $\mu_b \sim m_b$

$$C_i(\mu_b) = C_i^{(0)}(\mu_b) + \frac{\alpha_s(\mu_b)}{4\pi} C_i^{(1)}(\mu_b) + \left(\frac{\alpha_s(\mu_b)}{4\pi}\right)^2 C_i^{(2)}(\mu_b) + \ldots . \tag{26}$$

Here, $C_i^{(n)}(\mu_b)$ depend on α_s only via the ratio $\eta \equiv \alpha_s(\mu_0)/\alpha_s(\mu_b)$, where $\mu_0 \sim m_W$. In the Leading Order (LO) calculations, everything but $C_i^{(0)}(\mu_b)$ is neglected in Eq. (26). At the Next-to-Leading Order (NLO), one takes $C_i^{(1)}(\mu_b)$ into account. The Wilson coefficients contain information on the short-distance QCD effects due to hard gluon exchanges between the quark lines of the leading one-loop electroweak diagrams (Fig. 6.9). Such effects enhance the perturbative branching ratio $\mathcal{B}(b \to s\gamma)$ by roughly a factor of three [29].

The same formalism applies to $b \to d\gamma$, too. The corresponding operators Q_i are obtained by replacing $\bar{s} \to \bar{d}$ in Eq. (25), and by including the u-quark analogues of $Q_{1,2}$. The latter operators are no longer CKM-suppressed. The matching conditions $C_i(\mu_0)$ and the solutions of the RG equations, yielding $C_i(\mu_b)$, coincide with those needed for the process $b \to s\gamma$.

2.1. Inclusive $\overline{\rm B} \to X_{s(d)}\gamma$ decay

The inclusive branching ratio $\mathcal{B}(\overline{\rm B} \to X_s\gamma)$ was measured for the first time by CLEO in 1995 [30]. The present world averages

$$\mathcal{B}(\overline{\rm B} \to X_s\gamma \ \ (E_\gamma > 1.6 \text{ GeV})) \ = \ \left(3.28\ ^{+0.41}_{-0.36}\right) \times 10^{-4}, \tag{27}$$

$$\mathcal{B}(\overline{\rm B} \to X_s\gamma \ \ (E_\gamma > \ \tfrac{1}{20} m_b \ )) \ = \ \left(3.40\ ^{+0.42}_{-0.37}\right) \times 10^{-4} \tag{28}$$

are found from the following four measurements

$$\mathcal{B}(\overline{\rm B} \to X_s\gamma\,(E_\gamma > \tfrac{1}{20} m_b)) \ = \ \left[3.88 \pm 0.36_{\rm stat} \pm 0.37_{\rm sys}\ \left(^{+0.43}_{-0.23}\right)_{\rm theory}\right] \times 10^{-4}, \quad \text{(BABAR [31])},$$

$$\mathcal{B}(\overline{\rm B} \to X_s\gamma\,(E_\gamma > \tfrac{1}{20} m_b)) \ = \ \left[3.21 \pm 0.43_{\rm stat} \pm 0.27_{\rm sys}\ \left(^{+0.18}_{-0.10}\right)_{\rm theory}\right] \times 10^{-4}, \quad \text{(CLEO [32])},$$

$$\mathcal{B}(\overline{\rm B} \to X_s\gamma\,(E_\gamma > \tfrac{1}{20} m_b)) \ = \ \left[3.36 \pm 0.53_{\rm stat} \pm 0.42_{\rm sys}\ \left(^{+0.50}_{-0.54}\right)_{\rm theory}\right] \times 10^{-4}, \quad \text{(BELLE [33])},$$

$$\mathcal{B}(b \to s\gamma) \ = \ (3.11 \pm 0.80_{\rm stat} \pm 0.72_{\rm sys}) \times 10^{-4}, \quad \text{(ALEPH [34])},$$

in which full correlation of the "theory" errors has been assumed. The averages (27) and (28) are perfectly consistent with the SM predictions [35,36]

$$\mathcal{B}(\overline{\rm B} \to X_s\gamma \ \ (E_\gamma > 1.6 \text{ GeV}))_{\rm SM} \ = \ (3.57 \pm 0.30) \times 10^{-4}, \tag{29}$$

$$\mathcal{B}(\overline{\rm B} \to X_s\gamma \ \ (E_\gamma > \ \tfrac{1}{20} m_b \ ))_{\rm SM} \ = \ 3.70 \times 10^{-4}. \tag{30}$$

By convention, contributions to $\overline{\rm B} \to X_s\gamma$ from the intermediate real ψ and ψ' are treated as background, while all the continuum $c\bar{c}$ states are included assuming quark-hadron duality. Non-continuum states other than ψ and ψ' have negligible effect.

When the theoretical result (29) is reevaluated without use of the CKM unitarity in the dominant contributions (i.e. everywhere except for three small ($< 2.5\%$) corrections), comparison with the experiment (27) leads to the following constraint on the CKM matrix elements

$$| \, 1.69 \, \lambda_u \, + \, 1.60 \, \lambda_c \, + \, 0.60 \, \lambda_t \, | \; = \; (\, 0.94 \; \pm \; 0.07 \,) \, |V_{cb}|. \tag{31}$$

After using the numerical values of $\lambda_c \simeq |V_{cb}| = (41.0 \pm 2.1) \times 10^{-3}$ and λ_u from the PDG [37], this equation yields $\lambda_t \simeq -47 \times 10^{-3}$ with an error of around 17%. This is consistent with the unitarity relation $\lambda_c \simeq -\lambda_t$. This relation, however, holds in the SM with much better accuracy than what has just been derived from Eq. (31). On the other hand, if the SM with 3 generations is not valid, Eq. (31) is not valid either.

Contrary to $\mathcal{B}(\overline{\rm B} \to X_s\gamma)$, the branching ratio $\mathcal{B}(\overline{\rm B} \to X_d\gamma)$, if measured, would provide us with useful constraints on the Wolfenstein parameters $\bar{\rho}$ and $\bar{\eta}$. After using the CKM unitarity, it can be written as

$$\mathcal{B}(\overline{\rm B} \to X_d\gamma) = \frac{|\xi_t|^2}{|V_{cb}|^2} D_t + \frac{|\xi_u|^2}{|V_{cb}|^2} D_u + \frac{Re(\xi_t^* \xi_u)}{|V_{cb}|^2} D_r + \frac{Im(\xi_t^* \xi_u)}{|V_{cb}|^2} D_i \, . \tag{32}$$

The factors ξ_i have been defined earlier. The quantities D_a ($a = t, u, r, i$), which depend on various input parameters such as m_t, m_b, m_c, μ_b and α_s, are given in Ref. [38]. Typical values of these quantities (in units of λ^4) are: $D_t = 0.154, D_u = 0.012, D_r = -0.028$, and $D_i = 0.042$, corresponding to the scale $\mu = 5$ GeV, and the pole quark mass ratio $m_c/m_b = 0.29$. The charge-conjugate averaged branching ratio $\langle \mathcal{B}(B \to X_d\gamma) \rangle$ is obtained by discarding the last term on the right hand side of Eq. (32).

It is convenient to consider the ratio

$$\begin{aligned} \frac{\langle \mathcal{B}(B \to X_d\gamma) \rangle}{\langle \mathcal{B}(B \to X_s\gamma) \rangle} \; &= \; \frac{|\xi_t|^2}{|\lambda_t|^2} + \frac{D_u}{D_t} \frac{|\xi_u|^2}{|\lambda_t|^2} + \frac{D_r}{D_t} \frac{Re(\xi_t^* \xi_u)}{|\lambda_t|^2} \\ &= \; \lambda^2 \left[(1-\bar{\rho})^2 + \bar{\eta}^2 + \frac{D_u}{D_t} (\bar{\rho}^2 + \bar{\eta}^2) + \frac{D_r}{D_t} (\bar{\rho}(1-\bar{\rho}) - \bar{\eta}^2) \right] + O(\lambda^4) \\ &\simeq \; 0.036 \quad [\text{for } (\bar{\rho}, \bar{\eta}) = (0.22, 0.35)] \; . \end{aligned} \tag{33}$$

The above result together with Eq. (30) implies $\langle \mathcal{B}(\overline{\rm B} \to X_d\gamma) \rangle \simeq 1.3 \times 10^{-5}$ in the SM. Thus, with $O(10^8)$ $\rm B\overline{B}$ events already collected at the B factories, $O(10^3)$ $b \to d\gamma$ decays are already produced. However, extracting them from the background remains a non-trivial issue.

Apart from the total branching ratios, the inclusive decays $\overline{\rm B} \to X_{s(d)}\gamma$ provide us with other observables that might be useful for the CKM phenomenology. First, as discussed in Chapt. 3, the $\overline{\rm B} \to X_s\gamma$ photon spectrum is used to extract the HQET parameters that are crucial for the determination of V_{ub} and $|V_{cb}|$. Second, CP-asymmetries contain information on the CKM phase. These asymmetries can be either direct (i.e. occur in the decay amplitudes) or induced by the $\rm B\overline{B}$ mixing.

The mixing-induced CP-asymmetries in $\overline{\rm B} \to X_{s(d)}\gamma$ are very small ($\mathcal{O}(m_{s(d)}/m_b)$) in the SM, so long as the photon polarizations are summed over. It follows from the particular structure of the dominant operator Q_7 in Eq. (25), which implies that photons produced in the decays of B and $\overline{\rm B}$ have opposite *circular* polarizations. Thus, in the absence of new physics, observation of the mixing-induced CP-violation would require selecting particular *linear* photon polarization with the help of matter-induced photon conversion into e^+e^- pairs [39].

The SM predictions for the direct CP-asymmetries read

$$\mathcal{A}_{\rm CP}({\rm B} \to X_s\gamma) \equiv \frac{\Gamma(\overline{\rm B} \to X_s\gamma) - \Gamma({\rm B} \to X_{\overline{s}}\gamma)}{\Gamma(\overline{\rm B} \to X_s\gamma) + \Gamma({\rm B} \to X_{\overline{s}}\gamma)} \simeq \frac{{\rm Im}(\lambda_t^* \lambda_u) D_i}{|\lambda_t|^2 \, D_t} \; \simeq \; 0.27 \, \lambda^2 \bar{\eta} \; \sim \; 0.5\%, \tag{34}$$

$$\mathcal{A}_{\rm CP}(\mathrm{B}\to \mathrm{X_d}\gamma) \equiv \frac{\Gamma(\overline{\mathrm{B}}\to \mathrm{X_d}\gamma)-\Gamma(\mathrm{B}\to \mathrm{X_{\overline{d}}}\gamma)}{\Gamma(\overline{\mathrm{B}}\to \mathrm{X_d}\gamma)+\Gamma(\mathrm{B}\to \mathrm{X_{\overline{d}}}\gamma)} \simeq \frac{\mathrm{Im}(\xi_{\rm t}^*\xi_{\rm u})\mathrm{D_i}}{|\xi_{\rm t}|^2\,\mathrm{D_t}} \;\simeq\; \frac{-0.27\,\bar\eta}{(1-\bar\rho)^2+\bar\eta^2} \sim -13\%, \quad (35)$$

where $\bar\rho = 0.22$ and $\bar\eta = 0.35$ have been used in the numerical estimates. As stressed in Ref. [38], there is considerable scale uncertainty in the above predictions, which would require a NLO calculation of D_i to be brought under theoretical control. The smallness of $\mathcal{A}_{\rm CP}(\mathrm{B}\to X_s\gamma)$ is caused by three suppression factors: λ_u/λ_t, α_s/π and m_c^2/m_b^2. This SM prediction is consistent with the CLEO bound $-0.27 < \mathcal{A}_{\rm CP}(\mathrm{B}\to X_s\gamma) < +0.10$ at 95% C.L. [40].

No experimental limit has been announced so far on either the branching ratio $\mathcal{B}(\overline{\mathrm{B}}\to X_d\gamma)$ or the CP asymmetry $\mathcal{A}_{\rm CP}(\mathrm{B}\to X_d\gamma)$. While experimentally challenging, the measurement of these quantities might ultimately be feasible at the B-factories which would provide valuable and complementary constraints on the CKM parameters.

2.2. Exclusive radiative B decays

The effective Hamiltonian sandwiched between the B-meson and a single meson state (say, $\mathrm{K^*}$ or ρ in the transitions $\mathrm{B}\to(\mathrm{K^\star},\rho)\gamma$) can be expressed in terms of matrix elements of bilinear quark currents inducing heavy-light transitions. These matrix elements are dominated by strong interactions at small momentum transfer and cannot be calculated perturbatively. They have to be obtained from a non-perturbative method, such as the lattice-QCD and the QCD sum rule approach. As the inclusive branching ratio $\mathcal{B}(\mathrm{B}\to X_s\gamma)$ in the SM is in striking agreement with data, the role of the branching ratio $\mathcal{B}(\mathrm{B}\to \mathrm{K^*}\gamma)$ is that it will determine the form factor governing the electromagnetic penguin transition, $T_1^{\mathrm{K^*}}(0)$.

To get a firmer theoretical prediction on the decay rate, one has to include the perturbative QCD radiative corrections arising from the vertex renormalization and the hard spectator interactions. To incorporate both types of QCD corrections, it is helpful to use a factorization Ansatz for the heavy-light transitions at large recoil and at leading order in the inverse heavy meson mass, introduced in Ref. [41]. Exemplified here by the $\mathrm{B}\to V\gamma^*$ transition, a typical amplitude $f_k(q^2)$ can be written in the form

$$f_k(q^2) = C_{\perp k}\xi_\perp(q^2) + C_{\parallel k}\xi_\parallel(q^2) + \Phi_B \otimes T_k(q^2)\otimes \Phi_V, \quad (36)$$

where $\xi_\perp(q^2)$ and $\xi_\parallel(q^2)$ are the two independent form factors in these decays remaining in the heavy quark and large energy limit; $T_k(q^2)$ is a hard-scattering kernel calculated to $O(\alpha_s)$; Φ_B and Φ_V are the light-cone distribution amplitudes of the B- and vector-meson, respectively, the symbol $\otimes$ denotes convolution with T_k, and $C_k = 1 + O(\alpha_s)$ are the hard vertex renormalization coefficients. In a number of papers [42–44], the factorization Ansatz of Eq. (36) is shown to hold in $O(\alpha_s)$, leading to the explicit $O(\alpha_s)$ corrections to the amplitudes $\mathrm{B}\to V\gamma$ and $\mathrm{B}\to V\ell^+\ell^-$.

Experiment	$\mathcal{B}_{\rm exp}(\mathrm{B^0}(\overline{\mathrm{B}}^0)\to \mathrm{K^{*0}}(\overline{\mathrm{K}}^{*0})+\gamma)$	$\mathcal{B}_{\rm exp}(\mathrm{B^\pm}\to \mathrm{K^{*\pm}}+\gamma)$
CLEO [45]	$(4.55^{+0.72}_{-0.68}\pm 0.34)\times 10^{-5}$	$(3.76^{+0.89}_{-0.83}\pm 0.28)\times 10^{-5}$
BELLE [46]	$(3.91\pm 0.23\pm 0.25)\times 10^{-5}$	$(4.21\pm 0.35\pm 0.31)\times 10^{-5}$
BABAR [47]	$(4.23\pm 0.40\pm 0.22)\times 10^{-5}$	$(3.83\pm 0.62\pm 0.22)\times 10^{-5}$

Table 6.2: *Experimental branching ratios for the decays* $\mathrm{B^0}(\overline{\mathrm{B}}^0)\to \mathrm{K^{*0}}(\overline{\mathrm{K}}^{*0})\gamma$ *and* $\mathrm{B^\pm}\to \mathrm{K^{*\pm}}\gamma$.

We first discuss the exclusive decay $\mathrm{B}\to \mathrm{K^*}\gamma$, for which data from the CLEO, BABAR, and BELLE measurements are available and given in Table 6.2 for the charge conjugated averaged branching ratios. We note that the BELLE data alone has reached a statistical accuracy of better than 10%.

Adding the statistical and systematic errors in quadrature, we get the following world averages for the branching ratios:

$$\begin{aligned}\mathcal{B}(\mathrm{B}^0 \to \mathrm{K}^{*0}\gamma) &= (4.08 \pm 0.26) \times 10^{-5}\,, \\ \mathcal{B}(\mathrm{B}^\pm \to \mathrm{K}^\pm\gamma) &= (4.05 \pm 0.35) \times 10^{-5}\,. \end{aligned} \tag{37}$$

The two branching ratios are completely consistent with each other, ruling out any significant isospin breaking in the respective decay widths, which is not expected in the SM [48] but anticipated in some beyond-the-SM scenarios. Likewise, the CP asymmetry in $\mathrm{B} \to \mathrm{K}^*\gamma$ decays, which in the SM is expected to be of the same order of magnitude as for the inclusive decay, namely $\mathcal{A}_{\rm CP}(\mathrm{B} \to \mathrm{K}^*\gamma) \le 1\%$, is completely consistent with the present experimental bounds, the most stringent of which is posted by the BELLE collaboration [46]: $\mathcal{A}_{\rm CP}(\mathrm{B} \to \mathrm{K}^*\gamma) = -0.022 \pm 0.048 \pm 0.017$. In view of this, we shall concentrate in the following on the branching ratios in $\mathrm{B} \to \mathrm{K}^*\gamma$ decays to determine the form factors.

Ignoring the isospin differences in the decay widths of $\mathrm{B} \to \mathrm{K}^*\gamma$ decays, the branching ratios for $\mathrm{B}^\pm \to \mathrm{K}^{*\pm}\gamma$ and $\mathrm{B}^0(\overline{\mathrm{B}}^0) \to \mathrm{K}^{*0}(\overline{\mathrm{K}}^{*0})\gamma$ can be expressed as:

$$\begin{aligned}\mathcal{B}_{\rm th}(\mathrm{B} \to \mathrm{K}^*\gamma) &= \tau_B\, \Gamma_{\rm th}(\mathrm{B} \to \mathrm{K}^*\gamma) \\ &= \tau_B\, \frac{G_F^2 \alpha |V_{tb}V_{ts}^*|^2}{32\pi^4}\, m_{b,\rm pole}^2\, M^3\, \left[\xi_\perp^{(\mathrm{K}^*)}\right]^2 \left(1 - \frac{M_{\mathrm{K}^*}^2}{M^2}\right)^3 \left|C_7^{(0)\rm eff} + A^{(1)}(\mu)\right|^2 ,\end{aligned} \tag{38}$$

where G_F is the Fermi coupling constant, $\alpha = \alpha(0) = 1/137$ is the fine-structure constant, $m_{b,\rm pole}$ is the pole b-quark mass, M and M_{K^*} are the B- and K*-meson masses, and τ_B is the lifetime of the B^0- or B^+-meson. The quantity $\xi_\perp^{K^*}$ is the soft part of the form factor $T_1^{K^*}(q^2 = 0)$ in the $\mathrm{B} \to \mathrm{K}^*\gamma$ transition, to which the symmetries in the large energy limit apply. The two form factors $\xi_\perp^{K^*}$ and $T_1^{K^*}(q^2 = 0)$ are related by perturbative $(O(\alpha_s))$ and power $(O(\Lambda_{\rm QCD}/m_b))$ corrections [50]. Thus, one could have equivalently expressed the $O(\alpha_s)$-corrected branching ratio for $\mathrm{B} \to \mathrm{K}^*\gamma$ in terms of the QCD form factor $T_1^{K^*}(q^2 = 0)$, and a commensurately modified expression for the explicit $O(\alpha_s)$ correction in the above equation [43]. In any case, the form factor $T_1^{K^*}(q^2 = 0)$ or $\xi_\perp^{K^*}$ has to be determined by a non-perturbative method.

The function $A^{(1)}$ in Eq. (38) can be decomposed into the following three components:

$$A^{(1)}(\mu) = A_{C_7}^{(1)}(\mu) + A_{\rm ver}^{(1)}(\mu) + A_{\rm sp}^{(1)K^*}(\mu_{\rm sp})\,. \tag{39}$$

Here, $A_{C_7}^{(1)}$ and $A_{\rm ver}^{(1)}$ are the $O(\alpha_s)$ (i.e. NLO) corrections due to the Wilson coefficient $C_7^{\rm eff}$ and in the $b \to s\gamma$ vertex, respectively, and $A_{\rm sp}^{(1)K^*}$ is the $\mathcal{O}(\alpha_s)$ hard-spectator correction to the $\mathrm{B} \to \mathrm{K}^*\gamma$ amplitude computed in [42–44]. This formalism leads to the following branching ratio for $\mathrm{B} \to \mathrm{K}^*\gamma$ decays:

$$\mathcal{B}_{\rm th}(\mathrm{B} \to \mathrm{K}^*\gamma) \simeq (7.2 \pm 1.1) \times 10^{-5} \left(\frac{\tau_B}{1.6\ \mathrm{ps}}\right) \left(\frac{m_{b,\rm pole}}{4.65\ \mathrm{GeV}}\right)^2 \left(\frac{\xi_\perp^{(K^*)}}{0.35}\right)^2 , \tag{40}$$

where the default values of the three input parameters are made explicit, with the rest of the theoretical uncertainties indicated numerically; the default value for the form factor $\xi_\perp^{(K^*)}(0)$ is based on the light-cone QCD sum rule estimates [49].

The non-perturbative parameter $\xi_\perp^{(K^*)}(0)$ can now be extracted from the data on the branching ratios for $\mathrm{B} \to \mathrm{K}^*\gamma$ decays, given in Eq. (37), leading to the current world average $\langle \mathcal{B}(\mathrm{B} \to \mathrm{K}^*\gamma)\rangle = (4.06 \pm 0.21) \times 10^{-5}$, which then yields

$$\bar{\xi}_\perp^{(K^*)}(0) = 0.25 \pm 0.04, \qquad \left[\bar{T}_1^{(K^*)}(0, \bar{m}_b) = 0.27 \pm 0.04\right] , \tag{41}$$

where we have used the $O(\alpha_s)$ relation between the effective theory form factor $\xi_\perp^{(K^*)}(0)$ and the full QCD form factor $T_1^{(K^*)}(0,\bar{m}_b)$, worked out in [50]. This estimate is significantly smaller than the corresponding predictions from the QCD sum rules analysis $T_1^{(K^*)}(0) = 0.38 \pm 0.06$ [51,49] and from the lattice simulations $T_1^{(K^*)}(0) = 0.32^{+0.04}_{-0.02}$ [52]. Clearly, more work is needed to calculate the $\mathrm{B} \to \mathrm{K}^*\gamma$ decay form factors precisely.

As already discussed, inclusive $b \to d\gamma$ transitions are not yet available experimentally. This lends great importance to the exclusive decays, such as $\mathrm{B} \to \rho\gamma, \omega\gamma$, to whose discussion we now turn. These decays differ from their $\mathrm{B} \to \mathrm{K}^*\gamma$ counterparts, in that the annihilation contributions are not Cabibbo-suppressed. In particular, the isospin-violating ratios and CP-asymmetries in the decay rates involving the decays $\mathrm{B}^\pm \to \rho^\pm\gamma$ and $\mathrm{B}^0(\overline{\mathrm{B}^0}) \to \rho^0\gamma$ are sensitive to the penguin and annihilation interference in the amplitudes.

We recall that ignoring the perturbative QCD corrections to the penguin amplitudes the ratio of the branching ratios for the charged and neutral B-meson decays in $\mathrm{B} \to \rho\gamma$ can be written as [53,54]

$$\frac{\mathcal{B}(\mathrm{B}^- \to \rho^-\gamma)}{2\mathcal{B}(\mathrm{B}^0 \to \rho^0\gamma)} \simeq \left| 1 + \epsilon_A \mathrm{e}^{i\phi_A} \frac{V_{ub}V_{ud}^*}{V_{tb}V_{td}^*} \right|^2 , \tag{42}$$

where $\epsilon_A \mathrm{e}^{i\phi_A}$ includes the dominant W-annihilation and possible sub-dominant long-distance contributions. We shall use the value $\epsilon_A \simeq +0.30 \pm 0.07$ for the decays $\mathrm{B}^\pm \to \rho^\pm\gamma$ [55,56], obtained assuming factorization of the annihilation amplitude. The corresponding quantity for the decays $\mathrm{B}^0 \to \rho^0\gamma$ is suppressed due to the electric charge of the spectator quark in B^0 as well as by the unfavourable colour factors. Typical estimates for ϵ_A in $\mathrm{B}^0 \to \rho^0\gamma$ put it at around 5% [55,56]. The strong interaction phase ϕ_A vanishes in $\mathcal{O}(\alpha_s)$ in the chiral limit and to leading twist [54], giving theoretical credibility to the factorization-based estimates. Thus, in the QCD factorization approach the phase ϕ_A is expected to be small and one usually sets $\phi_A = 0$. Of course, $O(\alpha_s)$ vertex and hard spectator corrections generate non-zero strong phases, as discussed later. The isospin-violating correction depends on the unitarity triangle phase α due to the relation:

$$\frac{V_{ub}V_{ud}^*}{V_{tb}V_{td}^*} = -\left| \frac{V_{ub}V_{ud}^*}{V_{tb}V_{td}^*} \right| \mathrm{e}^{i\alpha} . \tag{43}$$

The NLO corrections to the branching ratios of the exclusive decays $\mathrm{B}^\pm \to \rho^\pm\gamma$ and $\mathrm{B}^0 \to \rho^0\gamma$ are derived very much along the same lines as outlined for the decays $\mathrm{B} \to \mathrm{K}^*\gamma$. Including the annihilation contribution, the $\mathrm{B} \to \rho\gamma$ branching ratios, isospin- and CP-violating asymmetries are given in [43,44].

Concentrating on the decays $\mathrm{B}^\pm \to \rho^\pm\gamma$, the expression for the ratio $R(\rho\gamma/\mathrm{K}^*\gamma) \equiv \mathcal{B}(B^\pm \to \rho^\pm\gamma)/\mathcal{B}(\mathrm{B}^\pm \to \mathrm{K}^{*\pm}\gamma)$ (where an average over the charge-conjugated modes is implied) can be written as [44]

$$R(\rho\gamma/\mathrm{K}^*\gamma) = S_\rho \left| \frac{V_{td}}{V_{ts}} \right|^2 \frac{(M_B^2 - M_\rho^2)^3}{(M_B^2 - M_{K^*}^2)^3} \zeta^2 (1 + \Delta R) , \tag{44}$$

where $S_\rho = 1$ for the $\rho^\pm$ meson, and $\zeta = \xi_\perp^\rho(0)/\xi_\perp^{K^*}(0)$, with $\xi_\perp^\rho(0)(\xi_\perp^{K^*}(0))$ being the form factors (at $q^2 = 0$) in the effective heavy quark theory for the decays $\mathrm{B} \to \rho\gamma(\mathrm{B} \to \mathrm{K}^*\gamma)$. The quantity $(1 + \Delta R)$ entails the explicit $O(\alpha_s)$ corrections, encoded through the functions $A_{\mathrm{R}}^{(1)K^*}$, $A_{\mathrm{R}}^{(1)t}$ and A_{R}^u, and the long-distance contribution L_{R}^u. For the decays $\mathrm{B}^\pm \to \rho^\pm\gamma$ and $\mathrm{B}^\pm \to \mathrm{K}^{*\pm}\gamma$, this can be written after charge conjugated averaging as

$$\begin{aligned} 1 + \Delta R^\pm &= \left| \frac{C_7^d + \lambda_u L_R^u}{C_7^s} \right|^2 \left(1 - 2A_R^{(1)K^*} \frac{\Re C_7^s}{|C_7^s|^2} \right) \\ &\quad + \frac{2}{|C_7^s|^2} \Re \left[(C_7^d + \lambda_u L_R^u)(A_R^{(1)t} + \lambda_u^* A_R^u) \right] . \end{aligned} \tag{45}$$

$\zeta = 0.76 \pm 0.10$ $A^{(1)K^*} = -0.113 - i0.043$ $A^u = -0.0181 + i0.0211$	$L_R^u = -0.095 \pm 0.022$ $A^{(1)t} = -0.114 - i0.045$
$\eta_{tt} = 0.57$ $\eta_{tc} = 0.47 \pm 0.04$ $\eta_B = 0.55$ $\xi_s = 1.18 \pm 0.04^{+0.12}_{-0}$	$\eta_{cc} = 1.38 \pm 0.53$ $\hat{B}_K = 0.86 \pm 0.15$ $F_{B_d}\sqrt{\hat{B}_{B_d}} = 235 \pm 33^{+0}_{-24}$ MeV
$\lambda = 0.221 \pm 0.002$ $\epsilon_K = (2.271 \pm 0.017)\ 10^{-3}$ $a_{\psi K_s} = 0.734 \pm 0.054$	$\lvert V_{ub}/V_{cb}\rvert = 0.097 \pm 0.010$ $\Delta M_{B_d} = 0.503 \pm 0.006\ \text{ps}^{-1}$ $\Delta M_{B_s} \geq 14.4\ \text{ps}^{-1}$ (95% C.L.)

Table 6.3: *Theoretical parameters and measurements used in* $\mathrm{B} \to \rho\gamma$ *observables and in the CKM unitarity fits. For details and references, see [57,17]*

In the SM, $C_7^d = C_7$, as in the $b \to s\gamma$ decays; however, in beyond-the-SM scenarios, this may not hold making the decays $\mathrm{B} \to \rho\gamma$ interesting for beyond-the-SM searches [57]. The definitions of the quantities $A^{(1)K^*}$, $A^{(1)t}$, A^u and $L_R^u = \epsilon_A\, C_7^{(0)\text{eff}}$ can be seen in [44]. Their default values together with that of ζ are summarized in Table 6.3, where we have also specified the theoretical errors in the more sensitive parameters ζ and L_R^u.

What concerns the quantity called ζ, we note that there are several model-dependent estimates of the same in the literature. Some representative values are: $\zeta = 0.76 \pm 0.06$ from the light-cone QCD sum rules [55]; a theoretically improved estimate in the same approach yields [49]: $\zeta = 0.75 \pm 0.07$; $\zeta = 0.88 \pm 0.02(!)$ using hybrid QCD sum rules [58], and $\zeta = 0.69 \pm 10\%$ in the quark model [59]. Except for the hybrid QCD sum rules, all other approaches yield a significant SU(3)-breaking in the magnetic moment form factors. In the light-cone QCD sum rule approach, this is anticipated due to the appreciable differences in the wave functions of the K^* and ρ-mesons. To reflect the current dispersion in the theoretical estimates of ζ, we take its value as $\zeta = 0.76 \pm 0.10$. A lattice-QCD based estimate of the same is highly desirable.

The isospin breaking ratio

$$\Delta(\rho\gamma) \equiv \frac{(\Delta^{+0} + \Delta^{-0})}{2}, \qquad \Delta^{\pm 0} = \frac{\Gamma(\mathrm{B}^\pm \to \rho^\pm\gamma)}{2\Gamma(\mathrm{B}^0(\overline{\mathrm{B}}^0) \to \rho^0\gamma)} - 1 \tag{46}$$

is given by

$$\begin{aligned}\Delta(\rho\gamma) &= \left|\frac{C_7^d + \lambda_u L_R^u}{C_7^d}\right|^2 \left(1 - \frac{2\Re C_7^d (A_R^{(1)t} + \lambda_u^* A_R^u)}{|C_7^d|^2}\right) \\ &\quad + \frac{2}{|C_7^d|^2}\Re\left[(C_7^d + \lambda_u L_R^u)(A_R^{(1)t} + \lambda_u^* A_R^u)\right] - 1\,,\end{aligned} \tag{47}$$

and the CP asymmetry $A_{CP}^\pm(\rho\gamma) = (\mathcal{B}(\mathrm{B}^- \to \rho^-\gamma) - \mathcal{B}(\mathrm{B}^+ \to \rho^+\gamma))/(\mathcal{B}(\mathrm{B}^- \to \rho^-\gamma) + \mathcal{B}(\mathrm{B}^+ \to \rho^+\gamma))$ is

$$A_{CP}^\pm(\rho\gamma) = -\frac{2\Im\left[(C_7^d + \lambda_u L_R^u)(A_I^{(1)t} + \lambda_u^* A_I^u)\right]}{|C_7^d + \lambda_u L_R^u|^2}\,. \tag{48}$$

The observables $R^0(\rho\gamma/\mathrm{K}^*\gamma) \equiv \bar{\mathcal{B}}(\mathrm{B}^0 \to \rho^0\gamma)/\mathcal{B}(\overline{\mathrm{B}}^0 \to \mathrm{K}^{*0}\gamma)$ (where $\bar{\mathcal{B}}$ is the average of the B^0 and $\overline{\mathrm{B}}^0$ modes) and $A_{CP}^0(\rho\gamma) = (\mathcal{B}(\mathrm{B}^0 \to \rho^0\gamma) - \mathcal{B}(\overline{\mathrm{B}}^0 \to \rho^0\gamma))/(\mathcal{B}(\mathrm{B}^0 \to \rho^-\gamma) + \mathcal{B}(\overline{\mathrm{B}}^0 \to \rho^0\gamma))$ are

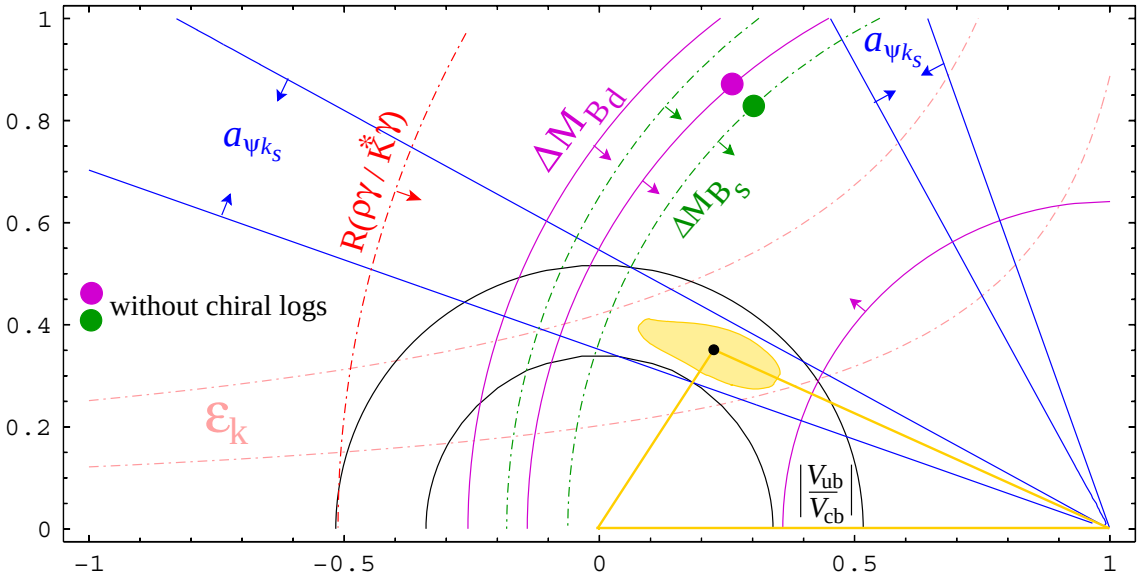

Fig. 6.10: Unitary triangle fit in the SM and the resulting 95% C.L. contour in the $\bar{\rho}$ - $\bar{\eta}$ plane. The impact of the $R(\rho\gamma/\mathrm{K}^*\gamma) < 0.047$ constraint is also shown (from Ref. [57]).

obtained from Eqs. (44, 45, 48) in the limit $L_R^u = 0$ and $S_\rho = 1/2$. The numerical estimates for the various observables depend, apart from the hadronic parameters specific to the $\mathrm{B} \to V\gamma$ ($V = \mathrm{K}^*, \rho$) decays, also on the CKM parameters, in particular $\bar{\rho}$ and $\bar{\eta}$. A typical analysis of the constraints in the $(\bar{\rho}, \bar{\eta})$ plane from the unitarity of the CKM matrix [57], including the measurements of the CP asymmetry $a_{\psi K_s}$ in the decays $\mathrm{B}^0/\overline{\mathrm{B}^0} \to J/\psi \mathrm{K}_s$ (and related modes) [60] is shown in Fig. 6.10. Note that for the hadronic parameters $F_{B_d}\sqrt{\hat{B}_{B_d}}$ and ξ_s, the recent lattice estimates [61] have been adopted that take into account uncertainties induced by the so-called chiral logarithms [62]. These errors are extremely asymmetric and, once taken into account, reduce sizeably the impact of the $\Delta M_{B_s}/\Delta M_{B_d}$ lower bound on the unitarity triangle analysis, as shown in Fig. 6.10. The 95% CL contour is drawn taking into account chiral logarithms uncertainties. The fitted values for the Wolfenstein parameters are $\bar{\rho} = 0.22 \pm 0.07$ and $\bar{\eta} = 0.35 \pm 0.04$. This yields $\Delta R^{\pm} = 0.055 \pm 0.130$ and $\Delta R^0 = 0.015 \pm 0.110$ [44,57]. The impact of the current upper limit $R(\rho\gamma/\mathrm{K}^*\gamma) \leq 0.047$ [63] is also shown. While not yet competitive to the existing constraints on the unitarity triangle, this surely is bound to change with the anticipated $O(1\ (\mathrm{ab})^{-1}))$ $\Upsilon(4S) \to \mathrm{B}\overline{\mathrm{B}}$ data over the next three years at the B-factories.

Taking into account these errors and the uncertainties on the theoretical parameters presented in Table 6.3, leads to the following SM expectations for the $\mathrm{B} \to (\mathrm{K}^*, \rho)\gamma$ decays [57]:

$$R^{\pm}(\rho\gamma/\mathrm{K}^*\gamma) = 0.023 \pm 0.012\ , \tag{49}$$

$$R^0(\rho\gamma/\mathrm{K}^*\gamma) = 0.011 \pm 0.006\ , \tag{50}$$

$$\Delta(\rho\gamma) = 0.04^{+0.14}_{-0.07}\ , \tag{51}$$

$$A_{CP}^{\pm}(\rho\gamma) = 0.10^{+0.03}_{-0.02}\ , \tag{52}$$

$$A_{CP}^{0}(\rho\gamma) = 0.06 \pm 0.02\ . \tag{53}$$

The above estimates of $R^{\pm}(\rho\gamma/\mathrm{K}^*\gamma)$ and $R^0(\rho\gamma/\mathrm{K}^*\gamma)$ can be combined with the measured branching ratios for $\mathrm{B} \to \mathrm{K}^*\gamma$ decays given earlier to yield:

$$\mathcal{B}(\mathrm{B}^{\pm} \to \rho^{\pm}\gamma) = (0.93 \pm 0.49) \times 10^{-6}\ , \quad \mathcal{B}(\mathrm{B}^0 \to \rho^0\gamma) = (0.45 \pm 0.24) \times 10^{-6}\ . \tag{54}$$

The errors include the uncertainties on the hadronic parameters and the CKM parameters $\bar{\rho}$, $\bar{\eta}$, as well as the current experimental error on $\mathcal{B}(\mathrm{B} \to \mathrm{K}^*\gamma)$. While there is as yet no experimental bounds

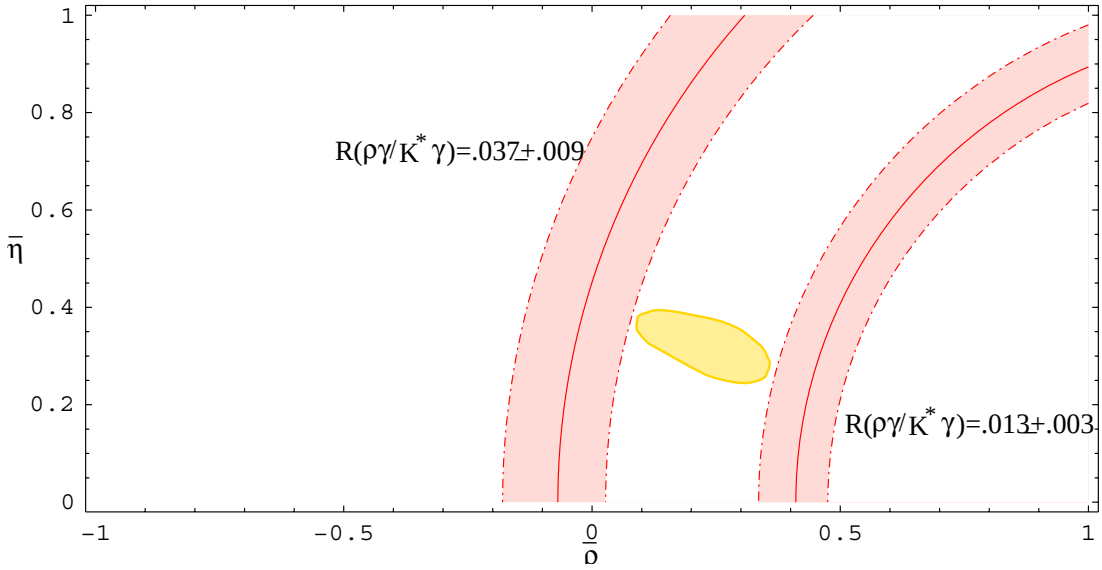

Fig. 6.11: Extremal values of $R(\rho\gamma/\mathrm{K}^*\gamma)$ t hat are compatible with the SM unitarity triangle analysis (from Ref. [57]).

on the isospin- and CP-violating quantities, $\Delta(\rho\gamma)$, $A_{CP}^{\pm}(\rho\gamma)$ and $A_{CP}^{0}(\rho\gamma)$, the upper limits on the branching ratios $R^{\pm}(\rho\gamma/\mathrm{K}^*\gamma)$ and $R^{0}(\rho\gamma/\mathrm{K}^*\gamma)$ have been significantly improved by the BABAR [63] and BELLE [46] collaborations recently. Averaged over the charge conjugated modes, the current best upper limits are [63]: $\mathcal{B}(\mathrm{B}^0 \to \rho^0\gamma) < 1.4 \times 10^{-6}$, $\mathcal{B}(\mathrm{B}^{\pm} \to \rho^{\pm}\gamma) < 2.3 \times 10^{-6}$ and $\mathcal{B}(\mathrm{B}^0 \to \omega\gamma) < 1.2 \times 10^{-6}$ (at 90% C.L.). They have been combined, using isospin weights for $\mathrm{B} \to \rho\gamma$ decays and assuming $\mathcal{B}(\mathrm{B}^0 \to \omega\gamma) = \mathcal{B}(\mathrm{B}^0 \to \rho^0\gamma)$, to yield the improved upper limit $\mathcal{B}(\mathrm{B} \to \rho\gamma) < 1.9 \times 10^{-6}$. The current measurements of the branching ratios for $\mathrm{B} \to \mathrm{K}^*\gamma$ decays by BABAR [47], $\mathcal{B}(\mathrm{B}^0 \to \mathrm{K}^{*0}\gamma) = (4.23\pm0.40\pm0.22)\times10^{-5}$ and $\mathcal{B}(\mathrm{B}^+ \to \mathrm{K}^{*+}\gamma) = (3.83\pm0.62\pm0.22)\times10^{-5}$, are then used to set an upper limit on the ratio of the branching ratios $R(\rho\gamma/\mathrm{K}^*\gamma) \equiv \mathcal{B}(\mathrm{B} \to \rho\gamma)/\mathcal{B}(\mathrm{B} \to \mathrm{K}^*\gamma) < 0.047$ (at 90% C.L.) [63]. This bound is typically a factor 2 away from the SM estimates given above [44,57]. However, in beyond-the-SM scenarios, this bound provides highly significant constraints on the relative strengths of the $b \to d\gamma$ and $b \to s\gamma$ transitions [57].

The extremal values of $R(\rho\gamma/\mathrm{K}^*\gamma)$ compatible with the SM UT-analysis are shown in Fig. 6.11 where the bands correspond to the values 0.037 ± 0.007 and 0.013 ± 0.003 (the errors are essentially driven by the uncertainty on ζ). The meaning of this figure is as follows: any measurement of $R(\rho\gamma/\mathrm{K}^*\gamma)$, whose central value lies in the range $(0.013, 0.037)$ would be compatible with the SM, irrespective of the size of the experimental error. The error induced by the imprecise determination of the isospin breaking parameter ζ limits currently the possibility of having a very sharp impact from $R(\rho\gamma/\mathrm{K}^*\gamma)$ on the UT analysis. This aspect needs further theoretical work.

3. Weak phases from hadronic B decays

M. Beneke, G. Buchalla (coordinator), M. Ciuchini, R. Fleischer, E. Franco, Y.-Y. Keum, G. Martinelli, M. Pierini, J.L. Rosner and L. Silvestrini

The next five contributions discuss the problem of extracting weak phases from hadronic B decays. The emphasis is on determining the CKM parameters γ and α, or equivalent constraints on $\bar{\rho}$ and $\bar{\eta}$, from exclusive modes with two light mesons in the final state, such as $\mathrm{B} \to \pi\mathrm{K}$ and $\mathrm{B} \to \pi\pi$. This problem is difficult since the underlying weak interaction processes are dressed by QCD dynamics, which is prominent in purely hadronic decays. Despite the general difficulty, there are several circumstances that help us to control strong interaction effects and to isolate the weak couplings:

- **Flavour symmetries:** The impact of strong interactions may be reduced by eliminating hadronic matrix elements through a combination of different channels, exploiting approximate flavour symmetries of QCD. Important examples are isospin, U-spin (doublet (d, s)) or, more generally, $SU(3)_F$.
- **Heavy-quark limit:** The fact that $m_b \gg \Lambda_{QCD}$ can be used to simplify the theoretical description of QCD dynamics in B decays. Within this framework amplitudes are expanded in Λ_{QCD}/m_b, long-distance and short-distance contributions are factorized, and the latter can be treated in perturbative QCD. As a result the impact of nonperturbative hadronic physics is reduced.
- **Rich phenomenology:** A large number of decay channels exists, which allows us to explore different approaches, to apply various strategies based on QCD flavour symmetries and to obtain cross-checks for dynamical calculations based on factorization.

It has to be emphasized that this field is in a state of ongoing development, both theoretically and experimentally. On the theory side important questions still need further study (general proof of factorization, light-cone dynamics of the B meson, numerical accuracy of heavy-quark limit in various situations, size of $SU(3)_F$-breaking corrections), while many valuable new data continue to be collected by the experiments. It is worth noting that the approaches based on flavour symmetries and those using dynamical calculations in the heavy-quark limit are complementary to each other. For instance, corrections from flavour symmetry breaking can be estimated within factorization. One may expect that the most important results might eventually be obtained from the combined use of all the available options mentioned above.

The following contributions summarize the status of the subject as it was discussed at this workshop. The contributions of J.L. Rosner and R. Fleischer highlight strategies based on QCD flavour symmetries to extract α and γ from $\mathrm{B} \to \pi\mathrm{K}$, $\pi\pi$ decays. The status of factorization is outlined by M. Beneke. A critical point of view on extracting γ from global fits to hadronic modes is presented by M. Ciuchini et al.. Finally, a phenomenological analysis based on the hypothesis of hard-gluon dominance of $\mathrm{B} \to \pi$ form factors is described by Y.-Y. Keum.

3.1. Weak coupling phases

J.L. Rosner[*]

The phases of CKM matrix elements describing charge-changing weak couplings of quarks are fundamental quantities. They are sometimes described in terms of angles $\alpha = \phi_2$, $\beta = \phi_1$, and $\gamma = \phi_3$ in the unitarity triangle. Now that BaBar and Belle are converging on a value of $\sin(2\beta)$, attention has turned to ways of learning α and $\gamma = \pi - \beta - \alpha$. This summary describes some recent work on the subject.

In Sec. 3.1.1. we discuss $\mathrm{B}^0 \to \pi^+\pi^-$ in the light of recent measurements at BaBar [64] and Belle [24] of time-dependent asymmetries. This work was performed in part in collaboration with M. Gronau [11,65,66] and in part with Z. Luo [12]. We then mention how to learn γ from various $\mathrm{B} \to \mathrm{K}\pi$ decays (Sec. 3.1.2., collaboration with M. Gronau [11] and with M. Neubert [67,68]), $2\beta + \gamma$ from $\mathrm{B} \to \mathrm{D}^{(*)}\pi$ (Sec. 3.1.3., collaboration with D. Suprun and C.W. Chiang [69]), and α and γ from tree-penguin interference in $\mathrm{B} \to PP,\ PV$ decays, where P is a light pseudoscalar and V a light vector meson (Sec. 3.1.4., collaboration with C.W. Chiang [70]). Sec. 3.1.5. is a short guide to other recent work, while we summarize in Sec. 3.1.6.

[*]J.L. Rosner would like to thank C.-W. Chiang, M. Gronau, Z. Luo, M. Neubert, and D. Suprun for enjoyable collaborations on these subjects.

3.1.1. *Determination of α from $\mathrm{B}^0 \to \pi^+\pi^-$ decays*

We regard α, γ as uncertain to about $\pi/4$: $126^\circ \geq \alpha \geq 83^\circ$, $32^\circ \leq \gamma \leq 75^\circ$ [11], in accord with $122^\circ \geq \alpha \geq 75^\circ$, $37^\circ \leq \gamma \leq 80^\circ$ [71]. If $\mathrm{B}^0 \to \pi^+\pi^-$ were dominated by the "tree" amplitude T with phase $\gamma = \mathrm{Arg}(V_{ub}^* V_{ud})$, the parameter $\lambda_{\pi\pi} \equiv e^{-2i\beta} A(\overline{\mathrm{B}}^0 \to \pi^+\pi^-)/A(\mathrm{B}^0 \to \pi^+\pi^-)$ would be just $e^{2i\alpha}$ and the indirect CP-violating asymmetry $S_{\pi\pi} = 2\mathrm{Im}\lambda_{\pi\pi}/(1+|\lambda_{\pi\pi}|^2)$ would be $\sin 2\alpha$. Here

$$\frac{d\Gamma}{dt}\left\{ \begin{array}{l} \mathrm{B}^0|_{t=0} \to f \\ \overline{\mathrm{B}}^0|_{t=0} \to f \end{array} \right\} \propto e^{-\Gamma t}[1 \mp S_{\pi\pi}\sin\Delta M_d t \pm C_{\pi\pi}\cos\Delta M_d t] \quad , \tag{55}$$

$C_{\pi\pi} = (1-|\lambda_{\pi\pi}|^2)/(1+|\lambda_{\pi\pi}|^2)$, and $\Delta\Gamma \simeq \Delta M_d/200$ has been neglected. In the presence of non-zero $\Delta\Gamma$ one can also measure $A_{\pi\pi} = 2\mathrm{Re}\lambda_{\pi\pi}/(1+|\lambda_{\pi\pi}|^2)$. Since $|S_{\pi\pi}|^2 + |C_{\pi\pi}|^2 + |A_{\pi\pi}|^2 = 1$ one has $|S_{\pi\pi}|^2 + |C_{\pi\pi}|^2 \leq 1$. However, one also has a penguin amplitude P involving a $\bar{b} \to \bar{d}$ loop transition involving contributions $\sim V_{ud}^* V_{ub}$, $V_{cd}^* V_{cb}$, and $V_{td}^* V_{tb} = -V_{ud}^* V_{ub} - V_{cd}^* V_{cb}$. The decay amplitudes are then

$$A(\mathrm{B}^0 \to \pi^+\pi^-) = -(|T|e^{i\delta_T}e^{i\gamma} + |P|e^{i\delta_P}),\ A(\overline{\mathrm{B}}^0 \to \pi^+\pi^-) = -(|T|e^{i\delta_T}e^{-i\gamma} + |P|e^{i\delta_P}), \tag{56}$$

where the strong phase difference $\delta \equiv \delta_P - \delta_T$. It will be convenient to define $R_{\pi\pi} \equiv \overline{\mathcal{B}}(\mathrm{B}^0 \to \pi^+\pi^-)/\overline{\mathcal{B}}(\mathrm{B}^0 \to \pi^+\pi^-)_{\mathrm{tree}}$, where $\overline{\mathcal{B}}$ refers to a branching ratio averaged over B^0 and $\overline{\mathrm{B}}^0$. One may use $S_{\pi\pi}$ and $C_{\pi\pi}$ to learn α, δ, resolving a discrete ambiguity with the help of $R_{\pi\pi}$ [65]. Alternatively, one may directly use $S_{\pi\pi}$, $C_{\pi\pi}$, and $R_{\pi\pi}$ to learn α, δ, and $|P/T|$ [66,72].

Explicit expressions for $R_{\pi\pi}$, $S_{\pi\pi}$ and $C_{\pi\pi}$ may be found in [65,66]. In [65] we estimated $|P/T| = 0.276 \pm 0.064$ (see also [10]), obtaining $|P|$ from $\mathrm{B}^+ \to \mathrm{K}^0\pi^+$ via (broken) flavor SU(3) and $|T|$ from $\mathrm{B} \to \pi\ell\nu$. Plotting $C_{\pi\pi}$ against $S_{\pi\pi}$ for various values of α in the likely range, one obtains curves parametrized by δ which establish a one-to-one correspondence between a pair $(S_{\pi\pi}, C_{\pi\pi})$ and a pair (α, δ) as long as $|\delta| \leq 90^\circ$. However, if $|\delta|$ is allowed to exceed about 90° these curves can intersect with one another, giving rise to a discrete ambiguity corresponding to as much as 30° uncertainty in α when $C_{\pi\pi} = 0$. In this case, when $\delta = 0$ or π, one has $|\lambda_{\pi\pi}| = 1$ and $S_{\pi\pi} = \sin 2(\alpha + \Delta\alpha)$, where $\tan(\Delta\alpha) = \pm(|P/T|\sin\gamma)/(1 \pm (|P/T|\cos\gamma)$ is typically $\pm 15^\circ$. One can resolve the ambiguity either by comparing the predicted $R_{\pi\pi}$ with experiment (see [65] for details) , or by comparing the allowed (ρ, η) region with that determined by other observables [71]. An example is shown in [11].

Once errors on $R_{\pi\pi}$ are reduced to ± 0.1 (they are now about three times as large [65]), a distinction between $\delta = 0$ and $\delta = \pi$ will be possible when $S_{\pi\pi} \simeq 0$, as appears to be the case for BaBar [64]. For the Belle data [24], which suggest $S_{\pi\pi} < 0$, the distinction becomes easier; it becomes harder for $S_{\pi\pi} > 0$. With 100 fb^{-1} at each of BaBar and Belle, it will be possible to reduce $\Delta|T|^2/|T|^2$ from its present error of 44% and $\overline{\mathcal{B}}(\mathrm{B}^0 \to \pi^+\pi^-)$ from its present error of 21% each to about 10% [12], which will go a long way toward this goal. In an analysis independent of $|P/T|$ performed since the workshop, the somewhat discrepant BaBar and Belle values of $S_{\pi\pi}$ and $C_{\pi\pi}$, when averaged, favor α between about 90° and 120° (see Fig. 1 of [66]).

3.1.2. *Determination of γ from $\mathrm{B} \to \mathrm{K}\pi$ decays*

γ from $\mathrm{B}^0 \to \mathrm{K}^+\pi^-$ and $\mathrm{B}^+ \to \mathrm{K}^0\pi^+$

We mention some results of [11] on information provided by $\mathrm{B}^0 \to \mathrm{K}^+\pi^-$ decays, which involve both a penguin P' and a tree T' amplitude. One can use the flavor-averaged branching ratio $\overline{\mathcal{B}}$ and the CP asymmetry in these decays, together with P' information from the $\mathrm{B}^+ \to \mathrm{K}^0\pi^+$ decay rate (assuming it is equal to the charge-conjugate rate, which must be checked) and T' information from $\mathrm{B} \to \pi\ell\nu$ and flavor SU(3), to obtain constraints on γ. One considers the ratio $R \equiv [\overline{\mathcal{B}}(\mathrm{B}^0 \to \mathrm{K}^+\pi^-)/\overline{\mathcal{B}}(B^+ \to \mathrm{K}^0\pi^+)][\tau_+/\tau_0]$, where the $\mathrm{B}^+/\mathrm{B}^0$ lifetime ratio τ_+/τ_0 is about 1.07. Once the error on this quantity is reduced to ± 0.05 from its value of ± 0.14 as of February 2002, which should be possible with 200 fb^{-1}

at each of BaBar and Belle, one should begin to see useful constraints arising from the value of R, especially if errors on the ratio $r \equiv |T'/P'|$ can be reduced with the help of better information on $|T'|$.

γ from $B^+ \to K^+\pi^0$ and $B^+ \to K^0\pi^+$

One can use the ratio $R_c \equiv 2\overline{\mathcal{B}}(B^+ \to K^+\pi^0)/\overline{\mathcal{B}}(B^+ \to K^0\pi^+)$ to determine γ [11,67,68]. Given the values as of February 2002, $R_c = 1.25 \pm 0.22$, $A_c \equiv [\mathcal{B}(B^- \to K^-\pi^0) - \mathcal{B}(B^+ \to K^+\pi^0)]/\overline{\mathcal{B}}(B^+ \to K^0\pi^+) = -0.13 \pm 0.17$, and $r_c \equiv |T' + C'|/|p'| = 0.230 \pm 0.035$ (here C' is a color-suppressed amplitude, while p' is a penguin amplitude including an electroweak contribution), and an estimate [67,68] of the electroweak penguin contribution, one finds $\gamma \leq 90^\circ$ or $\gamma \geq 140^\circ$ at the 1σ level, updating an earlier bound [11] $\gamma \geq 50^\circ$. A useful determination would involve $\Delta R_c = \pm 0.1$, achievable with 150 fb^{-1} each at BaBar and Belle.

3.1.3. Determination of $2\beta + \gamma$ from $B \to D^{(*)}\pi$ decays

The "right-sign" (RS) decay $B^0 \to D^{(*)-}\pi^+$, governed by the CKM factor $V_{cb}^* V_{ud}$, and the "wrong-sign" (WS) decay $\overline{B}^0 \to D^{(*)-}\pi^+$, governed by $V_{cd}^* V_{ub}$, can interfere through B^0–$\overline{B}^0$ mixing, leading to information on the weak phase $2\beta + \gamma$. One must separate out the dependence on a strong phase δ between the RS and WS amplitudes, measuring time-dependent observables

$$A_\pm(t) = (1 + R^2) \pm (1 - R^2)\cos\Delta mt, \;\; B_\pm(t) = -2R\sin(2\beta + \gamma \pm \delta)\sin\Delta mt, \qquad (57)$$

where $R \equiv |\mathrm{WS}/\mathrm{RS}| = r|V_{cd}^* V_{ub}/V_{cb}^* V_{ud}| \simeq 0.02r$, with r a parameter of order 1 which needs to be known better. In Ref. [69] we use the fact that R can be measured in the decay $B^+ \to D^{*+}\pi^0$ to conclude that with 250 million $B\bar{B}$ pairs one can obtain an error of less than ± 0.05 on $\sin(2\beta + \gamma)$, which is expected to be greater than about 0.89 in the standard model. Thus, such a measurement is not likely to constrain CKM parameters, but has potential for an interesting non-standard outcome.

3.1.4. Determination of α and γ from $B \to PP,\ PV$ decays

Some other processes which have a near-term potential for providing information on tree-penguin interference (and hence on α and γ) are the following [70: (1) the CP asymmetries in $B^+ \to \pi^+\eta$ and $\pi^+\eta'$; (2) rates in $B^+ \to \eta' K^+$ and $B^0 \to \eta' K^0$; (3) rates in $B^+ \to \eta K^{*+}$ and $B^0 \to \eta K^{*0}$; and (4) rates in $B^+ \to \omega K^+$ and $B^0 \to \omega K^0$. Other interesting branching ratios include those for $B^0 \to \pi^- K^{*+}$, $B^0 \to K^+\rho^-$, $B^+ \to \pi^+\rho^0$, $B^+ \to \pi^+\omega$, and $B^{(+,0)} \to \eta' K^{*(+,0)}$, with a story for each [70]. In order to see tree-penguin interference at the predicted level one needs to measure branching ratios at the level of $\Delta\overline{\mathcal{B}} = (1-2) \times 10^{-6}$.

3.1.5. References to other work

For other recent suggestions on measuring α and γ, see the review of [73] and the contributions of [74] on the isospin triangle in $B \to \pi\pi$ (α), [75,76] on $B^+ \to DK^+$ (γ), [77] on $B^0 \to DK_S$ ($2\beta+\gamma$), [78] on $B^0 \to K\pi$ (γ), [79] on $B^0 \to \pi^+\pi^-$ and $B_s \to K^+K_-$ (γ), and [80] on $B^0 \to K^+\pi^-$ and $B_s \to K^-\pi^+$ (γ). These contain references to earlier work.

3.1.6. Summary

CKM phases will be learned in many ways. While β is well-known now and will be better-known soon, present errors on α and γ are about 45°. To reduce them to 10° or less, several methods will help. (1) Time-dependent asymmetries in $B^0 \to \pi^+\pi^-$ already contain useful information. The next step will come when both BaBar and Belle accumulate samples of at least 100 fb^{-1}. (2) In $B^0 \to \pi^+\pi^-$

an ambiguity between a strong phase δ near zero and one near π (if the direct asymmetry parameter $C_{\pi\pi}$ is small) can be resolved experimentally, for example by better measurement of the $\mathrm{B}^0 \to \pi^+\pi^-$ branching ratio and the $\mathrm{B} \to \pi\ell\nu$ spectrum. (3) Several $\mathrm{B} \to \mathrm{K}\pi$ modes, when compared, can constrain γ through penguin-tree interference. This has been recognized, for example, in [71]. (4) The rates in several $\mathrm{B} \to \mathrm{PP}, \mathrm{PV}$ modes are sensitive to tree-penguin interference. One needs to measure branching ratios with errors less than 2×10^{-6} to see such effects reliably.

3.2. Extracting γ through flavour-symmetry strategies

R. Fleischer[†]

An important element in the testing of the Kobayashi–Maskawa picture of CP violation is the direct determination of the angle γ of the unitarity triangle of the CKM matrix. Here the goal is to overconstrain this angle as much as possible. In the presence of new physics, discrepancies may arise between different strategies, as well as with the "indirect" results for γ that are provided by the usual fits of the unitarity triangle, yielding at present $\gamma \sim 60^\circ$ [6,8,27].

There are many approaches on the market to determine γ (for a detailed review, see Ref. [81]). Here we shall focus on $\mathrm{B} \to \pi\mathrm{K}$ modes [11,78], [82–90], which can be analysed through flavour-symmetry arguments and plausible dynamical assumptions, and the U-spin-related decays $\mathrm{B}_d \to \pi^+\pi^-$, $\mathrm{B}_s \to \mathrm{K}^+\mathrm{K}^-$ [79]. The corresponding flavour-symmetry strategies allow the determination of γ and valuable hadronic parameters with a "minimal" theoretical input. Alternative approaches, relying on a more extensive use of theory, are provided by the recently developed "QCD factorization" [41,10] and "PQCD" [91] approaches, which allow furthermore a reduction of the theoretical uncertainties of the flavour-symmetry strategies discussed here. Let us note that these approaches are also particularly promising from a practical point of view: BaBar, Belle and CLEO-III may probe γ through $\mathrm{B} \to \pi\mathrm{K}$ modes, whereas the U-spin strategy, requiring also a measurement of the B_s-meson decay $\mathrm{B}_s \to \mathrm{K}^+\mathrm{K}^-$, is already interesting for run II of the Tevatron [3], and can be fully exploited in the LHC era [2]. A variant for the B-factories [92], where $\mathrm{B}_s \to \mathrm{K}^+\mathrm{K}^-$ is replaced by $\mathrm{B}_d \to \pi^\mp\mathrm{K}^\pm$, points already to an exciting picture [93].

3.2.1. Studies of $\mathrm{B} \to \pi\mathrm{K}$ *decays*

Using the isospin flavour symmetry of strong interactions, relations between $\mathrm{B} \to \pi\mathrm{K}$ amplitudes can be derived, which suggest the following combinations to probe γ: the "mixed" $\mathrm{B}^\pm \to \pi^\pm\mathrm{K}$, $\mathrm{B}_d \to \pi^\mp\mathrm{K}^\pm$ system [83–86], the "charged" $\mathrm{B}^\pm \to \pi^\pm\mathrm{K}$, $\mathrm{B}^\pm \to \pi^0\mathrm{K}^\pm$ system [67,68,88], and the "neutral" $\mathrm{B}_d \to \pi^0\mathrm{K}$, $\mathrm{B}_d \to \pi^\mp\mathrm{K}^\pm$ system [78,88]. Interestingly, already CP-averaged $\mathrm{B} \to \pi\mathrm{K}$ branching ratios may lead to non-trivial constraints on γ [84,67,68]. In order to *determine* this angle, also CP-violating rate differences have to be measured. To this end, we introduce the following observables [88]:

$$\left\{ \begin{array}{c} R \\ A_0 \end{array} \right\} \equiv \left[\frac{\mathrm{BR}(\mathrm{B}^0_\mathrm{d} \to \pi^-\mathrm{K}^+) \pm \mathrm{BR}(\overline{\mathrm{B}^0_\mathrm{d}} \to \pi^+\mathrm{K}^-)}{\mathrm{BR}(\mathrm{B}^+ \to \pi^+\mathrm{K}^0) + \mathrm{BR}(\mathrm{B}^- \to \pi^-\overline{\mathrm{K}^0})} \right] \frac{\tau_{B^+}}{\tau_{B^0_d}} \tag{58}$$

$$\left\{ \begin{array}{c} R_\mathrm{c} \\ A_0^\mathrm{c} \end{array} \right\} \equiv 2 \left[\frac{\mathrm{BR}(\mathrm{B}^+ \to \pi^0\mathrm{K}^+) \pm \mathrm{BR}(\mathrm{B}^- \to \pi^0\mathrm{K}^-)}{\mathrm{BR}(\mathrm{B}^+ \to \pi^+\mathrm{K}^0) + \mathrm{BR}(\mathrm{B}^- \to \pi^-\overline{\mathrm{K}^0})} \right] \tag{59}$$

$$\left\{ \begin{array}{c} R_\mathrm{n} \\ A_0^\mathrm{n} \end{array} \right\} \equiv \frac{1}{2} \left[\frac{\mathrm{BR}(\mathrm{B}^0_d \to \pi^-\mathrm{K}^+) \pm \mathrm{BR}(\overline{\mathrm{B}^0_d} \to \pi^+\mathrm{K}^-)}{\mathrm{BR}(\mathrm{B}^0_d \to \pi^0\mathrm{K}^0) + \mathrm{BR}(\overline{\mathrm{B}^0_d} \to \pi^0\overline{\mathrm{K}^0})} \right]. \tag{60}$$

[†]R. Fleischer would like to thank Andrzej Buras, Thomas Mannel and Joaquim Matias for pleasant collaborations on the topics discussed below.

If we employ the isospin flavour symmetry and make plausible dynamical assumptions, concerning mainly the smallness of certain rescattering processes, we obtain parametrizations of the following structure [86,88] (for alternative ones, see Ref. [87]):

$$R_{(\mathrm{c,n})},\, A_0^{(\mathrm{c,n})} = \text{functions}\left(q_{(\mathrm{c,n})}, r_{(\mathrm{c,n})}, \delta_{(\mathrm{c,n})}, \gamma\right). \tag{61}$$

Here $q_{(\mathrm{c,n})}$ denotes the ratio of electroweak (EW) penguins to "trees", $r_{(\mathrm{c,n})}$ is the ratio of "trees" to QCD penguins, and $\delta_{(\mathrm{c,n})}$ the strong phase between "trees" and QCD penguins. The EW penguin parameters $q_{(\mathrm{c,n})}$ can be fixed through theoretical arguments: in the mixed system [83–85], we have $q \approx 0$, as EW penguins contribute only in colour-suppressed form; in the charged and neutral $\mathrm{B} \to \pi\mathrm{K}$ systems, q_{c} and q_{n} can be fixed through the $SU(3)$ flavour symmetry without dynamical assumptions [67,68,78,88]. The $r_{(\mathrm{c,n})}$ can be determined with the help of additional experimental information: in the mixed system, r can be fixed through arguments based on factorization [83,85,41,10] or U-spin [80], whereas r_{c} and r_{n} can be determined from the CP-averaged $\mathrm{B}^{\pm} \to \pi^{\pm}\pi^0$ branching ratio by using only the $SU(3)$ flavour symmetry [82,67,68]. The uncertainties arising in this programme from $SU(3)$-breaking effects can be reduced through the QCD factorization approach [41,10], which is moreover in favour of small rescattering processes. For simplicity, we shall neglect such FSI effects in the discussion given below.

Since we are in a position to fix the parameters $q_{(\mathrm{c,n})}$ and $r_{(\mathrm{c,n})}$, we may determine $\delta_{(\mathrm{c,n})}$ and γ from the observables given in (61). This can be done separately for the mixed, charged and neutral $\mathrm{B} \to \pi\mathrm{K}$ systems. It should be emphasized that also CP-violating rate differences have to be measured to this end. Using just the CP-conserving observables $R_{(\mathrm{c,n})}$, we may obtain interesting constraints on γ. In contrast to $q_{(\mathrm{c,n})}$ and $r_{(\mathrm{c,n})}$, the strong phase $\delta_{(\mathrm{c,n})}$ suffers from large hadronic uncertainties. However, we can get rid of $\delta_{(\mathrm{c,n})}$ by keeping it as a "free" variable, yielding minimal and maximal values for $R_{(\mathrm{c,n})}$:

$$R^{\mathrm{ext}}_{(\mathrm{c,n})}\Big|_{\delta_{(\mathrm{c,n})}} = \text{function}\left(q_{(\mathrm{c,n})}, r_{(\mathrm{c,n})}, \gamma\right). \tag{62}$$

Keeping in addition $r_{(\mathrm{c,n})}$ as a free variable, we obtain another – less restrictive – minimal value

$$R^{\mathrm{min}}_{(\mathrm{c,n})}\Big|_{r_{(\mathrm{c,n})},\delta_{(\mathrm{c,n})}} = \text{function}\left(q_{(\mathrm{c,n})}, \gamma\right) \sin^2\gamma. \tag{63}$$

These extremal values of $R_{(\mathrm{c,n})}$ imply constraints on γ, since the cases corresponding to $R^{\mathrm{exp}}_{(\mathrm{c,n})} < R^{\mathrm{min}}_{(\mathrm{c,n})}$ and $R^{\mathrm{exp}}_{(\mathrm{c,n})} > R^{\mathrm{max}}_{(\mathrm{c,n})}$ are excluded. Present experimental data seem to point towards values for γ that are *larger* than 90°, which would be in conflict with the CKM fits, favouring $\gamma \sim 60^\circ$ [6,8,27]. Unfortunately, the present experimental uncertainties do not yet allow us to draw definite conclusions, but the picture should improve significantly in the future.

An efficient way to represent the situation in the $\mathrm{B} \to \pi\mathrm{K}$ system is provided by allowed regions in the $R_{(\mathrm{c,n})}$–$A_0^{(\mathrm{c,n})}$ planes [89,93], which can be derived within the Standard Model and allow a direct comparison with the experimental data. A complementary analysis in terms of γ and $\delta_{\mathrm{c,n}}$ was performed in Ref. [90]. Another recent $\mathrm{B} \to \pi\mathrm{K}$ study can be found in Ref. [11], where the R_{c} were calculated for given values of $A_0^{(\mathrm{c})}$ as functions of γ, and were compared with the B-factory data. In order to analyse $\mathrm{B} \to \pi\mathrm{K}$ modes, also certain sum rules may be useful [94].

3.2.2. The $\mathrm{B}_d \to \pi^+\pi^-$ and the $\mathrm{B}_s \to \mathrm{K}^+\mathrm{K}^-$ decays

As can be seen from the corresponding Feynman diagrams, $\mathrm{B}_s \to \mathrm{K}^+\mathrm{K}^-$ is related to $\mathrm{B}_d \to \pi^+\pi^-$ through an interchange of all down and strange quarks. The decay amplitudes read as follows [79]:

$$A(\mathrm{B}_d^0 \to \pi^+\pi^-) \propto \left[e^{i\gamma} - d e^{i\theta}\right], \quad A(\mathrm{B}_s^0 \to \mathrm{K}^+\mathrm{K}^-) \propto \left[e^{i\gamma} + \left(\frac{1-\lambda^2}{\lambda^2}\right) d' e^{i\theta'}\right], \tag{64}$$

where the CP-conserving strong amplitudes $de^{i\theta}$ and $d'e^{i\theta'}$ measure, sloppily speaking, ratios of penguin to tree amplitudes in $\mathrm{B}^0_d \to \pi^+\pi^-$ and $\mathrm{B}^0_s \to \mathrm{K}^+\mathrm{K}^-$, respectively. Using these general parametrizations, we obtain expressions for the direct and mixing-induced CP asymmetries of the following kind:

$$\mathcal{A}_{\mathrm{CP}}^{\mathrm{dir}}(\mathrm{B}_d \to \pi^+\pi^-) = \text{function}(d,\theta,\gamma),\ \mathcal{A}_{\mathrm{CP}}^{\mathrm{mix}}(\mathrm{B}_d \to \pi^+\pi^-) = \text{function}(d,\theta,\gamma,\phi_d = 2\beta) \tag{65}$$

$$\mathcal{A}_{\mathrm{CP}}^{\mathrm{dir}}(\mathrm{B}_s \to \mathrm{K}^+\mathrm{K}^-) = \text{function}(d',\theta',\gamma),\ \mathcal{A}_{\mathrm{CP}}^{\mathrm{mix}}(\mathrm{B}_s \to \mathrm{K}^+\mathrm{K}^-) = \text{function}(d',\theta',\gamma,\phi_s \approx 0). \tag{66}$$

Consequently, we have four observables at our disposal, depending on six "unknowns". However, since $\mathrm{B}_d \to \pi^+\pi^-$ and $\mathrm{B}_s \to \mathrm{K}^+\mathrm{K}^-$ are related to each other by interchanging all down and strange quarks, the U-spin flavour symmetry of strong interactions implies

$$d'e^{i\theta'} = d\,e^{i\theta}. \tag{67}$$

Using this relation, the four observables in (65,66) depend on the four quantities d, θ, $\phi_d = 2\beta$ and γ, which can hence be determined [79]. The theoretical accuracy is only limited by the U-spin symmetry, as no dynamical assumptions about rescattering processes have to be made. Theoretical considerations give us confidence into (67), as it does not receive U-spin-breaking corrections in factorization [79]. Moreover, we may also obtain experimental insights into U-spin breaking [79,95].

The U-spin arguments can be minimized, if the B^0_d–$\overline{\mathrm{B}}^0_d$ mixing phase $\phi_d = 2\beta$, which can be fixed through $\mathrm{B}_d \to J/\psi\mathrm{K}_{\mathrm{S}}$, is used as an input. The observables $\mathcal{A}_{\mathrm{CP}}^{\mathrm{dir}}(\mathrm{B}_d \to \pi^+\pi^-)$ and $\mathcal{A}_{\mathrm{CP}}^{\mathrm{mix}}(\mathrm{B}_d \to \pi^+\pi^-)$ allow us then to eliminate the strong phase θ and to determine d as a function of γ. Analogously, $\mathcal{A}_{\mathrm{CP}}^{\mathrm{dir}}(\mathrm{B}_s \to \mathrm{K}^+\mathrm{K}^-)$ and $\mathcal{A}_{\mathrm{CP}}^{\mathrm{mix}}(\mathrm{B}_s \to \mathrm{K}^+\mathrm{K}^-)$ allow us to eliminate the strong phase θ' and to determine d' as a function of γ. The corresponding contours in the γ–d and γ–d' planes can be fixed in a *theoretically clean* way. Using now the U-spin relation $d' = d$, these contours allow the determination both of the CKM angle γ and of the hadronic quantities d, θ, θ'; for a detailed illustration, see Ref. [79]. This approach is very promising for run II of the Tevatron and the experiments of the LHC era, where experimental accuracies for γ of $\mathcal{O}(10^\circ)$ [3] and $\mathcal{O}(1^\circ)$ [2] may be achieved, respectively. It should be emphasized that not only γ, but also the hadronic parameters d, θ, θ' are of particular interest, as they can be compared with theoretical predictions, thereby allowing valuable insights into hadron dynamics. For other recently developed U-spin strategies, the reader is referred to [80,96].

3.2.3. The $\mathrm{B}_d \to \pi^+\pi^-$ and the $\mathrm{B}_d \to \pi^\mp\mathrm{K}^\pm$ decays and implications for $\mathrm{B}_s \to \mathrm{K}^+\mathrm{K}^-$ decay

A variant of the $\mathrm{B}_d \to \pi^+\pi^-$, $\mathrm{B}_s \to \mathrm{K}^+\mathrm{K}^-$ approach was developed for the e^+e^- B-factories [92], where $\mathrm{B}_s \to \mathrm{K}^+\mathrm{K}^-$ is not accessible: as $\mathrm{B}_s \to \mathrm{K}^+\mathrm{K}^-$ and $\mathrm{B}_d \to \pi^\mp\mathrm{K}^\pm$ are related to each other through an interchange of the s and d spectator quarks, we may replace the B_s mode approximately through its B_d counterpart, which has already been observed by BaBar, Belle and CLEO. Following these lines and using experimental information on the CP-averaged $\mathrm{B}_d \to \pi^\mp\mathrm{K}^\pm$ and $\mathrm{B}_d \to \pi^+\pi^-$ branching ratios, the relevant hadronic penguin parameters can be constrained, implying certain allowed regions in observable space [93]. An interesting situation arises now in view of the recent B-factory measurements of CP violation in $\mathrm{B}_d \to \pi^+\pi^-$, allowing us to obtain new constraints on γ as a function of the B^0_d–$\overline{\mathrm{B}}^0_d$ mixing phase ϕ_d, which is fixed through $\mathcal{A}_{\mathrm{CP}}^{\mathrm{mix}}(\mathrm{B}_d \to J/\psi\mathrm{K}_{\mathrm{S}})$ up to a twofold ambiguity, $\phi_d \sim 51^\circ$ or 129°. If we assume that $\mathcal{A}_{\mathrm{CP}}^{\mathrm{mix}}(\mathrm{B}_d \to \pi^+\pi^-)$ is positive, as indicated by recent Belle data, and that ϕ_d is in agreement with the "indirect" fits of the unitarity triangle, i.e. $\phi_d \sim 51^\circ$, also the corresponding values for γ around 60° can be accommodated. On the other hand, for the second solution $\phi_d \sim 129^\circ$, we obtain a gap around $\gamma \sim 60^\circ$, and could easily accommodate values for γ larger than 90°. Because of the connection between the two solutions for ϕ_d and the resulting values for γ, it is very desirable to resolve the twofold ambiguity in the extraction of ϕ_d directly. As far as $\mathrm{B}_s \to \mathrm{K}^+\mathrm{K}^-$ is concerned, the data on the CP-averaged $\mathrm{B}_d \to \pi^+\pi^-$, $\mathrm{B}_d \to \pi^\mp\mathrm{K}^\pm$ branching ratios imply a very constrained allowed region in the space of $\mathcal{A}_{\mathrm{CP}}^{\mathrm{mix}}(\mathrm{B}_s \to \mathrm{K}^+\mathrm{K}^-)$ and $\mathcal{A}_{\mathrm{CP}}^{\mathrm{dir}}(\mathrm{B}_s \to \mathrm{K}^+\mathrm{K}^-)$ within the Standard Model, thereby providing a narrow target range for run II of the Tevatron and the experiments of the LHC era [93]. Other recent studies related to $\mathrm{B}_d \to \pi^+\pi^-$ can be found in Refs. [11,97].

3.3. Determining γ with QCD factorization

M. Beneke [‡]

3.3.1. Outline of the method

The QCD factorization approach [41,98] puts the well-known factorization ansatz [99] for hadronic two-body B decay matrix elements on a firm theoretical basis. It replaces the factorization ansatz by a factorization formula that includes radiative corrections and spectator scattering effects. Where it can be justified, the factorization ansatz emerges in the simultaneous limit, when m_b becomes large and when radiative corrections are neglected.

The QCD factorization approach uses heavy quark expansion methods ($m_b \gg \Lambda_{\rm QCD}$) and soft-collinear factorization (particle energies $\gg \Lambda_{\rm QCD}$) to compute the matrix elements $\langle f|O_i|\bar{\rm B}\rangle$ relevant to hadronic B decays in an expansion in $1/m_b$ and α_s. Only the leading term in $1/m_b$ assumes a simple form. The basic formula is

$$\begin{aligned}\langle M_1M_2|O_i|\overline{\rm B}\rangle \;=\; & F^{B\to M_1}(0)\int_0^1 du\, T^I(u)\Phi_{M_2}(u)\\ & +\int d\xi du dv\, T^{II}(\xi,u,v)\,\Phi_B(\xi)\Phi_{M_1}(v)\Phi_{M_2}(u),\end{aligned}\tag{68}$$

where $F^{B\to M_1}$ is a (non-perturbative) form factor, Φ_{M_i} and Φ_B are light-cone distribution amplitudes and $T^{I,II}$ are perturbatively calculable hard scattering kernels. Although not strictly proven to all orders in perturbation theory, the formula is presumed to be valid when both final state mesons are light. (M_1 is the meson that picks up the spectator quark from the B meson.) The formula shows that there is no long-distance interaction between the constituents of the meson M_2 and the (BM_1) system at leading order in $1/m_b$. This is the precise meaning of factorization. For a detailed discussion of (68) I refer to [10,98]. A summary of results that have been obtained in the QCD factorization approach is given in [100].

Factorization as embodied by (68) is not expected to hold at subleading order in $1/m_b$. Some power corrections related to scalar currents are enhanced by factors such as $m_\pi^2/((m_u+m_d)\Lambda_{\rm QCD})$. Some corrections of this type, in particular those related to scalar penguin amplitudes nevertheless appear to be calculable and turn out to be important numerically. On the other hand, attempts to compute subleading power corrections to hard spectator-scattering in perturbation theory usually result in infrared divergences, which signal the breakdown of factorization. At least these effects should be estimated and included into the error budget. All weak annihilation contributions belong to this class of effects and often constitute the dominant source of theoretical error.

3.3.2. Uses of QCD factorization

If the corrections to (68) were negligible and if all the quantities in (68) were known or computed with sufficient accuracy, the QCD factorization approach would allow one to determine directly weak CP-violating phases from branching fraction or CP asymmetry measurements, if the corresponding decay has two interfering amplitudes with different phases. In practice, depending on the particular decay mode, one is often far from this ideal situation. Depending on the theoretical uncertainty or one's confidence in theoretical error estimates, I can imagine the following uses of the QCD factorization approach, where in ascending order one makes stronger use of theoretical rather than experimental input.

1) Many strategies to determine γ are based on relating the strong interaction dynamics of different decay channels such that a sufficient set of measurements yields the weak phase together with the

[‡]M. Beneke would like to thank Gerhard Buchalla, Matthias Neubert and Chris Sachrajda for collaborations on the topics discussed in this article.

strong amplitudes (see the contributions by Fleischer and Rosner in this Chapter). QCD factorization can complement this approach where it has to rely on assumptions. For instance, it may be used to estimate SU(3) flavour symmetry breaking or to provide an estimate of small contributions to the decay amplitude that one would otherwise have to neglect to make use of the amplitude relations.

2) The QCD factorization approach generically predicts small strong rescattering phases, because rescattering is either perturbatively loop-suppressed, or power-suppressed in the heavy-quark limit. (Exceptions to the rule of small phases occur when the leading term in the α_s- or $1/m_b$-expansion is suppressed, for instance by small Wilson coefficients.) Even if the quantitative prediction of the strong phases turns out to be difficult, the qualitative result of small phases can be used to sharpen the bounds on γ that follow from some amplitude relations, or to turn the bounds into determinations of γ. An example of this in the context of a method suggested in [68] will be discussed below.
3) For predicting CP violation the ratio of two strong interaction amplitudes, P/T, (often a ratio of a pure penguin and a dominantly tree amplitude, which are multiplied by different weak phases) is a particularly important quantity. While P/T is computed in the QCD factorization approach, one may decide to use only the calculation of the absolute value $|P/T|$ and to dismiss the quantitative phase information. The rationale for this procedure could be that the calculation of the imaginary part is usually less accurate than the real part, because a one-loop calculation determines the phase only to leading order. For the same reason the value of the phase is more sensitive to uncalculable power corrections. In this procedure the phase information must be provided by an additional measurement, for instance a direct CP asymmetry.
4) The full information of the QCD factorization approach is employed to compute two-body branching fractions as functions of the parameters of the CKM matrix. Since the b quark mass is not very large it will be important to estimate the theoretical error from power corrections.

The development of QCD factorization has not yet reached the stage where one can decide which of these strategies will turn out to be most useful. (The strategy of choice obviously also depends on the amount of experimental information available that would allow one to drop one or the other piece of theoretical input.) Calculations of $\pi\pi$ and πK final states showed [10] that one obtains naturally the right magnitude of penguin and tree amplitudes. The accuracy of the calculation of strong phases is less clear at present, but forthcoming measurements of direct CP asymmetries should shed light on this question. The current limits favour small strong phases, but a quantitative comparison may require a complete next-to-leading order calculation of the absorptive parts of the amplitudes. It will also be important to clarify the relevance of weak annihilation effects in the decay amplitudes. While the current data do not favour the assumption of large annihilation contributions, they can also not yet be excluded. Bounds on rare annihilation-dominated decays will limit the corresponding amplitudes.

3.3.3. Results related to the determination of γ

The possibility to determine the CP-violating angle γ by comparing the calculation of branching fractions into $\pi\pi$ and πK final states with the corresponding data has been investigated in [10] (see also [101]). In the following I summarize the main results, referring to [10] for details and to [102,103] for partial updates of the analysis of [10].

γ from CP-averaged charged $\mathrm{B} \to \pi\mathrm{K}$ decay

The ratio

$$R_* = \frac{\mathrm{Br}(\mathrm{B}^+ \to \pi^+\mathrm{K}^0) + \mathrm{Br}(\mathrm{B}^- \to \pi^-\bar{\mathrm{K}}^0)}{2[\mathrm{Br}(\mathrm{B}^+ \to \pi^0\mathrm{K}^+) + \mathrm{Br}(\mathrm{B}^- \to \pi^0\mathrm{K}^-)]}\,, \tag{69}$$

currently measured as 0.71 ± 0.10, provides a useful bound on γ [68,87]. The theoretical expression is

$$\begin{aligned} R_*^{-1} &= 1 + 2\bar{\varepsilon}_{3/2}\cos\phi\,(q - \cos\gamma) + \bar{\varepsilon}_{3/2}^2(1 - 2q\cos\gamma + q^2) \\ &< \left(1 + \bar{\varepsilon}_{3/2}\,|q - \cos\gamma|\right)^2 + \bar{\varepsilon}_{3/2}^2\sin^2\gamma, \end{aligned} \tag{70}$$

where $\bar{\epsilon}_{3/2}e^{i\phi}$ is a tree-to-penguin ratio, whose magnitude can be fixed with SU(3) symmetry, and q an electroweak penguin contribution, which can be determined theoretically. (In this expression, a rescattering contribution ε_a, which QCD factorization predicts to be small, is neglected.) The inequality is obtained by allowing the relative strong phase ϕ to take any value. If R_* is smaller than one, the bound implies an exclusion region for $\cos\gamma$. The bound can be considerably sharpened, and the requirement $R_* < 1$ relaxed, if the phase is known to be small. QCD factorization as well as bounds on direct CP asymmetries suggest that $\cos\phi > 0.9$. In [10] it was shown that assuming the more conservative range $\cos\phi > 0.8$, the measurement of R_* combined with $|V_{ub}/V_{cb}|$ provides a determination of γ with a theoretical error of about 10°, if R_* is close to 1.

γ from $\mathrm{B}_d(t) \to \pi^+\pi^-$ decay

The QCD factorization approach allows us to interpret directly the mixing-induced and direct CP asymmetry in $\mathrm{B}_d \to \pi^+\pi^-$ decay without resort to other decay modes, since the tree and penguin amplitudes are both computed. The time-dependent asymmetry is defined by

$$\begin{aligned} A_{\mathrm{CP}}^{\pi\pi}(t) &= \frac{\mathrm{Br}(\mathrm{B}^0(t) \to \pi^+\pi^-) - \mathrm{Br}(\overline{\mathrm{B}}^0(t) \to \pi^+\pi^-)}{\mathrm{Br}(\mathrm{B}^0(t) \to \pi^+\pi^-) + \mathrm{Br}(\overline{\mathrm{B}}^0(t) \to \pi^+\pi^-)} \\ &= -S_{\pi\pi}\sin(\Delta M_B\,t) + C_{\pi\pi}\cos(\Delta M_B\,t). \end{aligned} \tag{71}$$

Assuming that the $\mathrm{B}\bar{\mathrm{B}}$ mixing phase is determined experimentally via the mixing-induced CP asymmetry in $\mathrm{B}_d(t) \to J/\psi\mathrm{K}$ decay, both $S_{\pi\pi}$ and $C_{\pi\pi}$ are measures of CP violation in the decay amplitude and determine γ. In [10] it was shown that even a moderately accurate measurement of $S_{\pi\pi}$ translates into a stringent constraint in the $(\bar{\rho}, \bar{\eta})$ plane. The predicted correlation between $S_{\pi\pi}$ and $C_{\pi\pi}$ is shown in [102].

3.3.4. γ from CP-averaged $\mathrm{B} \to \pi\mathrm{K}$, $\pi\pi$ decay

Since the branching fractions are computed as functions of the Wolfenstein parameters $(\bar{\rho}, \bar{\eta})$, one can perform a fit of $(\bar{\rho}, \bar{\eta})$ to the six measured CP-averaged $\mathrm{B} \to \pi\pi, \pi\mathrm{K}$ branching fractions. The result of this fit is shown in Fig. 6.12 based on the data as of May 2002. (The details of the fit procedure can be found in [10], the input data in [102]). The result of the fit is consistent with the standard fit based on meson mixing and $|V_{ub}|$. However, the $\pi\pi$, $\pi\mathrm{K}$ data persistently exhibit a preference for γ near 90°, or, for smaller γ, smaller $|V_{ub}|$. The significance and interpretation of this observation remains to be clarified.

3.3.5. Weak annihilation

Weak annihilation contributions are power-suppressed and not calculable in the QCD factorization approach. (This is one of the important differences between the QCD factorization approach and the pQCD approach described by Y. Keum in this Chapter.) The results discussed above include an estimate of annihilation effects together with an uncertainty derived from a $\pm 100\%$ variation of this estimate, encoded in the constraint $|\rho_A| < 1$ for a certain weak annihilation parameter [10]. Since this constraint is often a key factor in the overall theoretical uncertainty estimate, it will be important to obtain experimental information on weak annihilation. The current data on $\pi\pi$ and $\pi\mathrm{K}$ final states do not favour large annihilation contributions, but also do not exclude this possibility. The upper limits on annihilation-dominated

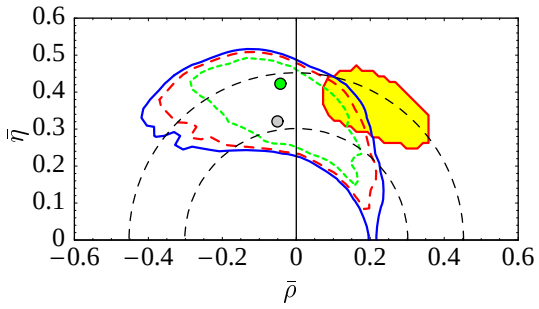

Fig. 6.12: *95% (solid), 90% (dashed) and 68% (short-dashed) confidence level contours in the* $(\bar{\rho}, \bar{\eta})$ *plane obtained from a global fit to the CP averaged* $\mathrm{B} \to \pi\mathrm{K}, \pi\pi$ *branching fractions, using the scanning method as described in [8]. The darker dot shows the overall best fit, whereas the lighter dot indicates the best fit for the default hadronic parameter set. The light-shaded region indicates the region preferred by the standard global fit [8], including the direct measurement of* $\sin(2\beta)$.

charmless decays are not yet tight enough to provide interesting constraints. However, we can adapt the estimate of annihilation contributions to $\bar{\mathrm{B}}_d \to \mathrm{D}^+\pi^-$ performed in [98] to the annihilation-dominated decay $\bar{\mathrm{B}}_d \to \mathrm{D}_s^+\mathrm{K}^-$, recently observed with a branching fraction $(3.8 \pm 1.1) \cdot 10^{-5}$ [104]. This results in a branching fraction estimate of $1.2 \cdot 10^{-5}$ for central parameters, or an upper limit $5 \cdot 10^{-5}$ upon assigning a 100% error to the annihilation amplitude. While the annihilation mechanism in $\bar{\mathrm{B}}_d \to \mathrm{D}_s^+\mathrm{K}^-$ is not identical to the dominant penguin annihilation term in $\mathrm{B} \to \pi\mathrm{K}$ decay, the comparison nevertheless supports the phenomenological treatment of annihilation suggested in [10,98].

3.4. $\mathrm{B} \to \mathrm{K}\pi$, charming penguins and the extraction of γ

M. Ciuchini, E. Franco, G. Martinelli, M. Pierini and L. Silvestrini

3.4.1. Main formulae

In this section we collect the main formulae for the amplitudes of $\mathrm{B} \to \mathrm{K}\pi, \pi\pi$, introducing the parametrization used in the analysis. We refer the reader to the literature for any detail on the origin and the properties of these parameters [105,106,107,108]. From Ref. [107], one reads

$$\begin{aligned}
A(\mathrm{B}_d \to \mathrm{K}^+\pi^-) &= \frac{G_F}{\sqrt{2}}\Big(\lambda_t^s P_1 - \lambda_u^s (E_1 - P_1^{GIM})\Big) \\
A(\mathrm{B}^+ \to \mathrm{K}^+\pi^0) &= \frac{G_F}{2}\Big(\lambda_t^s P_1 - \lambda_u^s (E_1 + E_2 - P_1^{GIM} + A_1)\Big) + \Delta A \\
A(\mathrm{B}^+ \to \mathrm{K}^0\pi^+) &= \frac{G_F}{\sqrt{2}}\Big(- \lambda_t^s P_1 + \lambda_u^s (A_1 - P_1^{GIM})\Big) + \Delta A \\
A(\mathrm{B}_d \to \mathrm{K}^0\pi^0) &= \frac{G_F}{2}\Big(- \lambda_t^s P_1 - \lambda_u^s (E_2 + P_1^{GIM})\Big) + \Delta A \\
A(\mathrm{B}_d \to \pi^+\pi^-) &= \frac{G_F}{\sqrt{2}}\Big(\lambda_t^d (P_1 + P_3) - \lambda_u^d (E_1 + A_2 - P_1^{GIM}) - P_3^{GIM}\Big) \\
A(\mathrm{B}_d \to \pi^+\pi^0) &= \frac{G_F}{2}\Big(- \lambda_u^d (E_1 + E_2)\Big) + \Delta A \\
A(\mathrm{B}_d \to \pi^0\pi^0) &= \frac{G_F}{2}\Big(- \lambda_t^s (P_1 + P_3) - \lambda_u^s (E_2 + P_1^{GIM} + P_3^{GIM} - A_2)\Big) + \Delta A\,,
\end{aligned} \tag{72}$$

$\lvert V_{cb}\rvert\times10^3$	$\lvert V_{ub}\rvert\times10^3$	$\hat{B}_K$	$F_{B_d}\sqrt{B_d}$ (MeV)	ξ
40.9 ± 1.0	3.70 ± 0.42	$0.86\pm0.06\pm0.14$	$230\pm30\pm15$	$1.16\pm0.03\pm0.04$
$f_K(M_K^2)$	$\mathcal{B}(\mathrm{K}^+\pi^-)\times10^6$	$\mathcal{B}(\mathrm{K}^+\pi^0)\times10^6$	$\mathcal{B}(\mathrm{K}^0\pi^+)\times10^6$	$\mathcal{B}(K^0\pi^0)\times10^6$
0.32 ± 0.12	18.6 ± 1.1	11.5 ± 1.3	17.9 ± 1.7	8.9 ± 2.3
$f_\pi(M_\pi^2)$	$\mathcal{B}(\pi^+\pi^-)\times10^6$	$\mathcal{B}(\pi^+\pi^0)\times10^6$	$\mathcal{B}(\pi^0\pi^0)\times10^6$	
0.27 ± 0.08	5.2 ± 0.6	4.9 ± 1.1	<3.4 *BaBar*	

Table 6.4: *Values of the input parameters used in our analysis. The CP-averaged branching ratios $\mathcal{B}$ are taken from Ref. [109].*

where $\lambda^q_{q'} = V_{q'q}V^*_{q'b}$. Neglecting the A_i, these parameters can be rewritten as

$$\begin{aligned} &E_1 = a_1^c A_{\pi\mathrm{K}}\,, \quad E_2 = a_2^c A_{K\pi}\,, \quad A_1 = A_2 = 0\,, \\ &P_1 = a_4^c A_{\pi K} + \tilde{P}_1\,, \quad P_1^{GIM} = (a_4^c - a_4^u)A_{\pi K} + \tilde{P}_1^{GIM}\,. \end{aligned} \tag{73}$$

The terms proportional to a_i^q give the parameters computed in the limit $m_b \to \infty$ using QCD factorization. Their definition, together with those of $A_{\pi K}$, $A_{K\pi}$, etc., can be found for instance in Refs. [41,98,10], although power-suppressed terms included there, proportional to the chiral factors $r^\chi_{K,\pi}$, should be discarded in eqs. (73). In our case, in fact, terms of $O(\Lambda_{QCD}/m_b)$ are accounted for by two phenomenological parameters: the charming-penguin parameter $\tilde{P}_1$ and the GIM-penguin parameter $\tilde{P}_1^{GIM}$. In $\mathrm{B}\to\mathrm{K}\pi$ there are no other contributions, once flavour $SU(2)$ symmetry is used and few other doubly Cabibbo-suppressed terms, including corrections to emission parametes E_1 and E_2, some annihilations (A_1) and the Zweig-suppressed contractions (ΔA), are neglected [107]. On the contrary, further power-suppressed terms (A_2, P_3, P_3^{GIM}) enter the $\mathrm{B}\to\pi\pi$ amplitudes, all with the same power of the Cabibbo angle. Therefore, these modes are subject to a larger uncertainty than the $\mathrm{B}\to\mathrm{K}\pi$ ones.

Using the inputs collected in Table 6.4, we fit the value of the complex parameter $\tilde{P}_1 = (0.13 \pm 0.02)\, e^{\pm i(114\pm35)^\circ}$. Notice that the sign of the phase is practically not constrained by the data. This result is almost independent of the inputs used for the CKM parameters ρ and η, namely whether these parameters are taken from the usual unitarity triangle analysis (UTA) [27,110] or only the constraint from $|V_{ub}/V_{cb}|$ is used.

Mode	UTA		$\lvert V_{ub}/V_{cb}\rvert$	
	$\mathcal{B}$ (10^{-6})	$\lvert\mathcal{A}_{CP}\rvert$	$\mathcal{B}$ (10^{-6})	$\lvert\mathcal{A}_{CP}\rvert$
$\pi^+\pi^-$	8.9 ± 3.3	0.37 ± 0.17	8.7 ± 3.6	0.39 ± 0.20
$\pi^+\pi^0$	5.4 ± 2.1	–	5.5 ± 2.2	–
$\pi^0\pi^0$	0.44 ± 0.13	0.61 ± 0.26	0.69 ± 0.27	0.45 ± 0.27
$\mathrm{K}^+\pi^-$	18.4 ± 1.0	0.21 ± 0.10	18.8 ± 1.0	0.21 ± 0.12
$\mathrm{K}^+\pi^0$	10.3 ± 0.9	0.22 ± 0.11	10.7 ± 1.0	0.22 ± 0.13
$\mathrm{K}^0\pi^+$	19.3 ± 1.2	0.00 ± 0.00	18.1 ± 1.5	0.00 ± 0.00
$\mathrm{K}^0\pi^0$	8.7 ± 0.8	0.04 ± 0.02	8.2 ± 1.2	0.04 ± 0.03

Table 6.5: *Predictions for CP-averaged branching ratios $\mathcal{B}$ and absolute value of the CP asymmetries $|\mathcal{A}_{CP}|$. The left (right) columns show results obtained using constraints on the CKM parameters ρ and η obtained from the UTA (the measurement of $|V_{ub}/V_{cb}|$). The last four channels are those used for fitting the charming penguin parameter $\tilde{P}_1$.*

For the sake of simplicity, we also neglect here the contribution of $\tilde{P}_1^{GIM}$. The $\mathrm{B} \to \mathrm{K}\pi$ data do not constrain this parameter very effectively, since its contribution is doubly Cabibbo suppressed with respect to $\tilde{P}_1$. The remaining $\pi^+\pi^-$ mode alone is not sufficient to fully determine the complex parameter $\tilde{P}_1^{GIM}$. It is interesting, however, to notice that the GIM-penguin contribution is potentially able to enhance the $\mathcal{B}(\mathrm{B} \to \pi^0\pi^0)$ up to few $\times 10^{-6}$ [108].

Table 6.5 shows the predicted values of the CP-averaged branching ratios $\mathcal{B}$ and the absolute value of the CP-asymmetries $|\mathcal{A}_{CP}|$ for the $\mathrm{B} \to \mathrm{K}\pi$ and $\mathrm{B} \to \pi\pi$ modes, since the data are not able to fix the sign of asymmetries. Charming penguins are able to reproduce the $\mathrm{K}\pi$ data and are also consistent with the only $\pi\pi$ mode measured so far. It is interesting to notice that the latest measurements improve the consistency, for a comparison see refs. [106,108].

3.4.2. Remarks on different approaches

Since the different approaches aiming at evaluating power-suppressed terms contain phenomenological parameters, it is natural to ask whether, after all, they are equivalent or not, even if the physical mechanism invoked to introduce the parameters is not the same. To answer this question, it is useful to compute the parameters $\tilde{P}_1$ and $\tilde{P}_1^{GIM}$ within *improved* QCD factorization. They read

$$\tilde{P}_1 = r_K^\chi a_6^c A_{\pi K} + b_3 B_{\pi K}\,,\ \tilde{P}_1^{GIM} = r_K^\chi (a_6^c - a_6^u) A_{\pi K}\,, \tag{74}$$

where the functions a_i^q (b_i) contain the complex parameter ρ_H (ρ_A), see Ref. [10] for the definitions. These two parameters account for chirally-enhanced terms, originating from hard-spectator interactions and annihilations respectively, which are not computable within the *improved* QCD factorization.

The functional dependence of the amplitudes on the phenomenological parameters in the two approaches is different. For instance, the GIM-penguin parameter is a pure short-distance correction in the *improved* QCD factorization, since the ρ_H dependence cancels out in the difference $a_6^c - a_6^u$. In practice, however, the main contribution of the phenomenological parameters to the $\mathrm{B} \to \mathrm{K}\pi$ amplitudes comes from the annihilation term b_3, i.e. from ρ_A . This term behaves effectively as the charming-penguin parameter, enhancing the Cabibbo-favored amplitude.

Notice that a vanishing ρ_A (and ρ_H), which turns out to be compatible with the data, does not mean that the phenomenological contribution is negligible. In fact, the parameters are defined so that the phenomenological terms are functions of $X_{A(H)} = (1 + \rho_{A(H)}) \log(m_B/\mu_h)$, where the scale μ_h is assumed to be 0.5 GeV [10].

3.4.3. On the possibility of extracting γ

The presence of complex phenomenological parameters in the amplitudes makes the extraction of γ very problematic. Using the $|V_{ub}/V_{cb}|$-constrained fit, almost any value of γ is allowed, given the uncertainty on $\tilde{P}_1$, see Fig. 6.13 (left). This seems a general problem which make us doubt recent claims proposing non-leptonic B decays as an effective tool for the CKM matrix determination. Even more, we think that the combination of the constraint from $\mathrm{B} \to \mathrm{K}\pi$ decays on γ with the others can even be misleading. The reason is very simple: γ is looked for through the effect of interefence terms in the branching ratios. The presence of a competing amplitude with a new phase, i.e. the one containing the phenomenological parameter, makes the extraction of γ much more complicated. Although weak and strong phases can be disentangled in principle, in practice we checked that not only the task is very difficult now, but the situation improves slowly as data become more accurate, even when the CP asymmetries will be measured.

Concerning various analyses based on the *improved* QCD factorization claiming to find a "large" value of $\gamma \sim 90^\circ$, we just notice that, as far as we know, they all assume the bound $|\rho_A| < 1$, suggested in Ref. [10] as a theoretical prejudice and supported by the observation that even $|\rho_A| = 0$ produces a

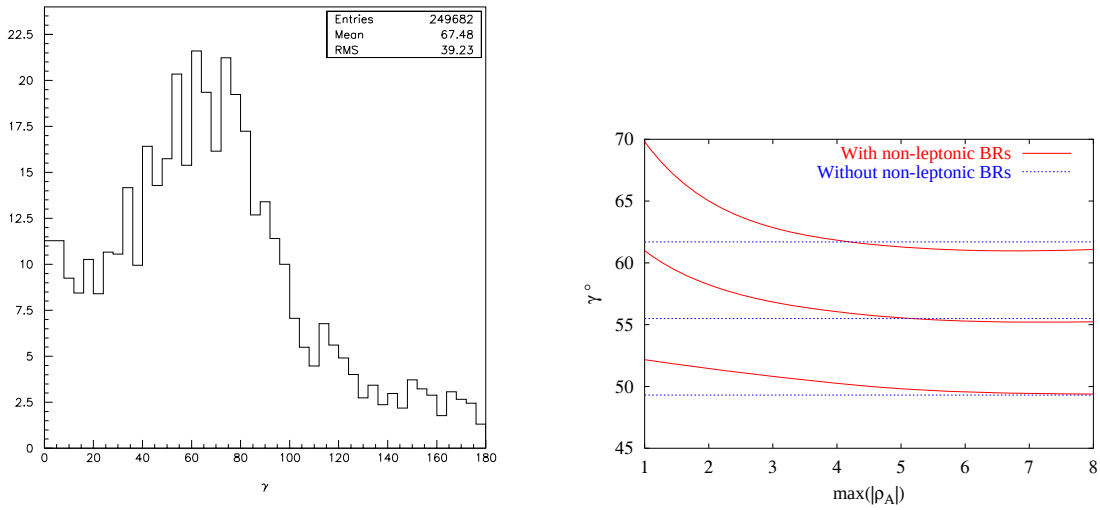

Fig. 6.13: *Fits of γ from* $\mathrm{B} \to \mathrm{K}\pi$ *using charming penguins (left) and UTA + improved QCD factorization as a function of* $\max|\rho_A|$ *(right).*

good fit to $\mathcal{B}(\mathrm{B} \to \mathrm{K}\pi)$. A better fit, however, can be obtained letting $|\rho_A|$ take values up to about 3. As shown in the right plot of Fig. 6.13, by doing so, the contribution of the constraint from non-leptonic B decays to a global fit of γ becomes totally negligible. In other words, for $|\rho_A| \sim 3$, the annihilation amplitude containing ρ_A becomes competitive with the others, improving the fit to the $\mathcal{B}$s on the one hand and weakening the predictivity on γ on the other.

3.5. Determination of the weak phases ϕ_2 and ϕ_3 from $\mathrm{B} \to \pi\pi, \mathrm{K}\pi$ in the pQCD method

Y.-Y. Keum[§].

In this section, we focus on the $\mathrm{B} \to \pi^+\pi^-$ and $\mathrm{K}\pi$ processes, providing promising strategies to determine the weak phases of ϕ_2 and ϕ_3, by using the perturbative QCD method. The perturbative QCD method (pQCD) has a predictive power demonstrated sucessfully in exclusive two body B-meson decays, specially in charmless B-meson decay processes[111]. By introducing parton transverse momenta $k_\perp$, we can generate naturally the Sudakov suppression effect due to resummation of large double logarithms $Exp[-\frac{\alpha_s C_F}{4\pi}\ln^2(\frac{Q^2}{k_\perp^2})]$, which suppress the long-distance contributions in the small $k_\perp$ region and give a sizable average $< k_\perp^2 > \sim \bar{\Lambda} M_B$. This can resolve the end point singularity problem and allow the applicability of pQCD to exclusive decays. We found that almost all of the contribution to the exclusive matrix elements come from the integration region where $\alpha_s/\pi < 0.3$ and the pertubative treatment can be justified.

In the pQCD approach, we can predict the contribution of non-factorizable term and annihilation diagram on the same basis as the factorizable one. A folklore for annihilation contributions is that they are negligible compared to W-emission diagrams due to helicity suppression. However the operators $O_{5,6}$ with helicity structure $(S-P)(S+P)$ are not suppressed and give dominant imaginary values, which is the main source of strong phase in the pQCD approach. So we have a large direct CP violation in $\mathrm{B} \to \pi^\pm\pi^\mp, \mathrm{K}^\pm\pi^\mp$, since large strong phase comes from the factorized annihilation diagram, which can distinguish pQCD from other models (see the previous two subsections).

[§]Y.-Y. Keum would like to thank G. Buchalla and members of PQCD working group for fruitful collaboration and joyful discussions.

3.5.1. *Extraction of $\phi_2(=\alpha)$ from $B \to \pi^+\pi^-$ decay*

Even though isospin analysis of $B \to \pi\pi$ can provide a clean way to determine ϕ_2, it might be difficult in practice because of the small branching ratio of $B^0 \to \pi^0\pi^0$. In reality to determine ϕ_2, we can use the time-dependent rate of $B^0(t) \to \pi^+\pi^-$ including sizable penguin contributions. In our analysis we use the c-convention. The amplitude can be written as:

$$A(B^0 \to \pi^+\pi^-) = -(|T_c|\, e^{i\delta_T} e^{i\phi_3} + |P_c|\, e^{i\delta_P}) \tag{75}$$

Penguin term carries a different weak phase than the dominant tree amplitude, which leads to generalized form of the time-dependent asymmetry.

When we define $R_{\pi\pi} = \overline{Br}(B^0 \to \pi^+\pi^-)/\overline{Br}(B^0 \to \pi^+\pi^-)|_{tree}$, where $\overline{Br}$ stands for a branching ratio averaged over B^0 and $\bar{B}^0$, the explicit expression for $S_{\pi\pi}$ and $C_{\pi\pi}$ are given by:

$$\begin{aligned} R_{\pi\pi} &= 1 - 2\,R_c\,\cos\delta\,\cos(\phi_1+\phi_2) + R_c^2, & (76)\\ R_{\pi\pi}S_{\pi\pi} &= \sin 2\phi_2 + 2\,R_c\,\sin(\phi_1-\phi_2)\,\cos\delta - R_c^2 sin2\phi_1, & (77)\\ R_{\pi\pi}C_{\pi\pi} &= 2\,R_c\,\sin(\phi_1+\phi_2)\,\sin\delta. & (78) \end{aligned}$$

with $R_c = |P_c/T_c|$ and the strong phase difference between penguin and tree amplitudes $\delta = \delta_P - \delta_T$. The time-dependent asymmetry measurement provides two equations for $C_{\pi\pi}$ and $S_{\pi\pi}$ in terms of R_c, δ and ϕ_2.

If we know R_c and δ, then we can determine ϕ_2 from the experimental data on $C_{\pi\pi}$ versus $S_{\pi\pi}$.

Since the pQCD method provides $R_c = 0.23^{+0.07}_{-0.05}$ and $-41^\circ < \delta < -32^\circ$, the allowed range of ϕ_2 at present stage is determined as $55^\circ < \phi_2 < 100^\circ$ as shown in Fig. 6.14. Since we have a relatively large strong phase in pQCD, in contrast to the QCD-factorization ($\delta \sim 0^\circ$), we predict large direct CP violation effect of $A_{cp}(B^0 \to \pi^+\pi^-) = (23 \pm 7)\%$ which will be tested by more precise experimental measurement in future. Since the data by Belle Collaboration [24] is located outside allowed physical regions, we only considered in the numerical analysis the recent BaBar measurement[112] with 90% C.L. interval taking into account the systematic errors:

- $S_{\pi\pi} = \quad 0.02 \pm 0.34 \pm 0.05 \qquad$ [-0.54, +0.58]
- $C_{\pi\pi} = -0.30 \pm 0.25 \pm 0.04 \qquad$ [-0.72, +0.12].

The central point of BaBar data corresponds to $\phi_2 = 78^\circ$ in the pQCD method.

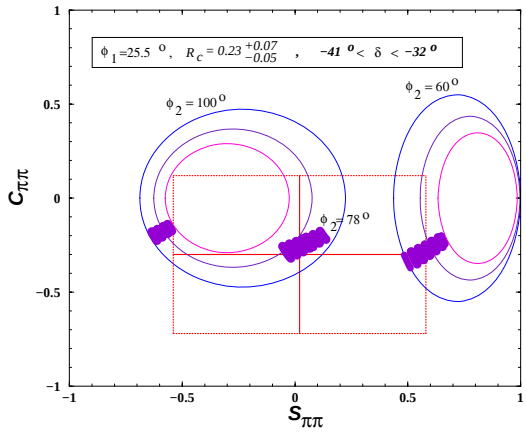

Fig. 6.14: *Plot of $C_{\pi\pi}$ versus $S_{\pi\pi}$ for various values of ϕ_2 with $\phi_1 = 25.5^\circ$, $0.18 < R_c < 0.30$ and $-41^\circ < \delta < -32^\circ$ in the pQCD method. Here we consider the allowed experimental ranges of BaBar measurment whinin 90% C.L. Dark areas is allowed regions in the pQCD method for different ϕ_2 values.*

3.5.2. *Extraction of $\phi_3(=\gamma)$ from $B^0 \to K^+\pi^-$ and $B^+ \to K^0\pi^+$ decays*

By using tree-penguin interference in $B^0 \to K^+\pi^-(\sim T' + P')$ versus $B^+ \to K^0\pi^+(\sim P')$, CP-averaged $B \to K\pi$ branching fraction may lead to non-trivial constraints on the ϕ_3 angle [84,67,68]. In order to determine ϕ_3, we need one more useful information on CP-violating rate differences[11]. Let's introduce the following observables :

$$\begin{aligned} R_K &= \frac{\overline{Br}(B^0 \to K^+\pi^-)\ \tau_+}{\overline{Br}(B^+ \to K^0\pi^+)\ \tau_0} = 1 - 2\ r_K\ \cos\delta\ \cos\phi_3 + r_K^2 \\ A_0 &= \frac{\Gamma(\bar{B}^0 \to K^-\pi^+) - \Gamma(B^0 \to K^+\pi^-)}{\Gamma(B^- \to \bar{K}^0\pi^-) + \Gamma(B^+ \to \bar{K}^0\pi^+)} \\ &= A_{cp}(B^0 \to K^+\pi^-)\ R_K = -2r_K\ \sin\phi_3\ \sin\delta. \end{aligned} \tag{79}$$

where $r_K = |T'/P'|$ is the ratio of tree to penguin amplitudes in $B \to K\pi$ and $\delta = \delta_{T'} - \delta_{P'}$ is the strong phase difference between tree and penguin amplitudes. After elimination of $\sin\delta$ in Eqs. (8)–(9), we have

$$R_K = 1 + r_K^2 \pm \sqrt{4r_K^2\cos^2\phi_3 - A_0^2\cot^2\phi_3}. \tag{80}$$

Here we obtain $r_K = 0.201 \pm 0.037$ from the pQCD analysis[111] and $A_0 = -0.11 \pm 0.065$ by combining recent BaBar measurement on CP asymmetry of $B^0 \to K^+\pi^-$: $A_{cp}(B^0 \to K^+\pi^-) = -10.2 \pm 5.0 \pm 1.6\%$ [112] with present world averaged value of $R_K = 1.10 \pm 0.15$ [113].

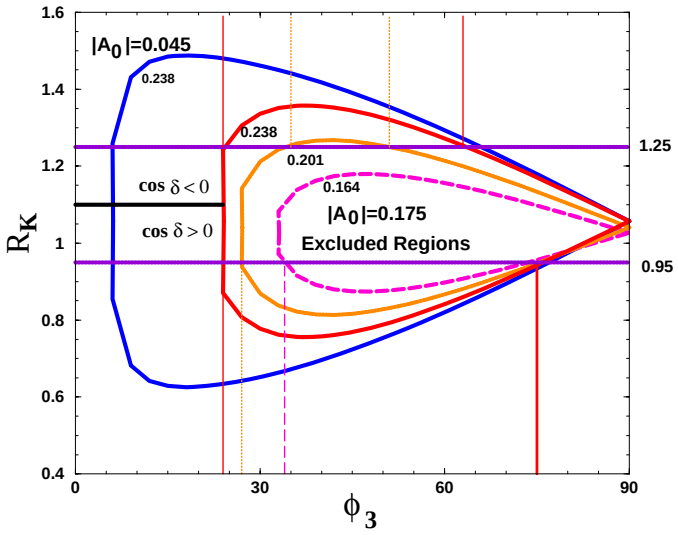

Fig. 6.15: *Plot of R_K versus ϕ_3 with $r_K = 0.164, 0.201$ and 0.238.*

From Table 2 of Ref. [114], we obtain $\delta_{P'} = 157^\circ$, $\delta_{T'} = 1.4^\circ$ and the negative $\cos\delta$: $\cos\delta = -0.91$. As shown in Fig. 6.15, we can constrain the allowed range of ϕ_3 within $1\,\sigma$ range of World Averaged R_K as follows:

- For $\cos\delta < 0$, $r_K = 0.164$: we can exclude $0^\circ \le \phi_3 \le 6^\circ$.
- For $\cos\delta < 0$, $r_K = 0.201$: we can exclude $0^\circ \le \phi_3 \le 6^\circ$ and $35^\circ \le \phi_3 \le 51^\circ$.
- For $\cos\delta < 0$, $r_K = 0.238$: we can exclude $0^\circ \le \phi_3 \le 6^\circ$ and $24^\circ \le \phi_3 \le 62^\circ$.

When we take the central value of $r_K = 0.201$, ϕ_3 is allowed within the ranges of $51^\circ \le \phi_3 \le 129^\circ$, which is consistent with the results of the model-independent CKM-fit in the $(\bar{\rho}, \bar{\eta})$ plane.

3.5.3. Conclusion

We discussed two methods to determine the weak phases ϕ_2 and ϕ_3 within the pQCD approach through 1) Time-dependent asymmetries in $B^0 \to \pi^+\pi^-$, 2) $B \to K\pi$ processes via penguin-tree interference. We can already obtain interesting bounds on ϕ_2 and ϕ_3 from present experimental measurements. Our predictions within pQCD method is in good agreement with present experimental measurements in charmless B-decays. Specially our pQCD method predicted a large direct CP asymmetry in $B^0 \to \pi^+\pi^-$ decay, which will be a crucial touch stone in order to distinguish our approach from others in future precise measurements. More detail works on other methods in $B \to K\pi$ and $D^{(*)}\pi$ processes will appear elsewhere [114].

4. $K \to \pi\nu\bar{\nu}$ decays

G. Isidori and D.E. Jaffe

4.1. Theoretical description

The $s \to d\nu\bar{\nu}$ transition is one of the rare examples of weak processes whose leading contribution starts at $\mathcal{O}(G_F^2)$. At the one-loop level it receives contributions only from Z-penguin and W-box diagrams, as shown in Fig. 6.16, or from pure quantum electroweak effects. Separating the contributions to the one-loop amplitude according to the intermediate up-type quark running inside the loop, we can write

$$\mathcal{A}(s \to d\nu\bar{\nu}) = \sum_{q=u,c,t} V_{qs}^* V_{qd} \mathcal{A}_q \quad \sim \quad \begin{cases} \mathcal{O}(\lambda^5 m_t^2) + i\mathcal{O}(\lambda^5 m_t^2) & (q=t) \\ \mathcal{O}(\lambda m_c^2) + i\mathcal{O}(\lambda^5 m_c^2) & (q=c) \\ \mathcal{O}(\lambda \Lambda_{\rm QCD}^2) & (q=u) \end{cases} \tag{81}$$

where V_{ij} denote the elements of the CKM matrix. The hierarchy of these elements would favour up- and charm-quark contributions; however, the *hard* GIM mechanism of the perturbative calculation implies $\mathcal{A}_q \sim m_q^2/M_W^2$, leading to a completely different scenario. As shown on the r.h.s. of (81), where we have employed the standard CKM phase convention ($\mathrm{Im}V_{us} = \mathrm{Im}V_{ud} = 0$) and expanded the V_{ij} in powers of the Cabibbo angle, the top-quark contribution dominates both real and imaginary parts. This structure implies several interesting consequences for $\mathcal{A}(s \to d\nu\bar{\nu})$: it is dominated by short-distance dynamics, therefore its QCD corrections are small and calculable in perturbation theory; it is very sensitive to V_{td}, which is one of the less constrained CKM matrix elements; it is likely to have a large CP-violating phase; it is very suppressed within the SM and thus very sensitive to possible new sources of quark-flavour mixing.

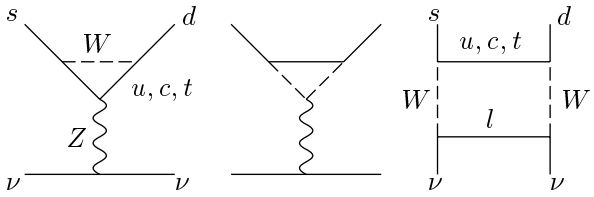

Fig. 6.16: *One-loop diagrams contributing to the $s \to d\nu\bar{\nu}$ transition.*

Short-distance contributions to $\mathcal{A}(s \to d\nu\bar{\nu})$, are efficiently described, within the SM, by the following effective Hamiltonian [115]

$$\mathcal{H}_{eff} = \frac{G_F}{\sqrt{2}} \frac{\alpha}{2\pi \sin^2\Theta_W} \sum_{l=e,\mu,\tau} \left[\lambda_c X_{NL}^l + \lambda_t X(x_t)\right] (\bar{s}d)_{V-A} (\bar{\nu}_l \nu_l)_{V-A} \,, \tag{82}$$

where $x_t = m_t^2/M_W^2$ and, as usual, $\lambda_q = V_{qs}^* V_{qd}$. The coefficients X_{NL}^l and $X(x_t)$, encoding charm- and top-quark loop contributions, are known at the NLO accuracy in QCD [116,117] and can be found

explicitly in [115]. The theoretical uncertainty in the dominant top contribution is very small and it is essentially determined by the experimental error on m_t. Fixing the $\overline{\rm MS}$ top-quark mass to $\overline{m}_t(m_t) = (166 \pm 5)$ GeV we can write

$$X(x_t) = 1.51 \left[\frac{\overline{m}_t(m_t)}{166\ {\rm GeV}}\right]^{1.15} = 1.51 \pm 0.05\ . \tag{83}$$

The simple structure of $\mathcal{H}_{eff}$ leads to two important properties of the physical $\mathrm{K} \to \pi\nu\bar{\nu}$ transitions:

- The relation between partonic and hadronic amplitudes is exceptionally accurate, since hadronic matrix elements of the $\bar{s}\gamma^\mu d$ current between a kaon and a pion can be derived by isospin symmetry from the measured K_{l3} rates.
- The lepton pair is produced in a state of definite CP and angular momentum, implying that the leading SM contribution to $\mathrm{K}_L \to \pi^0\nu\bar{\nu}$ is CP-violating.

The largest theoretical uncertainty in estimating $\mathcal{B}(\mathrm{K}^+ \to \pi^+\nu\bar{\nu})$ originates from the charm sector. Following the analysis of Ref. [115], the perturbative charm contribution is conveniently described in terms of the parameter

$$P_0(X) = \frac{1}{\lambda^4}\left[\frac{2}{3}X_{NL}^e + \frac{1}{3}X_{NL}^\tau\right] = 0.42 \pm 0.06\ . \tag{84}$$

The numerical error in the r.h.s. of Eq. (84) is obtained from a conservative estimate of NNLO corrections [115]. Recently also non-perturbative effects introduced by the integration over charmed degrees of freedom have been discussed [118]. Despite a precise estimate of these contributions is not possible at present (due to unknown hadronic matrix-elements), these can be considered as included in the uncertainty quoted in Eq. (84).[¶] Finally, we recall that genuine long-distance effects associated to light-quark loops are well below the uncertainties from the charm sector [119].

With these definitions the branching fraction of $\mathrm{K}^+ \to \pi^+\nu\bar{\nu}$ can be written as

$$\mathcal{B}(\mathrm{K}^+ \to \pi^+\nu\bar{\nu}) = \frac{\bar{\kappa}_+}{\lambda^2}\left[({\rm Im}\lambda_t)^2 X^2(x_t) + \left(\lambda^4 {\rm Re}\lambda_c P_0(X) + {\rm Re}\lambda_t X(x_t)\right)^2\right]\ , \tag{85}$$

where [115]

$$\bar{\kappa}_+ = r_{K^+}\frac{3\alpha^2 \mathcal{B}(\mathrm{K}^+ \to \pi^0 e^+\nu)}{2\pi^2 \sin^4\Theta_W} = 7.50 \times 10^{-6} \tag{86}$$

and $r_{K^+} = 0.901$ takes into account the isospin breaking corrections necessary to extract the matrix element of the $(\bar{s}d)_V$ current from $\mathcal{B}(\mathrm{K}^+ \to \pi^0 e^+\nu)$ [120].

The case of $\mathrm{K}_L \to \pi^0\nu\bar{\nu}$ is even cleaner from the theoretical point of view [121]. Because of the CP structure, only the imaginary parts in (82) –where the charm contribution is absolutely negligible– contribute to $\mathcal{A}(\mathrm{K}_2 \to \pi^0\nu\bar{\nu})$. Thus the dominant direct-CP-violating component of $\mathcal{A}(\mathrm{K}_L \to \pi^0\nu\bar{\nu})$ is completely saturated by the top contribution, where QCD corrections are suppressed and rapidly convergent. Intermediate and long-distance effects in this process are confined only to the indirect-CP-violating contribution [9] and to the CP-conserving one [122], which are both extremely small. Taking into account the isospin-breaking corrections to the hadronic matrix element [120], we can write an expression for the $\mathrm{K}_L \to \pi^0\nu\bar{\nu}$ rate in terms of short-distance parameters, namely

$$\mathcal{B}(\mathrm{K}_L \to \pi^0\nu\bar{\nu})_{\rm SM} = \frac{\bar{\kappa}_L}{\lambda^2}({\rm Im}\lambda_t)^2 X^2(x_t) = 4.16 \times 10^{-10} \times \left[\frac{\overline{m}_t(m_t)}{167\ {\rm GeV}}\right]^{2.30}\left[\frac{{\rm Im}\lambda_t}{\lambda^5}\right]^2\ , \tag{87}$$

which has a theoretical error below 3%.

[¶] The natural order of magnitude of these non-perturbative corrections, relative to the perturbative charm contribution is $m_K^2/(m_c^2 \ln(m_c^2/M_W^2)) \sim 2\%$.

At present the SM predictions of the two $\mathrm{K} \to \pi\nu\bar{\nu}$ rates are not extremely precise owing to the limited knowledge of both real and imaginary parts of λ_t. Taking into account all the indirect constraints in a global Gaussian fit, the allowed ranges read [123,124][‖]

$$\mathcal{B}(\mathrm{K}^+ \to \pi^+\nu\bar{\nu})_{\mathrm{SM}} = (0.72 \pm 0.21) \times 10^{-10} \,, \tag{88}$$

$$\mathcal{B}(\mathrm{K}_L \to \pi^0\nu\bar{\nu})_{\mathrm{SM}} = (0.28 \pm 0.10) \times 10^{-10} \,. \tag{89}$$

The high accuracy of the theoretical predictions of $\mathcal{B}(\mathrm{K}^+ \to \pi^+\nu\bar{\nu})$ and $\mathcal{B}(\mathrm{K}_L \to \pi^0\nu\bar{\nu})$ in terms of modulus and phase of $\lambda_t = V_{ts}^* V_{td}$ clearly offers the possibility of very interesting tests of flavour dynamics. Within the SM, a measurement of both channels would provide two independent pieces of information on the unitary triangle, or a complete determination of $\bar{\rho}$ and $\bar{\eta}$ from $\Delta S = 1$ transitions. In particular, $\mathcal{B}(\mathrm{K}^+ \to \pi^+\nu\bar{\nu})$ defines an ellipse in the $\bar{\rho}$–$\bar{\eta}$ plane and $\mathcal{B}(\mathrm{K}_{\mathrm{L}}^0 \to \pi^0\nu\bar{\nu})$ an horizontal line (the height of the unitarity triangle). Note, in addition, that the determination of $\sin 2\beta$ which can be obtained by combining $\mathcal{B}(\mathrm{K}_{\mathrm{L}}^0 \to \pi^0\nu\bar{\nu})$ and $\mathcal{B}(\mathrm{K}^+ \to \pi^+\nu\bar{\nu})$ is extremely clean, being independent from uncertainties due to m_t and V_{cb} (contrary to the separate determinations of $\bar{\rho}$ and $\bar{\eta}$) [9].

In principle a very precise and highly non-trivial test of the CKM mechanism could be obtained by the comparison of the following two sets of data [9]: the two $\mathrm{K} \to \pi\nu\bar{\nu}$ rates on one side, the ratio $\Delta M_{B_d}/\Delta M_{B_s}$ and $a_{\mathrm{CP}}(B \to J/\Psi K_S)$ on the other side. The two sets are determined by very different loop amplitudes ($\Delta S = 1$ FCNCs and $\Delta B = 2$ mixing) and both suffer from very small theoretical uncertainties. In particular, concerning the $\mathrm{K}^+ \to \pi^+\nu\bar{\nu}$ mode, we can write [123]

$$\mathcal{B}(\mathrm{K}^+ \to \pi^+\nu\bar{\nu}) = \bar{\kappa}_+ |V_{cb}|^4 X^2(x_t) \left[\sigma R_t^2 \sin^2\beta + \frac{1}{\sigma}\left(R_t\cos\beta + \frac{\lambda^4 P_0(X)}{|V_{cb}|^2 X(x_t)}\right)^2\right] \,, \tag{90}$$

where R_t is determined by $\Delta M_{B_d}/\Delta M_{B_s}$ [115],[**]

$$R_t = \frac{\xi}{\lambda}\sqrt{\frac{\Delta M_{B_d}}{\Delta M_{B_s}}} \tag{91}$$

and $\sin\beta$ from $a_{\mathrm{CP}}(B \to J/\Psi \mathrm{K}_S)$. In the next few years, when the experimental determination of $a_{\mathrm{CP}}(B \to J/\Psi \mathrm{K}_S)$, $\Delta M_{B_d}/\Delta M_{B_s}$, and $\mathcal{B}(\mathrm{K}^+ \to \pi^+\nu\bar{\nu})$ will substantially improve, this relation could provide one of the most significant tests of the Standard Model in the sector of quark-flavour dynamics.

Present experimental data on $\mathrm{K} \to \pi\nu\bar{\nu}$ rates do not allow yet to fully explore the high-discovery potential of these CKM tests. Nonetheless, we stress that the evidence of the $\mathrm{K}^+ \to \pi^+\nu\bar{\nu}$ decay obtained by BNL-E787 already provides highly non-trivial constraints on realistic scenarios with large new sources of flavour mixing (see e.g. Ref. [123,125,126]).

4.2. Experimental status and future prospects

The Brookhaven experiment E787 [127] searched for the decay $\mathrm{K}^+ \to \pi^+\nu\bar{\nu}$ by stopping approximately 25% of a 670, 710, 730 or 790 MeV/c K^+ beam at $\sim$ 5 MHz with $\sim 25\%$ π^+ contamination in a scintillating-fiber target along the axis of a 1-T solenoidal magnetic spectrometer. The range (R), momentum (P) and energy (E) of charged decay products are measured using the target, central drift chamber and a cylindrical range stack composed of 21 layers of plastic scintillator with two layers of

[‖] As pointed out in Ref. [124], the errors in Eqs. (88)–(89) can be reduced if $\mathrm{Re}\lambda_t$ and $\mathrm{Im}\lambda_t$ are directly extracted from $a_{\mathrm{CP}}(B \to J/\Psi \mathrm{K}_S)$ and ϵ_K; however, this procedure introduces a stronger sensitivity to the probability distribution of the (theoretical) estimate of B_K.

[**] As usual we define $\xi = (F_{B_s}/F_{B_d})\sqrt{B_{B_s}/B_{B_d}}$ and $\sigma = 1/(1-\frac{\lambda^2}{2})^2$.

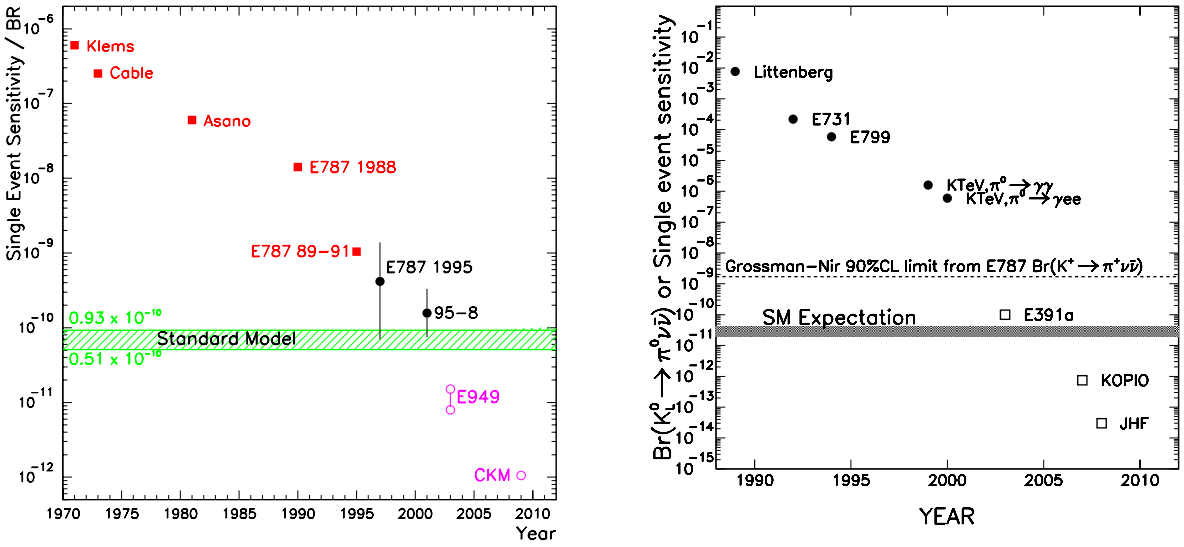

Fig. 6.17: *History and prospects for the study of $\mathcal{B}(\mathrm{K}^+ \to \pi^+\nu\bar{\nu})$(left) and $\mathcal{B}(\mathrm{K}^0_\mathrm{L} \to \pi^0\nu\bar{\nu})$(right). The points with error bars are measured branching fractions, the solid points are upper limits at 90% CL and the open points or squares are single event sensitivities. The dashed line is a nearly model-independent limit based on the E787's results for $\mathcal{B}(\mathrm{K}^+ \to \pi^+\nu\bar{\nu})$ [126]. The horizontal bands are the 68% CL SM expectations.*

tracking chambers. Detection of the decay sequence $\pi^+ \to \mu^+ \to e^+$ in the range stack provided a powerful tool against $\mathrm{K}^+ \to \mu^+\nu(\gamma)$ decays. A 4π-sr calorimeter consisting of lead/scintillator layers in the barrel (14 radiation lengths) and undoped CsI crystals in the endcap (13.5 radiation lengths) were used to veto photons and suppress $\mathrm{K}^+ \to \pi^+\pi^0$ background. Incident kaons were detected and identified by Čerenkov, tracking and energy loss detectors along the beam that aided in the suppression of backgrounds due to scattered beam pions and the charge exchange process that resulted in $\mathrm{K}^0_\mathrm{L} \to \pi^+\ell^-\nu$ decays ($\ell^- = e^-,\mu^-$) in the target.

E787 has a long history, summarized in Fig. 6.17, that has lead to the development of a relatively robust analysis strategy. The strategy begins with *a priori* identification of background sources and development of experimental tools to suppress each background source with at least two independent cuts. In the search for such rare processes, background rejection cannot be reliably simulated, instead it is measured by alternatively inverting independent cuts and measuring the rejection of each cut taking any correlations into account. To avoid bias, cuts are determined using 1/3 of the data and then the backgrounds rates are measured with the remaining 2/3 sample. Background estimates are verified by loosening cuts and comparing the observed and predicted rates, first in the 1/3 sample, then in the 2/3 sample. Simulated signal events are used to measure the geometrical acceptance for $\mathrm{K}^+ \to \pi^+\nu\bar{\nu}$ and the acceptance is verified with a measurement of $\mathcal{B}(\mathrm{K}^+ \to \pi^+\pi^0)$. The pre-defined signal region in R, P and E is not examined until all background estimates are verified. It is anticipated that similar strategies will be employed in further investigations of $\mathrm{K} \to \pi\nu\bar{\nu}$ decays.

Brookhaven E787 was completed in 1998 and has observed two candidates for the decay $\mathrm{K}^+ \to \pi^+\nu\bar{\nu}$ in the pion momentum region 211 to 229 MeV/c with an estimated background of 0.15 ± 0.05 in a sample of 5.9×10^{12} stopped K^+ that corresponds to [127]

$$\mathcal{B}(\mathrm{K}^+ \to \pi^+\nu\bar{\nu}) = (15.7^{+17.5}_{-8.2}) \times 10^{-11} \; . \tag{92}$$

The probability that the two candidates are entirely due to background is 0.02% . In addition a search

in the momentum interval 140 to 195 MeV/c in a sample of 1.1×10^{12} stopped K^+ yielded a single candidate upon an estimated background of 0.73 ± 0.18 corresponding to a limit $\mathcal{B}(K^+ \to \pi^+\nu\bar{\nu}) < 420 \times 10^{-11}$ at 90% C.L. [128]. Such a search below the peak of the two body $K^+ \to \pi^+\pi^0$ decays has the potential not only to augment the statistics of the higher momentum sample, but also to investigate the shape of the $P(\pi^+)$ distribution predicted by the SM. In addition, the search is somewhat complementary to that of the higher momentum interval because the background is dominated by $K^+ \to \pi^+\pi^0$ decays in which the charged pion undergoes a nuclear interaction in the target near the kaon decay vertex.

E949 is an upgraded version of E787 with an expected net increase in sensitivity of at least a factor of 5 based on 6000 hours of running time or 5-10 SM events [129]. The main detector upgrades are an increased photon veto capability, both in the endcap and barrel regions, as well as trigger and data acquisition improvements. E949 recently accumulated 1.9×10^{12} stopped kaons ($\sim 1/9$ of E949's goal) and additional running is expected in 2003 assuming sufficient funding is forthcoming.

The CKM experiment at Fermilab expects to attain a single event sensitivity of 1×10^{-12} that would correspond to ~ 100 $K^+ \to \pi^+\nu\bar{\nu}$ events assuming the SM value of the branching fraction [130]. Such a measurement would achieve a statistical precision comparable to the current theoretical uncertainty in the branching fraction. CKM departs from the E787/E949 technique by using kaon decays in flight in a 22 GeV/c, 50 MHz debunched beam with 60% kaon purity. The experiment will use photon veto technology similar to E787 and KTeV with the addition of ring-imaging Čerenkov detectors to aid in kinematic suppression of backgrounds. The use of in-flight kaon decays means that the dominant $K^+ \to \pi^+\pi^0$ background in E787's search in the lower momentum region should not be present at CKM [131]. CKM should be taking data in the second half of this decade.

The progress concerning the neutral mode is much slower. No dedicated experiment has started yet and the best direct limit is more than four orders of magnitude above the SM expectation [132]. An indirect model-independent upper bound on $\Gamma(K_L \to \pi^0\nu\bar{\nu})$ can be obtained by the isospin relation [126]

$$\Gamma(K^+ \to \pi^+\nu\bar{\nu}) = \Gamma(K_L \to \pi^0\nu\bar{\nu}) + \Gamma(K_S \to \pi^0\nu\bar{\nu}) \tag{93}$$

which is valid for any $s \to d\nu\bar{\nu}$ local operator of dimension ≤ 8 (up to small isospin-breaking corrections). Using the BNL-E787 result (92), this implies $\mathcal{B}(K_L \to \pi^0\nu\bar{\nu}) < 1.7 \times 10^{-9}$ (90% CL). Any experimental information below this figure can be translated into a non-trivial constraint on possible new-physics contributions to the $s \to d\nu\bar{\nu}$ amplitude.

The first $K_L \to \pi^0\nu\bar{\nu}$ dedicated experiments are E391a at KEK [133] and KOPIO at Brookhaven [134]. E391a is envisioned as a two-stage experiment and will attempt to use a highly collimated K_L^0 beam and a hermetic veto to observe high transverse momentum π^0 near the endpoint of the $K_L^0 \to \pi^0\nu\bar{\nu}$ spectrum with a technique similar to previous searches [132]. The first stage of E391a is regarded as a pilot experiment and will use the KEK 12 GeV/c proton beam and should begin data taking in 2003. If successful, it could push the limit on $\mathcal{B}(K_L^0 \to \pi^0\nu\bar{\nu})$ to within an order of magnitude of the SM expectation (Fig. 6.18). An aggressive second stage envisions use of the high intensity 50 GeV/c proton beam from the Japanese Hadron Facility(JHF) to reach a single event sensitivity of 3×10^{-14} or, equivalently, ~ 1000 SM events.

The KOPIO experiment will attempt a new approach, using a microbunched, low momentum beam, time-of-flight and a high precision electromagnetic preradiator and calorimeter to fully reconstruct the kinematics of the $K_L^0 \to \pi^0\nu\bar{\nu}$ decay. Coupled with highly efficient charged particle and photon vetoes, KOPIO will be able to exploit the E787 strategy of independent kinematic and veto cuts to measure all backgrounds with the data. The goal of KOPIO is a single event sensitivity of 7.5×10^{-13} or the capability to obtain 40 SM events with a signal to background of 2 corresponding to a precision on $\mathcal{J}$ or $\bar{\eta}$ of $\sim 10\%$.

As anticipated, one of the most interesting test of the CKM mechanism could be obtained by the comparison of the two $K \to \pi\nu\bar{\nu}$ rates on one side vs. the ratio $\Delta M_{B_d}/\Delta M_{B_s}$ and $a_{CP}(B \to$

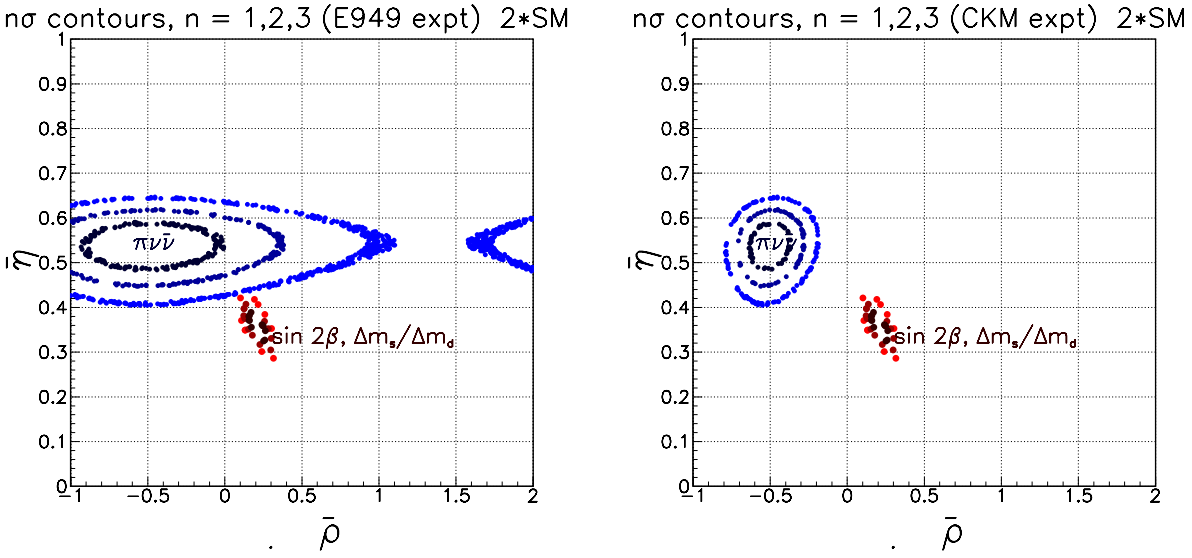

Fig. 6.18: *Comparison of the impact of hypothetical measurements of the* $\mathrm{K} \to \pi\nu\bar{\nu}$ *branching fractions by E949 and KOPIO(left) or CKM and KOPIO(right) in the* $\bar{\rho}, \bar{\eta}$ *plane with hypothetical measurements of* $\sin 2\beta$ *and* $\Delta M_s/\Delta M_d$*. Contours at 68.3, 95.45 and 99.7% CL are indicated for the K measurements. For the B measurements, the points indicating the three contours overlap. See text for details.*

$\mathrm{J}/\Psi\mathrm{K_S}$) on the other side. As an illustration, in Figure 6.18 we consider the comparison of the two B-physics measurements, assumed to be $a_{\mathrm{CP}}(B \to J/\Psi \mathrm{K}_S) = 0.75 \pm 0.02$ and $\Delta M_{B_d}/\Delta M_{B_s} = 17.0 \pm 1.7\ \mathrm{ps}^{-1}$, with the two $\mathrm{K} \to \pi\nu\bar{\nu}$ rates, both assumed to be twice the corresponding SM prediction. The uncertainties on $\mathcal{B}(\mathrm{K} \to \pi\nu\bar{\nu})$ measurements are those expected by E949, CKM and KOPIO experiments attaining their expected sensitivities. The corresponding constraints in the $\bar{\rho}$–$\bar{\eta}$ plane have been derived assuming Gaussian uncertainties for all quantities, using the Bayesian statistics option of the CKM fitter program [135]. Negligible uncertainty in $|V_{cb}|$ is assumed in placing the K measurements in this *B-centric* rendering of the UT. Note that the alternative, equally fundamental, parametrization of the UT using the λ_t plane would remove the need for this assumption [136].

References

[1] The BaBar Physics Book, eds. P. Harrison and H. Quinn, 1998, SLAC report 504.

[2] B Decays at the LHC, eds. P. Ball, R. Fleischer, G.F. Tartarelli, P. Vikas and G. Wilkinson, hep-ph/0003238.

[3] B Physics at the Tevatron, Run II and Beyond, K. Anikeev et al., hep-ph/0201071.

[4] A.J. Buras and R. Fleischer, Adv Ser. Direct. High. Energy Phys. **15** (1998) 65; [hep-ph/9704376].

[5] A.J. Buras, hep-ph/0101336, lectures at the International Erice School, August, 2000;
Y. Nir, hep-ph/0109090, lectures at 55th Scottish Univ. Summer School, 2001.

[6] A.J. Buras, F. Parodi and A. Stocchi, JHEP **0301** (2003) 029 [hep-ph/0207101].

[7] J.M. Soares and L. Wolfenstein, Phys. Rev. D **47** (1993) 1021; Y. Nir and U. Sarid, Phys. Rev. D **47** (1993) 2818; Y. Grossman and Y. Nir, Phys. Lett. B **313** (1993) 126; R. Barbieri, L.J. Hall and A. Romanino, Phys. Lett. B **401** (1997) 47; M. Ciuchini, E. Franco, L. Giusti, V. Lubicz and G. Martinelli, Nucl. Phys. B **573** (2000) 201-222; P. Paganini, F. Parodi, P. Roudeau and A. Stocchi, Physica Scripta **58** (1998) 556-569; F. Parodi, P. Roudeau and A. Stocchi Nuovo Cimento **112A (1999) 833.**

[8] A. Höcker, H. Lacker, S. Laplace and F. Le Diberder, Eur. Phys. J. C **21** (2001) 225.

[9] G. Buchalla and A.J. Buras, Phys. Rev. D **54** (1996) 6782.

[10] M. Beneke, G. Buchalla, M. Neubert, and C. Sachrajda, Nucl. Phys. B **606** (2001) 245.

[11] M. Gronau and J. L. Rosner, Phys. Rev. D **65** (2002) 013004 [E: D **65** (2002) 079901].

[12] Z. Luo and J. L. Rosner, Phys. Rev. D **65** (2002) 054027.

[13] A.J. Buras, M.E. Lautenbacher and G. Ostermaier, Phys. Rev. D **50** (1994) 3433.

[14] A.J. Buras, Phys. Lett. B **333** (1994) 476; Nucl. Instr. Meth. **A368** (1995) 1.

[15] R. Aleksan, B. Kayser and D. London, Phys. Rev. Lett. **73** (1994) 18;
J.P. Silva and L. Wolfenstein, Phys. Rev. D **55** (1997) 5331;
I.I. Bigi and A.I. Sanda, hep-ph/9909479.

[16] A.J. Buras, P. Gambino, M. Gorbahn, S. Jäger and L. Silvestrini, Phys. Lett. B **500** (2001) 161.

[17] A. Ali and D. London, Eur. Phys. J. C **9** (1999) 687 [hep-ph/9903535]; Phys. Rep. **320** (1999), 79 [hep-ph/9907243]; hep-ph/0002167; Eur. Phys. J. C **18** (2001) 665.

[18] A.J. Buras and R. Fleischer, Phys. Rev. D **64** (2001) 115010.

[19] A.J. Buras, P.H. Chankowski, J. Rosiek and L. Slawianowska, Nucl. Phys. B **619** (2001) 434.

[20] G. D'Ambrosio and G. Isidori, Phys. Lett. B **530** (2002) 108.

[21] G.C. Branco, L. Lavoura and J. Silva, (1999), CP Violation, Oxford Science Publications, Press Clarendon, Oxford.

[22] F.J. Botella, G.C. Branco, M. Nebot and M.N. Rebelo, Nucl. Phys. B **651** (2003) 174 [hep-ph/0206133].

[23] L. Wolfenstein, Phys. Rev. Lett. **51** (1983) 1945.

[24] Belle Collaboration, K. Abe et al., Phys. Rev. Lett. **89** (2002) 071801, hep-ex/0204002.

[25] Talk by A. Farbin (BaBar Collaboration), XXXVIIth Recontres de Moriond, Electroweak Interactions and Unified Theories, Les Arcs, France, 9-16 March 2002, *http://moriond.in2p3.fr/EW/2002/*.

[26] Average from Y. Nir hep-ph/0208080 based on: R. Barate et al. (ALEPH Collaboration) *Phys. Lett.* B **492** (2000), 259; K. Ackerstaff et al. (OPAL Collaboration) *Eur. Phys.* C **5** (1998) 379; T. Affolder at al. Phys. ReV. D61 (2000) 072005; B. Aubert et al. (Babar Collaboration) hep-ex/0207042; K. Abe at al. (Belle Collaboration) hep-ex/0207098.

[27] M. Ciuchini, G. D'Agostini, E. Franco, V. Lubicz, G. Martinelli, F. Parodi, P. Roudeau, A. Stocchi, JHEP **0107** (2001) 013 [hep-ph/0012308].

[28] T. Hurth, Rev. Mod. Phys. (to appear) [hep-ph/0212304]; A. J. Buras and M. Misiak, Acta Phys. Pol. B 33 (2002) 2597 [hep-ph/0207131].

[29] S. Bertolini, F. Borzumati and A. Masiero, Phys. Rev. Lett. **59** (1987) 180;
N.G. Deshpande *et al.*, Phys. Rev. Lett. **59** (1987) 183.

[30] M. S. Alam *et al.* (CLEO Collaboration), Phys. Rev. Lett. **74** (1995) 2885.

[31] B. Aubert *et al.* (BABAR Collaboration), hep-ex/0207076.

[32] S. Chen *et al.* (CLEO Collaboration), Phys. Rev. Lett. **87** (2001) 251807 [hep-ex/0108032].

[33] K. Abe *et al.* (BELLE Collaboration), Phys. Lett. B **511** (2001) 151 [hep-ex/0103042].

[34] R. Barate *et al.* (ALEPH Collaboration), Phys. Lett. B **429** (1998) 169.

[35] P. Gambino and M. Misiak, Nucl. Phys. B **611** (2001) 338 [hep-ph/0104034].

[36] A.J. Buras, A. Czarnecki, M. Misiak and J. Urban, Nucl. Phys. B **631** (2002) 219 [hep-ph/0203135].

[37] K. Hagiwara *et al.* (Particle Data Group Collaboration), Phys. Rev. D **66** (2002) 010001.

[38] A. Ali, H. Asatrian and C. Greub, Phys. Lett. B **429** (1998) 87 [hep-ph/9803314];
A. L. Kagan and M. Neubert, Phys. Rev. D **58** (1998) 094012 [hep-ph/9803368].

[39] Y. Grossman and D. Pirjol, JHEP **0006** (2000) 02 [hep-ph/0005069].

[40] T.E. Coan *et al.* (CLEO Collaboration), Phys. Rev. Lett. **86** (2001) 5661 [hep-ex/0010075].

[41] M. Beneke, G. Buchalla, M. Neubert and C. T. Sachrajda, Phys. Rev. Lett. **83** (1999) 1914 [hep-ph/9905312].

[42] M. Beneke, T. Feldmann and D. Seidel, Nucl. Phys. B **612** (2001) 25 [hep-ph/0106067].

[43] S. W. Bosch and G. Buchalla, Nucl. Phys. B **621** (2002) 459 [hep-ph/01060].

[44] A. Ali and A. Y. Parkhomenko, Eur. Phys. J. C **23** (2002) 89 [hep-ph/0105302].

[45] T. E. Coan *et al.* (CLEO Collaboration), Phys. Rev. Lett. **84** (2000) 5283 [hep-ex/9912057].

[46] S. Nishida (BELLE Collaboration), Talk presented at the 31st. International Conference on High Energy Physics, July 24 - 31, 2002, Amsterdam, The Netherlands.

[47] B. Aubert *et al.* (BABAR Collaboration) Phys. Rev. Lett. **88** (2002) 101805 [hep-ex/0110065].

[48] A. L. Kagan and M. Neubert, Phys. Lett. B **539**, 227 (2002) [hep-ph/0110078].

[49] P. Ball and V. M. Braun, Phys. Rev. D **58** (1998) 094016 [hep-ph/9805422].

[50] M. Beneke and T. Feldmann, Nucl. Phys. B **592** (2001) 3 [hep-ph/0008255].

[51] A. Ali, V. M. Braun and H. Simma, Z. Phys. C **63** (1994) 437 [hep-ph/9401277].

[52] L. Del Debbio, J. M. Flynn, L. Lellouch and J. Nieves (UKQCD Collaboration), Phys. Lett. B **416** (1998) 392 [hep-lat/9708008].

[53] A. Ali, L. T. Handoko and D. London, Phys. Rev. D **63** (2000) 014014 [hep-ph/0006175].

[54] B. Grinstein and D. Pirjol, Phys. Rev. D **62** (2000) 093002 [hep-ph/0002216].

[55] A. Ali and V. M. Braun, Phys. Lett. B **359** (1995) 223 [hep-ph/9506248].

[56] A. Khodjamirian, G. Stoll and D. Wyler, Phys. Lett. B **358** (1995) 129 [hep-ph/9506242].

[57] A. Ali and E. Lunghi, DESY-02-089, hep-ph/0206242.

[58] S. Narison, Phys. Lett. B **327** (1994) 354 [hep-ph/9403370].

[59] D. Melikhov and B. Stech, Phys. Rev. D **62** (2000) 014006 [hep-ph/0001113].

[60] Y. Nir, hep-ph/0208080.

[61] See, for example, L. Lellouch, plenary talk at the 31st. International Conference on High Energy Physics, July 24 - 31, 2002, Amsterdam, The Netherlands.

[62] A. S. Kronfeld and S. M. Ryan, Phys. Lett. B **543** [hep-ph/0206058].

[63] C. Jessop (BABAR Collaboration), Talk presented at the 31st. International Conference on High Energy Physics, July 24 - 31, 2002, Amsterdam, The Netherlands.

[64] BaBar Collaboration, B. Aubert et al., SLAC preprint SLAC-PUB-9229, hep-ex/0205082, presented at 37th Rencontres de Moriond on Electroweak Interactions and Unified Theories, Les Arcs, France, 9–16 Mar 2002.

[65] M. Gronau and J. L. Rosner, Phys. Rev. D **65** (2002) 093012.

[66] M. Gronau and J. L. Rosner, Phys. Rev. D **66** (2002) 119901.

[67] M. Neubert and J. L. Rosner, Phys. Lett. B **441** (1998) 403.

[68] M. Neubert and J. L. Rosner, Phys. Rev. Lett. **81** (1998) 5076.

[69] D. A. Suprun, C.-W. Chiang, and J. L. Rosner, Phys. Rev. D **65** (2002) 054025.

[70] C.-W. Chiang and J. L. Rosner, Phys. Rev. D **65** (2002) 074035.

[71] A. Höcker, H. Lacker, S. Laplace, and F. Le Diberder, in *Proceedings of the 9th International Symposium on Heavy Flavor Physics*, Pasadena, California, 10–13 Sep 2001, AIP Conf. Proc. **618** (2002) 27.

[72] J. Charles, Phys. Rev. D **59** (1999) 054007.

[73] R. Fleischer, in *Proceedings of the 9th International Symposium on Heavy Flavor Physics*, Pasadena, California, 10–13 Sep 2001, AIP Conf. Proc. **618** (2002) 266.

[74] M. Gronau, D. London, N. Sinha, and R. Sinha, Phys. Lett. B **514** (2001) 315.

[75] M. Gronau, Phys. Rev. D **58** (1998) 037301.

[76] D. Atwood, I. Dunietz, and A. Soni, Phys. Rev. D **63** (2001) 036005.

[77] B. Kayser and D. London, Phys. Rev. D **63** (2000) 116013.

[78] A. J. Buras and R. Fleischer, Eur. Phys. J. C **16** (2000) 97.

[79] R. Fleischer, Phys. Lett. B **459** (1999) 306.

[80] M. Gronau and J. L. Rosner, Phys. Lett. B **482** (2000) 71.

[81] R. Fleischer, Phys. Rep. **370** (2202) 537 [hep-ph/0207108].

[82] M. Gronau, J. L. Rosner and D. London, Phys. Rev. Lett. **73** (1994) 21.

[83] R. Fleischer, Phys. Lett. B **365** (1996) 399.

[84] R. Fleischer and T. Mannel, Phys. Rev. D **57** (1998) 2752.

[85] M. Gronau and J. L. Rosner, Phys. Rev. D **57** (1998) 6843.

[86] R. Fleischer, Eur. Phys. J. C **6** (1999) 451.

[87] M. Neubert, JHEP **9902** (1999) 014.

[88] A. J. Buras and R. Fleischer, Eur. Phys. J. C **11** (1999) 93.

[89] R. Fleischer and J. Matias, Phys. Rev. D **61** (2000) 074004.

[90] M. Bargiotti *et al.*, Eur. Phys. J. C **24** (2002) 361.

[91] H.-n. Li and H. L. Yu, Phys. Rev. D **53** (1996) 2480;
Y. Y. Keum, H.-n. Li and A. I. Sanda, Phys. Lett. B **504** (2001) 6;
Y. Y. Keum and H.-n. Li, Phys. Rev. D **63** (2001) 074006.

[92] R. Fleischer, Eur. Phys. J. C **16** (2000) 87.

[93] R. Fleischer and J. Matias, Phys. Rev. D. **66** (2002) 054009, [hep-ph/0204101].

[94] J. Matias, Phys. Lett. B **520** (2001) 131.

[95] M. Gronau, Phys. Lett. B **492** (2000) 297.

[96] R. Fleischer, Eur. Phys. J. C **10** (1999) 299, Phys. Rev. D **60** (1999) 073008;
P. Z. Skands, JHEP **0101** (2001) 008.

[97] M. Gronau and J. L. Rosner, Phys. Rev. D **65** (2002) 093012, 113008 and hep-ph/0205323;
C.-D. Lü and Z.-j. Xiao, Phys. Rev. D **66** (2002) 074011 [hep-ph/0205134].

[98] M. Beneke, G. Buchalla, M. Neubert and C. T. Sachrajda, Nucl. Phys. B **591** (2000) 313.

[99] M. Wirbel, B. Stech and M. Bauer, Z. Phys. C **29** (1985) 637;
M. Bauer, B. Stech and M. Wirbel, Z. Phys. C **34** (1987) 103.

[100] M. Beneke, in: Proceedings of the 5th KEK Topical Conference: Frontiers in Flavor Physics (KEKTC5), Tsukuba, Ibaraki, Japan, 20-22 Nov 2001 [hep-ph/0202056].

[101] D. Du, H. Gong, J. Sun, D. Yang and G. Zhu, Phys. Rev. D **65** (2002) 074001.

[102] M. Beneke, in: Proceedings of: Flavor Physics and CP Violation (FPCP), Philadelphia, Pennsylvania, 16-18 May 2002 [hep-ph/0207228].

[103] M. Neubert, in: Proceedings of the International Workshop on Heavy Quarks and Leptons, Salerno, Italy, 27 May - 1 Jun 2002 [hep-ph/0207327].

[104] BaBar Collaboration, hep-ex/0207053; P. Krokovny [Belle Collaboration], talk at ICHEP2002, Amsterdam, July 2002.

[105] M. Ciuchini, E. Franco, G. Martinelli and L. Silvestrini, Nucl. Phys. B **501** (1997) 271 [hep-ph/9703353].

[106] M. Ciuchini, R. Contino, E. Franco, G. Martinelli and L. Silvestrini, Nucl. Phys. B **512** (1998) 3 [Erratum-ibid. B **531** (1998) 656] [hep-ph/9708222].

[107] A. J. Buras and L. Silvestrini, Nucl. Phys. B **569** (2000) 3 [hep-ph/9812392].

[108] M. Ciuchini, E. Franco, G. Martinelli, M. Pierini and L. Silvestrini, Phys. Lett. B **515** (2001) 33 [hep-ph/0104126].

[109] R. Patterson, summary talk at FPCP02, *http://www.hep.upenn.edu/FPCP/talks/1803/180303Patterson.pdf*.

[110] M. Ciuchini, Nucl. Phys. Proc. Suppl. **109** (2002) 307 [hep-ph/0112133].

[111] Y.Y. Keum, H.n. Li and A.I. Sanda, Phys. Lett. B **504** (2001) 6; Phys. Rev. D **63** (2001) 054008; hep-ph/0201103; Y.Y. Keum and H.n. Li, Phys. Rev. D **63** (2001) 074006; C.D. Lu, K. Ukai and M.Z. Yang, Phys. Rev. D **63** (2001) 074009; C.-H. Chen, Y.Y. Keum and H.-n. Li, Phys.Rev.D **64** (2001) 112002; hep-ph/0204166; S. Mishima, Phys.Lett. B **521** (2001) 252.

[112] BaBar Collaboration (B. Aubert et al.), hep-ex/0207055.

[113] R. Bartoldus, talk on Review of rare two-body B decays at FPCP workshop, May 17, 2002.

[114] Y.Y. Keum, Proceeding at the 3rd workshop on Higher Luminosity B Factory, Aug. 6-7, 2002; hep-ph/0209002; hep-ph/0209014; Y.Y. Keum et al., in preparation.

[115] G. Buchalla and A. J. Buras, Nucl. Phys. B **548** (1999) 309 [hep-ph/9901288].

[116] G. Buchalla and A. J. Buras, Nucl. Phys. B **398** (1993) 285; **400** (1993) 225; **412** (1994) 106 [hep-ph/9308272];

[117] M. Misiak and J. Urban, Phys. Lett. B. **451** (1999) 161 [hep-ph/9901278].

[118] A. F. Falk, A. Lewandowski and A. A. Petrov, Phys. Lett. B. **505** (2001) 107 [hep-ph/0012099].

[119] M. Lu and M. Wise, Phys. Lett. B. **324** (1994) 461 [hep-ph/9401204].

[120] W.J. Marciano and Z. Parsa, Phys. Rev. D **53** (1996) R1.

[121] L. Littenberg, Phys. Rev. D39 (1989) 3322.

[122] G. Buchalla and G. Isidori, Phys. Lett. B. **440** (1998) 170 [hep-ph/9806501];
D. Rein and L.M. Sehgal, Phys. Rev. D39 (1989) 3325.

[123] G. D'Ambrosio and G. Isidori, Phys. Lett. B. **530** (2002) 108 [hep-ph/0112135].

[124] S. Kettell, L. Landsberg and H. Nguyen, hep-ph/0212321.

[125] A. J. Buras *et al.*, Nucl. Phys. B **566** (2000) 3 [hep-ph/9908371].

[126] Y. Grossman and Y. Nir, Phys. Lett. B **398** (1997) 163 [hep-ph/9701313].

[127] S. Adler *et al.* [E787 Collaboration], Phys. Rev. Lett. **88** (2002) 041803 and references therein.

[128] S. Adler *et al.* [E787 Collaboration], Phys. Lett. B **537** (2002) 211 [hep-ex/0201037].

[129] *http://www.phy.bnl.gov/e949/*

[130] P.S. Cooper, Nucl. Phys. Proc. Suppl. **99B** (2001) 121;
http://www.fnal.gov/projects/ckm/Welcome.html

[131] M.V.Diwan, hep-ex/0205089, La Thuile, Italy, 2002.

[132] A. Alavi-Harati *et al.* [KTeV Collaboration], Phys. Rev. D **61** (2000) 072006 [hep-ex/9907014].

[133] *http://psux1.kek.jp/∼e391/*

[134] A. Konaka, hep-ex/9903016; *http://pubweb.bnl.gov/people/e926/*

[135] H. Höcker, H. Lacker, S. Laplace and F. Le Diberder, Eur. Phys. J. C **21** (2001) 225, hep-ph/0104062, *http://ckmfitter.in2p3.fr/*

[136] L.S. Littenberg, hep-ex/0201026, to appear in the Proc. 9th Intl. Symp. on Heavy Flavor Physics.